MCEER
EARTHQUAKE ENGINEERING TO EXTREME EVENTS

U.S. Department of Transportation
Federal Highway Administration

ISSN 1520-295X

REDARS Validation Report

by
Sungbin Cho, Charles K. Huyck, Shubharoop Ghosh
and Ronald T. Eguchi

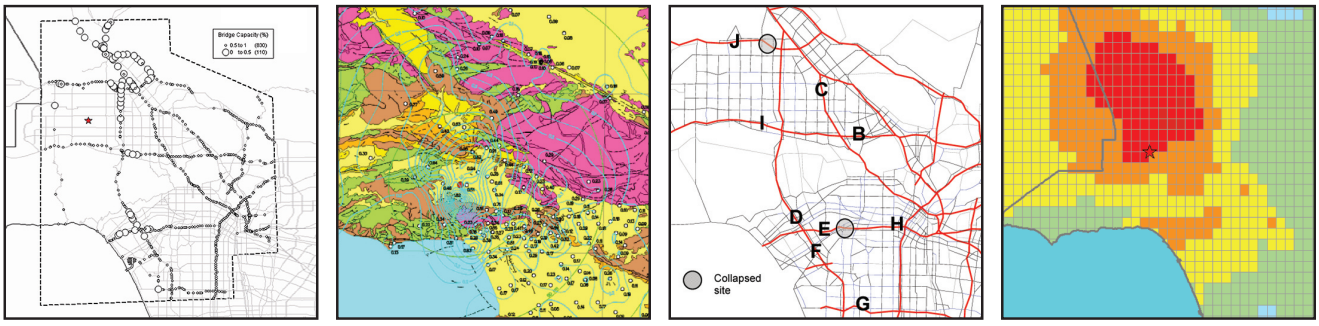

Technical Report MCEER-06-0007

August 8, 2006

This research was conducted at ImageCat, Inc. and was supported by the
Federal Highway Administration under contract number DTFH61-98-C-00094.

NOTICE

This report was prepared by ImageCat, Inc. as a result of research sponsored by MCEER through a contract from the Federal Highway Administration. Neither MCEER, associates of MCEER, its sponsors, ImageCat, Inc., nor any person acting on their behalf:

a. makes any warranty, express or implied, with respect to the use of any information, apparatus, method, or process disclosed in this report or that such use may not infringe upon privately owned rights; or

b. assumes any liabilities of whatsoever kind with respect to the use of, or the damage resulting from the use of, any information, apparatus, method, or process disclosed in this report.

Any opinions, findings, and conclusions or recommendations expressed in this publication are those of the author(s) and do not necessarily reflect the views of MCEER or the Federal Highway Administration.

MCEER
EARTHQUAKE ENGINEERING TO EXTREME EVENTS

U.S. Department of Transportation
Federal Highway Administration

REDARS Validation Report

by

Sungbin Cho[1], Charles K. Huyck[2], Shubharoop Ghosh[1]
and Ronald T. Eguchi[3]

Publication Date: August 8, 2006
Submittal Date: April 3, 2006

Technical Report MCEER-06-0007

Task Number 094-B-1.1

FHWA Contract Number DTFH61-98-C-00094
Contract Officer's Technical Representative: W. Phillip Yen, Ph.D., P.E. HRDI-7
Senior Research Structural Engineer/Seismic Research Program Manager
Federal Highway Administration

1 Transportation System Analyst, ImageCat, Inc., Long Beach, California
2 Senior Vice President, ImageCat, Inc., Long Beach, California
3 CEO and President, ImageCat, Inc., Long Beach, California

MCEER
University at Buffalo, The State University of New York
Red Jacket Quadrangle, Buffalo, NY 14261
Phone: (716) 645-3391; Fax (716) 645-3399
E-mail: *mceer@buffalo.edu*; WWW Site: *http://mceer.buffalo.edu*

Preface

The Multidisciplinary Center for Earthquake Engineering Research (MCEER) is a national center of excellence in advanced technology applications that is dedicated to the reduction of earthquake losses nationwide. Headquartered at the University at Buffalo, State University of New York, the Center was originally established by the National Science Foundation in 1986, as the National Center for Earthquake Engineering Research (NCEER).

Comprising a consortium of researchers from numerous disciplines and institutions throughout the United States, the Center's mission is to reduce earthquake losses through research and the application of advanced technologies that improve engineering, pre-earthquake planning and post-earthquake recovery strategies. Toward this end, the Center coordinates a nationwide program of multidisciplinary team research, education and outreach activities.

MCEER's research is conducted under the sponsorship of two major federal agencies, the National Science Foundation (NSF) and the Federal Highway Administration (FHWA), and the State of New York. Significant support is also derived from the Federal Emergency Management Agency (FEMA), other state governments, academic institutions, foreign governments and private industry.

The Center's Highway Project develops improved seismic design, evaluation, and retrofit methodologies and strategies for new and existing bridges and other highway structures, and for assessing the seismic performance of highway systems. The FHWA has sponsored three major contracts with MCEER under the Highway Project, two of which were initiated in 1992 and the third in 1998.

Of the two 1992 studies, one performed a series of tasks intended to improve seismic design practices for new highway bridges, tunnels, and retaining structures (MCEER Project 112). The other study focused on methodologies and approaches for assessing and improving the seismic performance of existing "typical" highway bridges and other highway system components including tunnels, retaining structures, slopes, culverts, and pavements (MCEER Project 106). These studies were conducted to:

- assess the seismic vulnerability of highway systems, structures, and components;
- develop concepts for retrofitting vulnerable highway structures and components;
- develop improved design and analysis methodologies for bridges, tunnels, and retaining structures, which include consideration of soil-structure interaction mechanisms and their influence on structural response; and
- develop, update, and recommend improved seismic design and performance criteria for new highway systems and structures.

The 1998 study, "Seismic Vulnerability of the Highway System" (FHWA Contract DTFH61-98-C-00094; known as MCEER Project 094), was initiated with the objective of performing studies to improve the seismic performance of bridge types not covered under Projects 106 or 112, and to provide extensions to system performance assessments for highway systems. Specific subjects covered under Project 094 include:

- development of formal loss estimation technologies and methodologies for highway systems;
- analysis, design, detailing, and retrofitting technologies for special bridges, including those with flexible superstructures (e.g., trusses), those supported by steel tower substructures, and cable-supported bridges (e.g., suspension and cable-stayed bridges);
- seismic response modification device technologies (e.g., hysteretic dampers, isolation bearings); and
- soil behavior, foundation behavior, and ground motion studies for large bridges.

In addition, Project 094 includes a series of special studies, addressing topics that range from non-destructive assessment of retrofitted bridge components to supporting studies intended to assist in educating the bridge engineering profession on the implementation of new seismic design and retrofitting strategies.

This report presents the results of an extensive review and evaluation of the Seismic Risk Assessment (SRA) methodology for highway systems, as documented in "A Risk-Based Methodology for Assessing the Seismic Performance of Highway Systems," by S.D. Werner, C.E. Taylor, J.E. Moore II, J.S. Walton and S. Cho, MCEER-00-0014. The efficacy of all key modules in the REDARS (Risk of Earthquake Damage for Roadway Systems) software program were evaluated. The modules included: bridge damage or fragility module, post-earthquake traffic state module, transportation module and economic loss module. The results from this review were evaluated by the REDARS development team and subsequently used to update the REDARS software program. The REDARS methodology and software for seismic risk analysis of highway systems is presented in a companion MCEER special report, "REDARS 2 Methodology and Software for Seismic Risk Analysis of Highway Systems," by S.D. Werner, C.E. Taylor, S. Cho, J.P. Lavoie, C.K. Huyck, C. Eitzel, H. Chung and R.T. Eguchi, MCEER-06-SP08.

ABSTRACT

This report represents the result of an extensive review and evaluation of the Seismic Risk Assessment (SRA) methodology for highway systems documented in Werner et al. (2000). The research team evaluated the efficacy of all key modules in the REDARS (Risk of Earthquake Damage for Roadway Systems) software program. The modules included: bridge damage or fragility module, post-earthquake traffic state module, transportation module, and economic loss module.

The reader should note that the version of REDARS that was evaluated in this study has since been updated based largely on the conclusions and recommendations of this report. Using the Northridge earthquake as a validation/calibration event, this early version of REDARS produced results that were measurably higher than expected or observed. For example, the number of bridges estimated with some level of damage was approximately two times higher than what was actually observed in the Northridge earthquake. Furthermore, post-earthquake traffic volumes and economic losses (derived primarily from travel time increases) were substantially higher when derived through REDARS. There are many reasons why these overestimations occurred; however, the primary reason appears to be the incompatibility between the ground motions that were actually observed during the Northridge earthquake and the bridge fragility models used in this study. This area certainly deserves more attention.

Some of the key recommendations that were identified in this study include: 1) the uncertainty factors in the bridge fragility model require further investigation, 2) additional events – beyond the 1994 Northridge earthquake – should be incorporated in the validation and/or calibration of the different loss modules, especially related to bridge fragilities, 3) further investigation of the traffic state model, particularly, in the relationship between link importance and duration of bridge closure should be conducted, 4) the travel demand model should be enhanced so that congestion level becomes a critical factor in establishing demand, 5) a more realistic post-earthquake, route choice model should be developed, and 6) other significant cost items (e.g., bridge repair costs, business interruption costs due to disrupted highway segments) should be included in future enhancements of REDARS.

ACKNOWLEDGMENTS

The authors gratefully acknowledge the Federal Highway Administration (FHWA) and the Multidisciplinary Center for Earthquake Engineering Research (MCEER) for their financial support of this research. We would also like to thank Ian Buckle of the University of Nevada at Reno, George C. Lee and Jerry O'Connor of MCEER, and Phil Yen of FHWA -- for their guidance throughout this research.

The authors would especially like to acknowledge the exceptional leadership and guidance provided by Stuart Werner of Seismic Systems and Engineering Consultants. Without this vision, this project would not have been possible. In addition, the special efforts of Jean-Paul Lavoie and Chip Eitzel of Geodesy, Craig E. Taylor of Natural Hazards Management, Inc., and James E. Moore II of the University of Southern California are acknowledged by the authors. The authors would also like to thank Clifford Roblee of the NEES Consortium, Inc., Nesrin Basöz of St. Paul Travelers, and Paul Somerville of URS Corporation for their help and guidance in the early part of our study. The authors would like to finally acknowledge the final editing performed on the report by Beverley J. Adams of ImageCat, and Jerry McMillan.

This research was conducted under MCEER master agreement DTFH61-98-C-00094 with the Federal Highway Administration.

TABLE OF CONTENTS

TABLE OF CONTENTS

TABLE OF CONTENTS (Cont'd)

LIST OF FIGURES

LIST OF FIGURES (Cont'd)

LIST OF TABLES

SECTION 1
INTRODUCTION

Loss estimation methods have become a key element in many earthquake loss reduction programs. Largely considered ancillary tools until recently, they are now essential components in many earthquake preparedness, response, mitigation, and recovery studies. For example, loss estimation methods are currently being used to quantify the long-term benefits (in terms of reduction of future losses) associated with specific retrofit strategies, to project possible losses immediately following significant earthquakes, and to evaluate the benefits of alternative reconstruction or recovery strategies, i.e., pre-planning for post-earthquake reconstruction.

The application of loss estimation methods for transportation planning is particularly important. Like any lifeline system, the failure of key transportation components can lead to larger system impacts, often affecting the entire community or region. Currently, the only means of gauging or assessing these larger impacts is through the application of system-type analyses that incorporate loss estimation models. With respect to transportation analyses, some studies have been performed to estimate the system-wide impacts after large earthquakes; however, the range of measures considered in these studies has generally been small and incomplete.

Beginning in the late 1990's, the Federal Highway Administration (FHWA) through the Multidisciplinary Center for Earthquake Engineering Research (MCEER) began funding research on the development of a loss estimation framework for highway transportation systems (Werner et al., 2000). This research resulted in a scenario-based methodology that estimated damage to bridges and impacts on the overall transportation network. Output from this methodology included: GIS displays of the spatial distribution of seismic hazards and their effects; component damage states; system states at various time periods after the earthquake; tabulations of economic losses; and travel time increases due to disrupted transportation links. In 2000, the basic methodology and framework (initially referred to as the Seismic Risk Assessment methodology or SRA) was established and a demonstration example was developed using Shelby County (including the city of Memphis), Tennessee as a pilot area (Werner, et al., 2000).

In 2001, formal activities were implemented to transform the methodology into a verified and publicly-available software tool, with technical documentation and a user's manual. As part of this process, a complimentary effort involving an independent evaluation and validation of the loss estimation methodology was launched. The purpose of this study was to 1) review the methodology for completeness and technical validity, 2) to perform a comparative analysis on each loss estimation module to assess its efficacy in producing reasonable results, 3) to perform a validation study of the methodology using empirical data collected after the 1994 Northridge earthquake, and 4) to recommend specific enhancements or improvements to the methodology in order to better match damage and performance data from real events. This report is a culmination of these tasks; its results have already been used to revise and update the current SRA software tool which is now called REDARS (Risk of Earthquake Damage to Roadway Systems).

1.1 Study Objectives

The objectives of this study were to review, validate and recommend changes and/or improvements to the loss estimation methodology and software program, *REDARS*. During this study, the following tasks were performed:

1. SRA Review. The project team provided a review and evaluation of the SRA methodology. Particular attention was given to those parameters and models that could be modified or replaced. Since one of the tasks below dealt with the sensitivity of results to changes in parameter values, it was important to determine the extent to which these models could be modified.
2. Implementation of REDARS 1.0[1] Code. During this phase of the project, REDARS 1.0 was installed at ImageCat for subsequent testing and evaluation. Several simple examples were implemented. As part of this subtask, the research team also evaluated the completeness and understandability of the User's Manual.
3. Develop Input Data for Los Angeles Case Study. To implement REDARS 1.0 for Los Angeles, the research team compiled data and information on local seismic hazards in the Los Angeles area (including soil data), bridge information (including bridge types, configurations, number of spans, etc.), highway network data, and traffic flow information. The project team also collected damage and post-earthquake traffic information on the 1994 Northridge earthquake. These data were used in both the sensitivity studies as well as the validation work.
4. Conduct Sensitivity Studies. The research team conducted sensitivity studies in order to identify key parameters and modules. The purpose of these sensitivity studies was to 1) identify the effect that parameter uncertainties had on the final loss estimation results, and 2) identify possible simplifications in the methodology to facilitate more rapid calculations of loss or impact. In particular, the research team focused on those simplifications that would help to improve the modeling of post-earthquake traffic patterns and levels. These sensitivity studies focused on Los Angeles area.
5. Conduct Validation Studies using Data from the 1994 Northridge Earthquakes. The research team began the validation process by developing the input required to run REDARS 1.0 for the 1994 Northridge earthquake. The Northridge earthquake would test REDARS' ability to identify changes in post-earthquake traffic patterns after a major earthquake.
6. Recommend Changes and/or Improvements to the Methodology to Better Assess the Performance of Transportation Systems in Earthquakes. Based on the results of the sensitivity analyses and the validation work completed above, the research team recommended specific areas where either the methodology or the software routines should be improved in order to better match actual earthquake performance data, e.g., the Northridge earthquake.

[1] This version of REDARS represents the first software implementation of the SRA methodology. At the time of publication, REDARS 2.0 was introduced which incorporated many of the recommended changes of this study.

1.2 Evaluation Approach

Figure 1-1 shows the evaluation approach for this study. In general, the approach was based on comparing REDARS results – at a module level - with actual earthquake information from of the 1994 Northridge earthquake. There were four different modules or levels that were evaluated: bridge damage states; post-earthquake traffic states; post-earthquake traffic volumes; and economic losses. In order to isolate the comparisons, the input to each REDARS module was information or data from the actual earthquake. In this way, we prevented the propagation of errors or variations from one module to another.

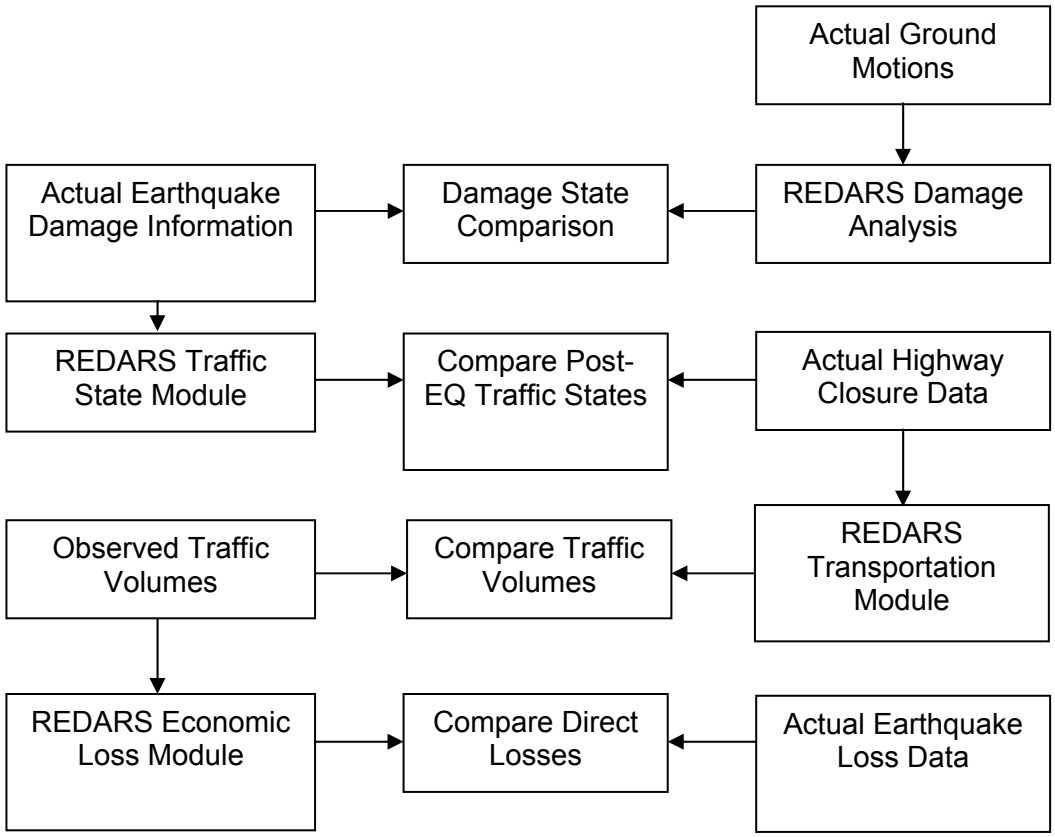

Figure 1-1 REDARS Evaluation Approach

1.3 Study Region and Basic Data Sources

The Los Angeles study area (Figure 1-2) selected for the validation of the methodology covered 772 square miles. For transportation network data, the National Highway Planning Network (NHPN) and the Highway Performance Monitoring System (HPMS) databases from Federal Highway Administration (FHWA) were used. The Transportation network included the freeways, the major arterials, and the corridors identified by the NHPN database with designated

route numbers. Nine hundred and forty (940) Caltrans maintained bridges were located within the study area. REDARS uses the National Bridge Inventory (NBI) database format and Mander's bridge fragility model (Mander et al., 1998, HAZUS-99 Chapter 7, Basöz and Mander, 1999) to develop bridge fragility functions for the bridges located in the study area. Traffic demand (Origin-Destination) data was provided by the Southern California Association of Governments (SCAG). Soil data used in REDARS came from the National Earthquake Hazards Reduction Program (NEHRP).

Ground motion data from the 1994 Northridge earthquake were used as input to REDARS. The TriNet ground motion data on this event was the most recent (1997). TriNet data were displayed as shaking maps with peak ground accelerations, peak ground velocities, and spectral accelerations at 0.3 second and 1.0 second mapped.

Caltrans data on observed bridge damage states from the Northridge earthquake were used to assess the efficacy of bridge damage or fragility models. In some cases, the project team re-evaluated the damage states compiled by Caltrans using aerial photographs taken immediately after the Northridge earthquake. In four cases, the damage states were modified from the original Caltrans database.

Table 1-1 Data and their Sources

Data	Data Source(s)
Event	1994 Northridge earthquake
Ground Motion	Tri-Net (http://www.trinet.org)
Bridge	National Bridge Inventory Database (FHWA) State Bridge Log (Caltrans)
Transportation Network	National Highway Planning Network (FHWA) Highway Performance Monitoring System (FHWA)
TAZ and OD	1990 OD survey by Southern California Association of Governments
Soil	NEHRP soil and amplification data
Damage States	Caltrans

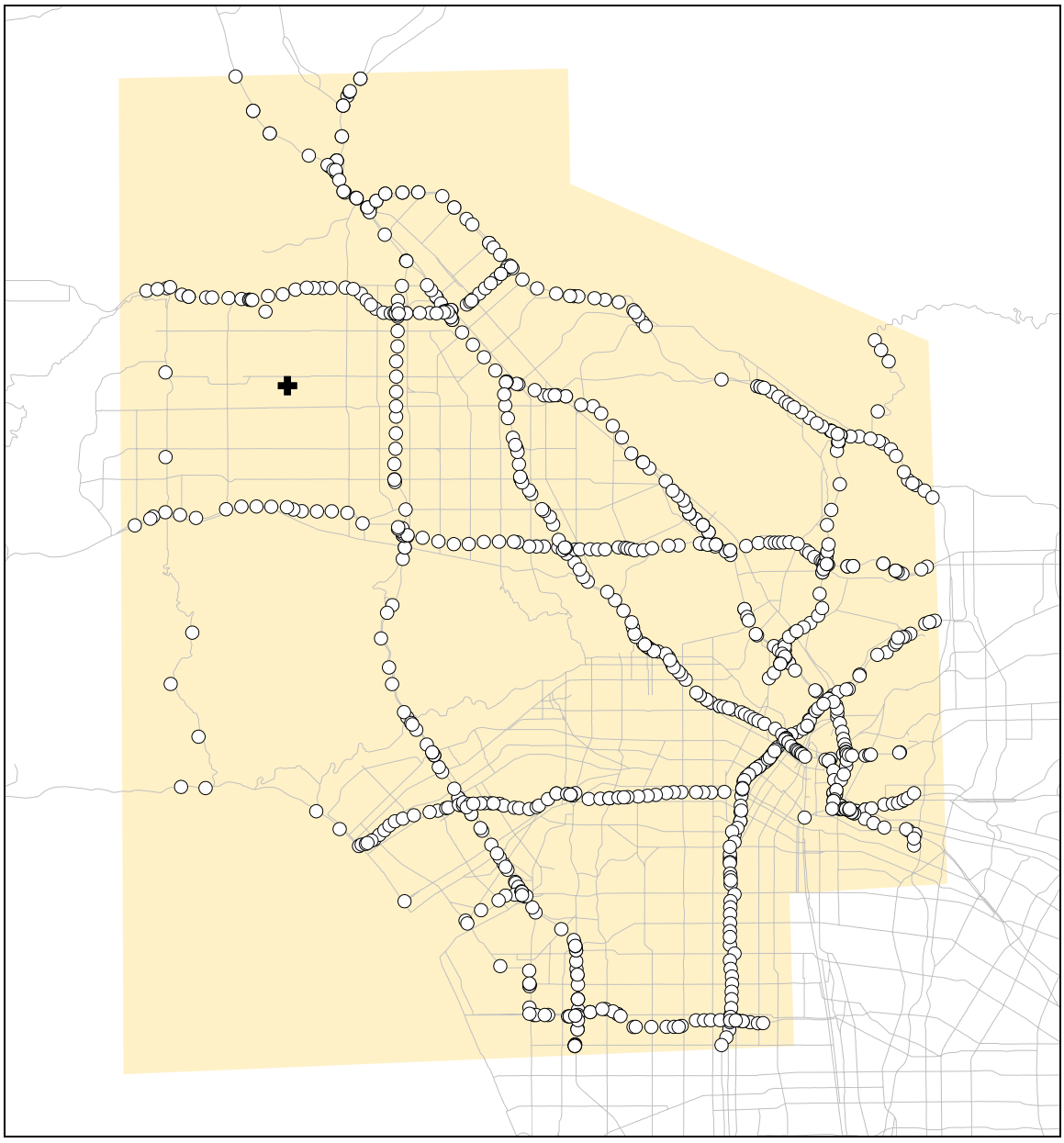

Note: cross indicates the epicenter of the 1994 Northridge earthquake

Figure 1-2 Study Area, Network and Bridges

1.4 Report Outline

This report contains seven major sections, including this introduction. Section 2 covers the different ground motion data sets used in this study to estimate shaking intensities from the 1994 Northridge earthquake. A key issue that is introduced in this section is the wide variation of results when regional ground motions are sought in this event. Section 3 deals with the evaluation of the bridge damage or fragility functions. A direct comparison is made between the number of bridges in each bridge damage state, as computed by the REDARS methodology and the actual number recorded by Caltrans, the operator of state-owned bridges in California.

Section 4 focuses on the comparison of REDARS-generated traffic states and those reported by Caltrans. In general, this comparison examines whether the REDARS model accurately predicts the number of open or closed lanes on bridges that suffered significant earthquake damage. Section 5 deals with traffic volumes, and how REDARS compared with post-Northridge data. This comparison is conducted at various levels; a regional comparison is made with traffic volumes across the Los Angeles basis, and a local comparison is made using arterial data and information around bridges that suffered major damage or complete collapse. Section 6 covers the comparison of economic losses. In this case, losses are defined as costs associated with increased travel times. This comparison does not address structural repair costs or losses associated with business interruptions. Finally, Section 7 summarizes the major conclusions and/or observations from the earlier sections. In addition, the research team makes a number of recommendations to improve the overall loss estimation methodology in REDARS.

SECTION 2
GROUND MOTION

This section describes the ground motion data sets used in this study to validate the different loss modules contained in REDARS. As described previously, the basis for these ground motions was the 1994 Northridge earthquake. As will be evident in later discussions, one serious issue that prevented a straightforward use of these data was the apparent disparity between the different data sets. A key consideration in the validation work was selecting a ground motion data set that most closely matched the input ground motions used to develop the bridge fragility functions used in REDARS. This section also contains guidelines that should be followed in selecting and implementing future ground motion data sets, e.g., ShakeMap.

2.1 Ground Motion

Although the different ground motion data sets from the Northridge Earthquake utilized the same seismic network data (614 short-period sensors, 1563 strong-motion sensors, 198 broadband sensors in California and western Nevada), differences in data interpretation, data interpolation and extrapolation, and data filtering led to vastly different ground motion contours for this event. From the standpoint of validating the REDARS methodology, these differences caused many problems, the least of which was matching damage data on bridges for the Northridge event. For various reasons, these data sets are not entirely consistent with loss modules in REDARS, nor are they consistent with each other. Two areas that contribute to these inconsistencies are 1) the way in which the ground motion parameters are represented (e.g., vector sum estimates of various ground motion components versus maximum of the two horizontal components), and the interpolation schemes used to estimate ground motions where no recording instruments were located. As it turns out, understanding these differences is crucial to explaining the wide variation of results in bridge fragility and damageability. Section 2 is organized as follows:

- Section 2.2 describes three available data sets for 1994 Northridge earthquake that are based upon observed ground motion recordings.
- Section 2.3 discusses the relationship used to represent the correlation between peak ground acceleration (PGA) and spectral acceleration (SA).
- Section 2.4 discusses the processing of the TriNet[2] data.
- Section 2.5 describes the calculation of site amplification factors that are required by the bridge damage function in REDARS.

The version of REDARS that was evaluated in this study is different than the currently available version that Caltrans is using (REDARS 1.0) and certainly different than the version that will ultimately be delivered to the Federal Highway Administration in 2006 (REDARS 2.0). These latter versions incorporate changes that reflect improvements to the version evaluated in this study. One specific difference is that the version reviewed in this study did not have the

[2] TriNet is the name of the organization that includes the three major seismic network operators, i.e., the California Institute of Technology (Caltech), the U.S. Geological Survey (USGS), and the California Geological Survey (CGS). This organization has since been subsumed under the California Integrated Seismic Network (CISN) which represents seismic networks throughout California.

capability of computing ground motions based on earthquake source information (e.g., magnitude and location). Therefore, in lieu of using computed ground motions (which would be consistent with the validation methodology described earlier), the REDARS validation team essentially bypassed any evaluation of ground motion models and proceeded directly to an assessment of bridge fragility, traffic and economic loss models using the Northridge earthquake as a baseline case.

2.2 Sources of Observed Ground Motion Data for the Northridge Earthquake

This section describes the three sources of ground motion data considered in this study. They include:

- TriNet ShakeMap files (March 1999),
- USGS Open File Report 94-197 (C.M. Wentworth, R.D. Borcherdt, 1994), and
- Data processed by Paul Somerville (URS Corp.) for the Applied Technology Council (ATC) in 1995.

2.2.1 TriNet ShakeMap

TriNet ShakeMaps provide near real-time ground shaking data for all significant Southern California earthquakes. The ShakeMaps incorporate data from three active seismic networks in Southern California, i.e., TriNet system. TriNet began in 1997, with the goal of unifying the three separate networks, and harnessing some existing efforts to transmit the ground shaking records to a centralized location for analysis. The three networks are the Southern California Seismic Network (SCSN) operated by Caltech and the USGS, the California Strong Motion Instrumentation Program (CSMIP) operated by the California Geological Survey, and the USGS National Strong Motion Program (NSMP). Figures 2-1 and 2-2 map the TriNet sensor locations throughout Southern California that contribute to the ShakeMap system.

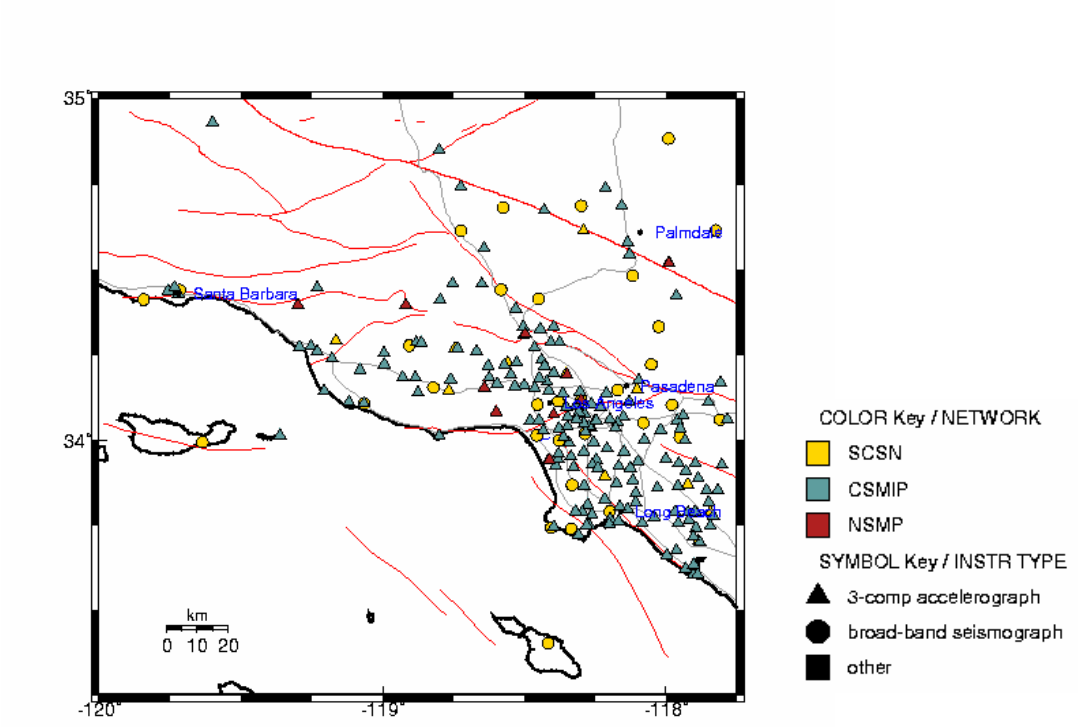

Figure 2-1 TriNet Sensors in the Greater Los Angeles Region

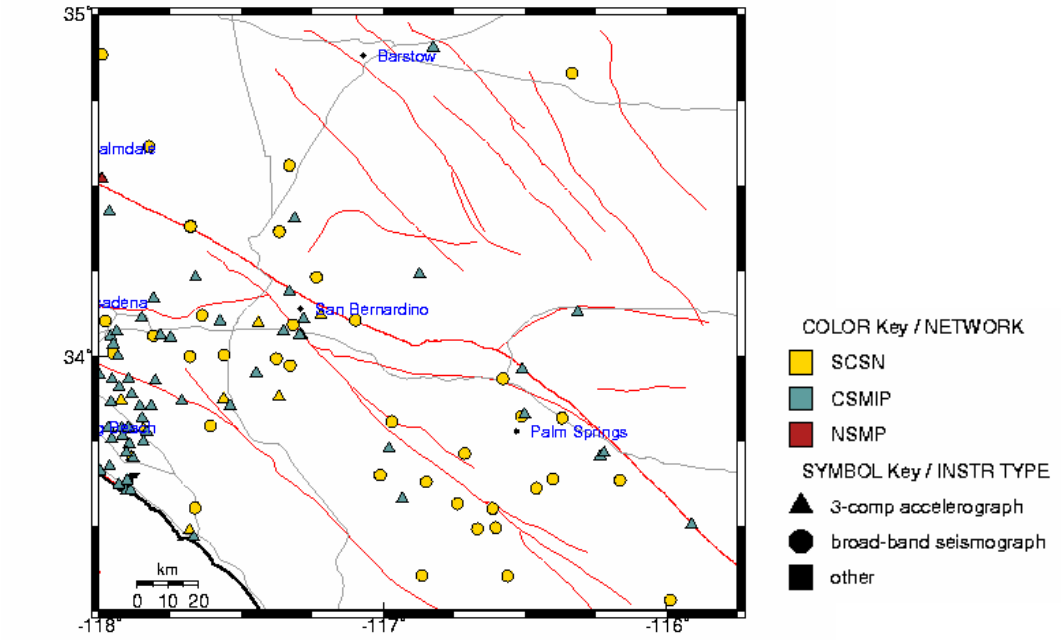

Figure 2-2 TriNet Sensors East and South of the Greater Los Angeles Region

After an event, TriNet interpolates a ground shaking surface from hundreds of accelerograms produced throughout the region and posts the results in standardized file formats, commonly known as ShakeMaps. There are two forms of interpolated data, a fine grid that is used for visualization (see Figure 2-3), and a coarser grid for analysis (Figure 2-4). The fine grid can be used to visualize results, but because there is a continuous change in color representation, it is difficult to infer more than an integer representation of instrumental intensity. This is by design, so that users will not infer more accuracy than is warranted by the number of accelerograms. The GIS files used to create this visualization are not available for downloading. However, this detailed interpolation is used to generate contour lines that can be imported into various programs for analysis.

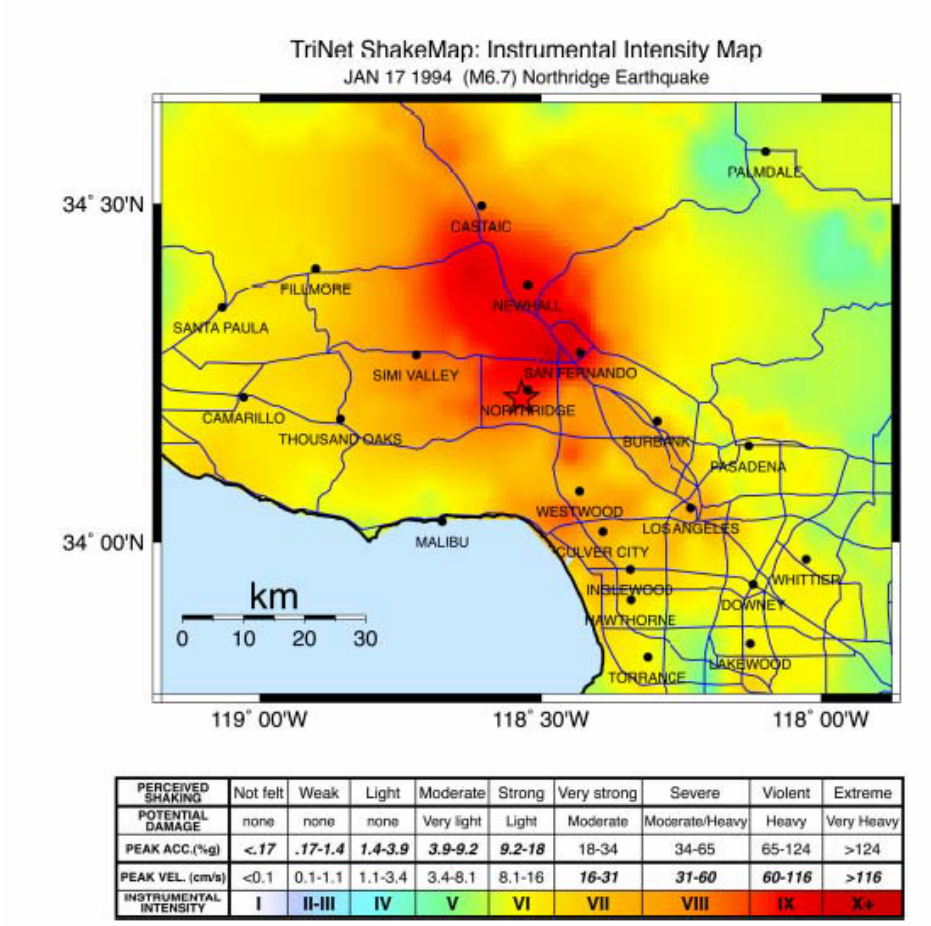

PERCEIVED SHAKING	Not felt	Weak	Light	Moderate	Strong	Very strong	Severe	Violent	Extreme
POTENTIAL DAMAGE	none	none	none	Very light	Light	Moderate	Moderate/Heavy	Heavy	Very Heavy
PEAK ACC.(%g)	*<.17*	*.17-1.4*	*1.4-3.9*	*3.9-9.2*	*9.2-18*	18-34	34-65	65-124	>124
PEAK VEL. (cm/s)	<0.1	0.1-1.1	1.1-3.4	3.4-8.1	8.1-16	*16-31*	*31-60*	*60-116*	*>116*
INSTRUMENTAL INTENSITY	I	II-III	IV	V	VI	VII	VIII	IX	X+

Figure 2-3 TriNet Media Map for Northridge: Data Available for Viewing

The data for the Northridge ShakeMap are not based on the TriNet sensors, which have been deployed since the Northridge Earthquake, but on existing analog networks including CGS (Coast and Geodetic Survey), USGS (U.S. Geological Survey), USC (University of Southern California), and SCE (Southern California Edison. There have been many versions of the TriNet map for the 1994 Northridge Earthquake (7/98, 10/98, 3/99, 10/02, 12/02, and 7/03). Some of the known differences in these versions are discussed below.

For the Northridge earthquake, the interpolated data set is available on a 0.025 decimal degree grid, which equates to a 2.3 km East-West by 2.8 km North-South irregular grid in the Northridge area. Ground Shaking values posted at this resolution for the Northridge Earthquake are displayed in Figure 2-4.

Ground shaking is estimated between instrument sites by first converting the surface ground motion at each site to a bedrock ground motion value. This is necessary in order to limit the interpolation to those factors that are influenced only by the source parameters of the earthquake, e.g., earthquake magnitude and location. The conversion to bedrock is accomplished by dividing surface ground motions by site amplification factors (see Table 2-1). The soil classification system is based on identifying different geologic units, i.e., Quaternary, Tertiary, Mesozoic (QTM) as described by Park and Ellrick (1998). The attenuation function used in interpolation scheme is one developed by Joyner et al. (1997) and Joyner and Boore (1988). After the interpolation is completed, the bedrock ground motions are then converted back to surface ground motions by multiplying the bedrock ground motions by the soil amplification factors in Table 2-1.

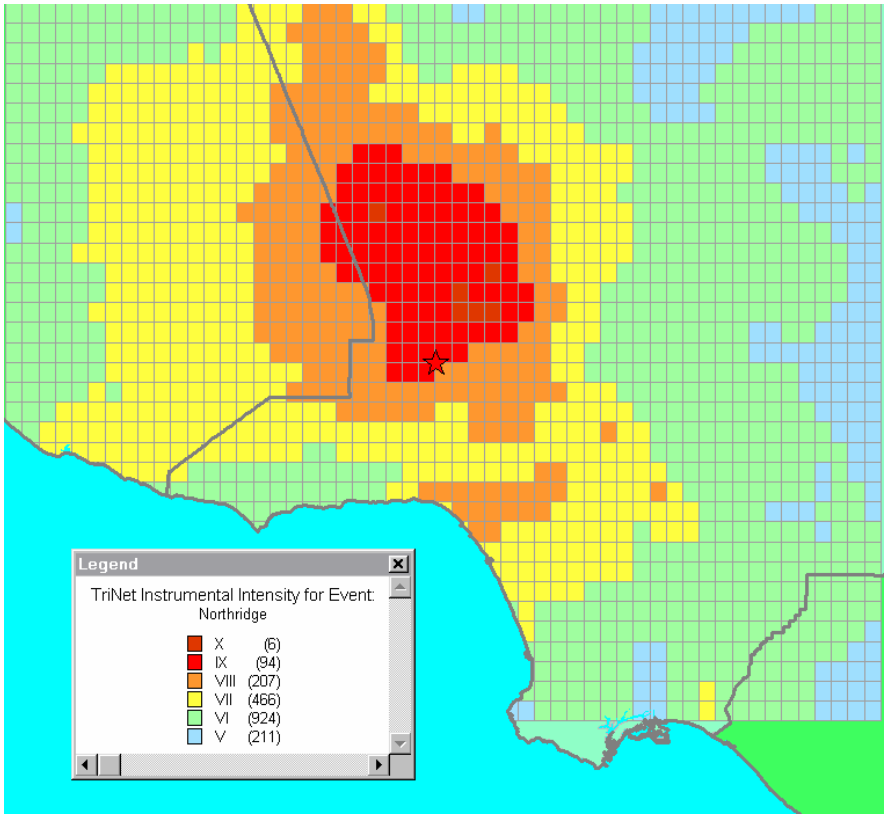

Figure 2-4 TriNet Instrumental Intensity ShakeMap for Northridge: Data Available for Modeling (1999)

Table 2-1 Site Amplification Factors Used in TriNet ShakeMap System (from Borcherdt, 1994)

Period (sec)	Input Rock Peak Ground Acceleration			
	< 15%g	15-25%g	25-35%g	> 35%g
Mesozoic (589 m/sec)				
0.1-0.5	1.00	1.00	1.00	1.00
0.4-2.0	1.00	1.00	1.00	1.00
Tertiary (406 m/sec)				
0.1-0.5	1.14	1.10	1.04	0.98
0.4-2.0	1.27	1.25	1.22	1.18
Quaternary (333 m/sec)				
0.1-0.5	1.22	1.15	1.06	0.97
0.4-2.0	1.45	1.41	1.35	1.29

The peak ground accelerations posted in ShakeMap represent the "maximum" peak ground acceleration from the two horizontal components of an accelerogram. The final interpolated ShakeMap is available in a standardized file format for importing into several loss estimation software programs (e.g., EPEDAT and HAZUS). In future versions of REDARS, the developers plan to build functions to read these file formats as well. The files are available on an anonymous FTP server: *ftp://seismo.gps.caltech.edu/pub/shake/*, and can be downloaded as soon as 5 minutes after an event. Also, TriNet has the ability to "Push," or transmit files automatically to key computers. These computers at key locations such as The California Office of Emergency Services, run loss estimation applications that can produce results based on TriNet ground motions as soon as they are "pushed" to the computers.

There have been several revisions to the "Northridge" ShakeMap ground shaking recordings since its first release on March 17, 1997. These changes have been based on improved interpolation techniques, refined geologic maps, revised amplification factors, and other factors (Dave Wald, personal communication). Additionally, there have been corrections to specific questionable readings from the Northridge earthquake, such as the anomously high ground shaking recorded at the Tarzana site. Recently, the site amplification factors used in "deamplifying" ground motions down to bedrock have been modified to correspond to the NEHRP soil classification system. The depth of the epicenter has also been added to the header file as additional information on the earthquake (see Section 2.2). In ShakeMap 2.4 (released during 2002), the "bias" used in the interpolation scheme has been changed. Dave Wald (USGS) described the bias in personal communication:

> "*The bias used in ShakeMap is a scalar correction ... applied to the predicted empirically-based ground motions used for infilling sparse data areas and for more stable interpolation*."

The release notes (s.dist_2_4) for ShakeMap version 2.4 (December 2002) describe this change in detail:

```
- Fixed a bias problem in grind.
  Because the attenuation curves are only good out to 100km or
  so, we included the bias_max_range parameter, which allowed
  only stations within the specified range to be used in the
```

```
bias calculation. Previously, however, stations beyond this
distance could still be flagged as outliers. The change in
this release is to discontinue the flagging of stations whose
data appear low with respect to the attenuation curve if they
are beyond the bias_max_range Data that are too high are still
flagged as outliers.

This fix does not solve all of the bias-related problems
(particularly those that result from deep earthquakes).
```

Additionally, during this revision, the reference grid by which the data was posted went from 1.5 minutes to 1 minute. Although the spacing of the grids is uniform within a geographic projection, the spacing of the grid depends upon location. In the Los Angeles area, a single 1.5 minute grid cell corresponds to approximately a 2.8 km (North South) by 2.3 km (East West) rectangle. The 1 minute grid cell corresponds to approximately a 1.9 km (North South) by 1.6 km (East West) rectangle.

The impact of these changes on the peak ground accelerations computed for a region is significant, as can be seen in Figures 2-5. Many of the bridges in the San Fernando Valley and around Santa Monica have much lower recorded peak ground accelerations in the newer data set. Figure 2-6 shows PGA values for the two data sets; this figure shows that the overall peak ground accelerations in the newer version is about 15% lower than the previous one, according to the linear regression slope, β=0.8532.

Additionally, TriNet ground motions produce *peak* ground motions, rather than *geometric means* (Wald, personal communication). It is unclear whether the bridge model is based on peak or mean ground motions, but the difference in shaking is approximately 14-15% (Somerville, personal communication). The relationship between ground shaking intensities and REDARS results is examined briefly in Appendix B.

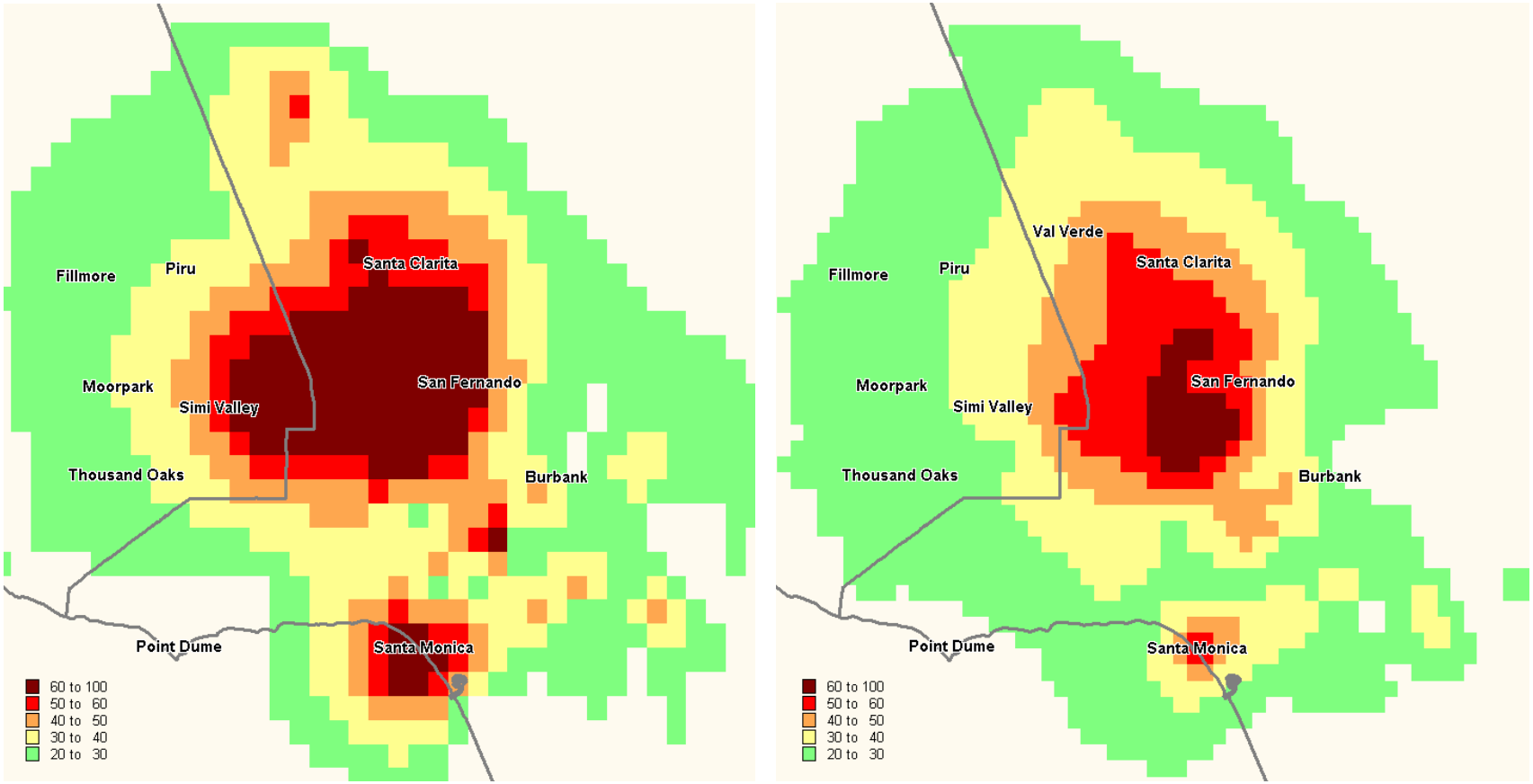

a) Data available on March 1997 **b) Data available on December 2002**

Figure 2-5 TriNet Peak Ground Acceleration (in percent g) ShakeMap for Northridge Earthquake

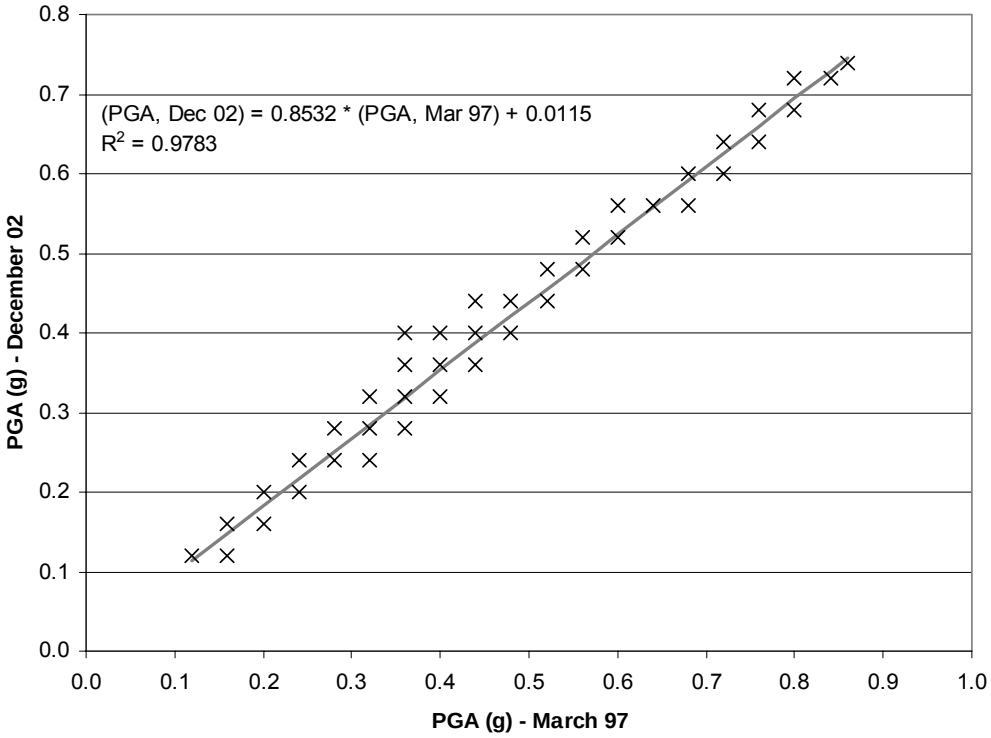

Figure 2-6 Comparison of Northridge TriNet ShakeMap Peak Ground Acceleration Between the March 1997 and December 2002 Versions (7,985 grid points for the study area)

2.2.2 USGS - Open File Report 94-197

Open-File Report 94-197 (USGS, 1994) contains maps of peak horizontal and vertical accelerations, as shown in Figures 2-7 and 2-8. This USGS open file report offers a preliminary account of the ground motion patterns experienced from the Northridge Earthquake. The contours that are presented in Figures 2-7 and 2-8 were developed from the initial instrument readings from the event, and thus include anomalous data, e.g., the Tarzana record. The maps also show zones of different geologic units. The maps are not available in GIS format. Furthermore, the ground motion data from the report does not include spectral acceleration measures, which is the basis of bridge fragility model in Chapter 3. Whenever spectral acceleration measures are required, the procedure in Section 2.3 is applied to estimate.

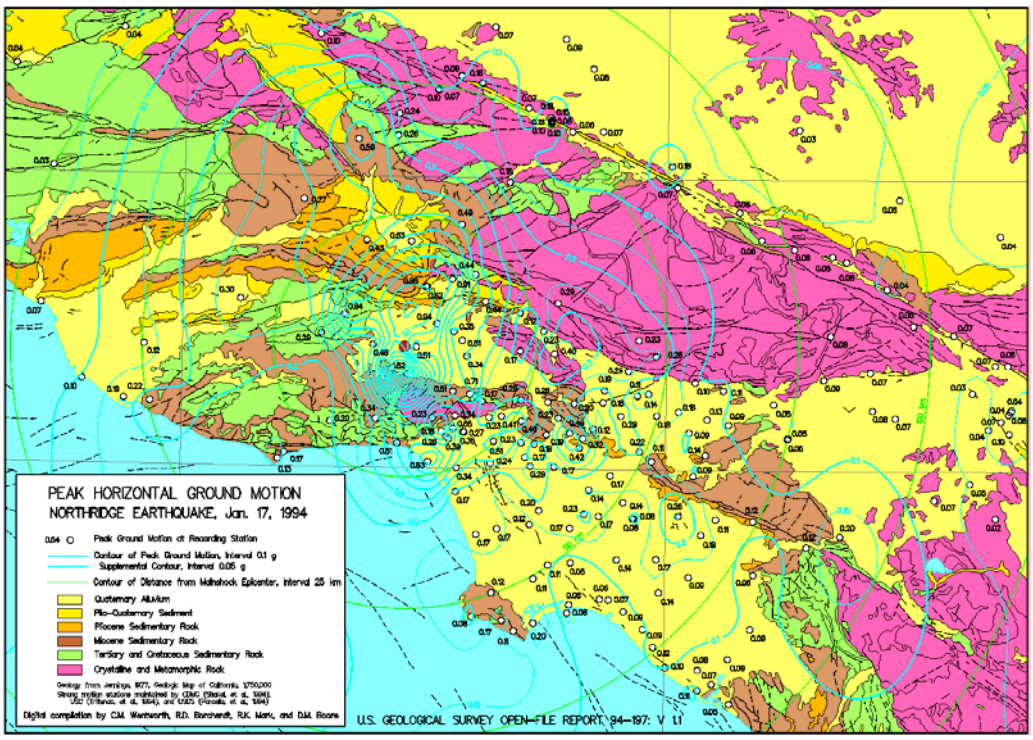

a) Peak Horizontal Ground Shaking

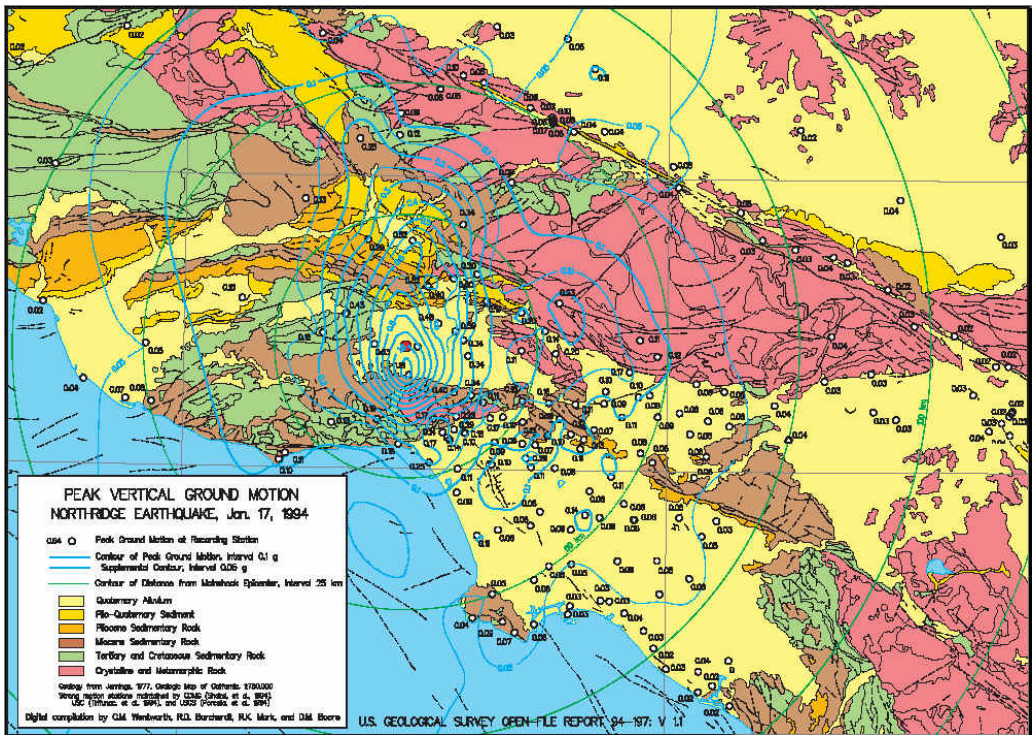

b) Peak Vertical Ground Shaking

Figure 2-7 Peak Ground Shaking from Open File Report 94-197

2.2.3 1996 Ground Shaking Update from Paul Somerville et al.

Somerville, et al., (1996) provides an additional interpretation of the regional ground shaking pattern from Northridge Earthquake.

2.3 Conversion of Peak Ground Acceleration to Spectral Accelerations

Since the bridge fragility functions use spectral acceleration and not peak ground acceleration as an input parameter, it was necessary to convert the peak ground acceleration data discussed earlier into spectral accelerations. Based on recommendations from the American Association of State and Transportation Officials (AASHTO), the conversion equation for spectral acceleration from peak ground acceleration on site class B (Friedland, et al. 2001) is:

$$SA_{0.3\text{sec}} = 2.5 \times PGA \text{ , and} \tag{1a}$$

$$SA_{1.0\text{sec}} = PGA \tag{1b}$$

Peak ground accelerations on any soil type can be derived from a number of different sources, including equations contained in HAZUS 99. According to Equations 4-15, and 4-18, in the HAZUS99 Technical Manual, peak ground acceleration and spectral acceleration at 1.0 second at a site with soil type *i* are:

$$PGA_i = PGA \times F_{Ai}$$

$$SA_{1.0\text{sec},\,i} = SA_{1.0\text{sec}} * F_{Vi}$$

where, F_{Ai}, and F_{Vi} are soil amplification factors for 0.3 second (short period) and 1.0 second (long period), respectively (see Table 4-10 in HAZUS99 Technical Manual). By combining these equations with Equation (1), spectral acceleration and peak ground acceleration for site class *i* has following relationship:

$$\begin{aligned} SA_{1.0\text{sec},\,i} &= [F_{Vi} \ / \ F_{Ai}] \ \times \ PGA_i \\ &= F_i \ \times \ PGA_i \end{aligned}$$

For soil types C and D, which cover most of Southern California, the ratio of the two respective amplification factors, $F_i = [F_{Vi} \ / \ F_{Ai}]$, ranges from 1.1 (when $SA_{0.3\text{sec}} \leq 0.25$, and $SA_{1.0\text{sec}} \geq 0.5$) to 2.4 (when $SA_{0.3\text{sec}} \geq 1.25$, and $SA_{1.0\text{sec}} \leq 0.1$). With soil type E, the ratio increases up to 3.9 (when $SA_{0.3\text{sec}} = 1.0$, and $SA_{1.0\text{sec}} \leq 0.1$).

Since the 1994 Northridge earthquake, spectral accelerations have been published along with peak ground acceleration from TriNet (July 1998, October 1998, March 1999, October 2002, December 2002, and July 2003) and Somerville, et al. (1996). Using these data, it is possible to examine the relationship between PGA and SA for the Northridge earthquake. The validation of ground motion predictions for the Northridge earthquake is not within the scope of this study;

however, it is important to understand on a general level how these different assumptions and model results affect the estimation of bridge damage or fragility.

Peak ground accelerations and spectral accelerations (at three periods, 0, 0.3 and 1.0 second) at 7985 locations were examined using a 500-meter rectangular grid within the study area. Using TriNet data from March 1999 and December 2002, the relationship between spectral accelerations at 0.3 seconds and peak ground accelerations is close to linear with a slope of about 2.5, which is consistent with the AASHTO scaling criteria in Equation 1 above. However, Figure 2.8 also shows that there is not a one-to-one correspondence between spectral accelerations at 1.0 second and peak ground accelerations. Although the relationship between these parameters is linear, spectral accelerations at 1.0 second are about 1.9 times higher than corresponding peak ground accelerations in the two data sets (March 1999 and December 2002). A similar conclusion is found in Somerville, et al. (1996). That is, Somerville found that spectral accelerations at 1.0 second were about 1.7 times higher than corresponding peak ground accelerations, see Figure 2-9.

For Southern California, where soil types are either C, D, or E, these spectral amplification factors also correspond to the AASHTO spectral shape. The relationship between peak ground acceleration and spectral acceleration at 0.3 second in Somerville's (1996) is higher than that found in the TriNet data sets. Figure 2.9 shows that spectral accelerations at 0.3 seconds is more than 5 times higher than corresponding peak ground accelerations. Note that the regression coefficients, R^2, in Figure 2-8 for spectral accelerations at 0.3 seconds and 1.0 seconds are identical. According to the developers of the data, this is because the spectral accelerations for 0.3 second, and 1.0 second are both calculated based on the peak ground velocity, using following equation:

$$SA\left(cm/\sec^2\right) = \frac{2\pi \cdot PGV\left(cm/\sec\right)}{T} \tag{2}$$

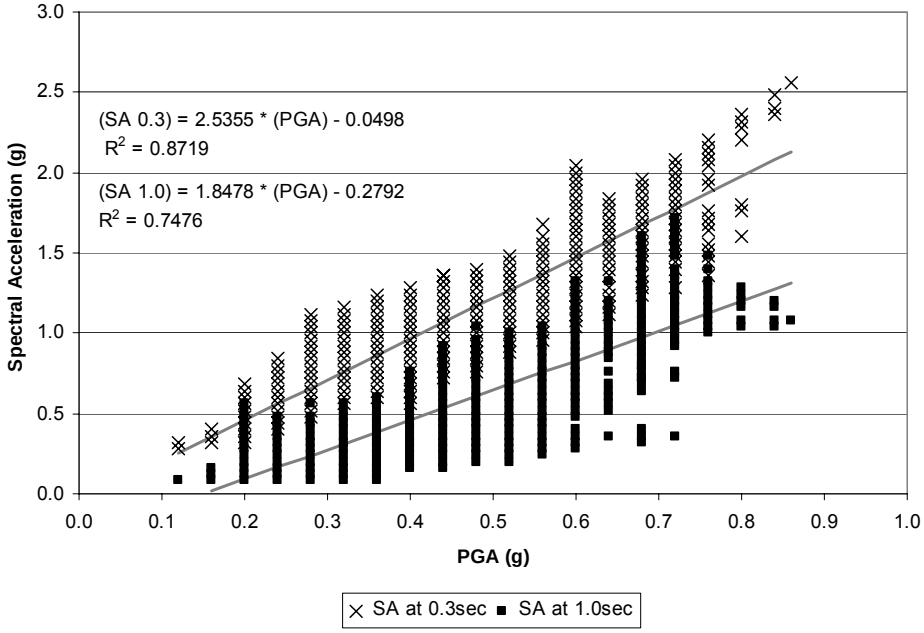

a) March 1997

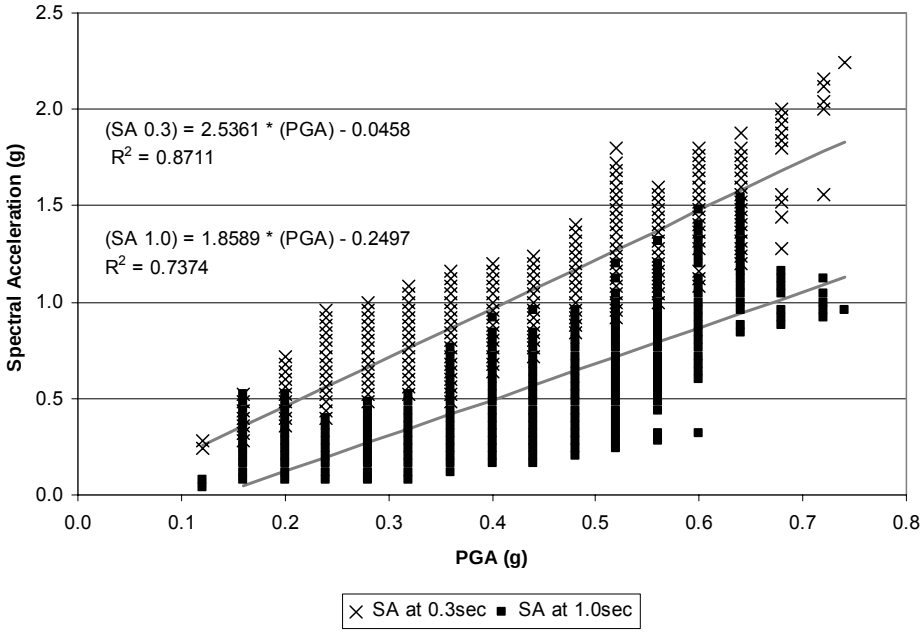

b) December 2002

Figure 2-8 A Comparison of TriNet Peak Ground Acceleration and Spectral Acceleration Data from the 1994 Northridge Earthquake

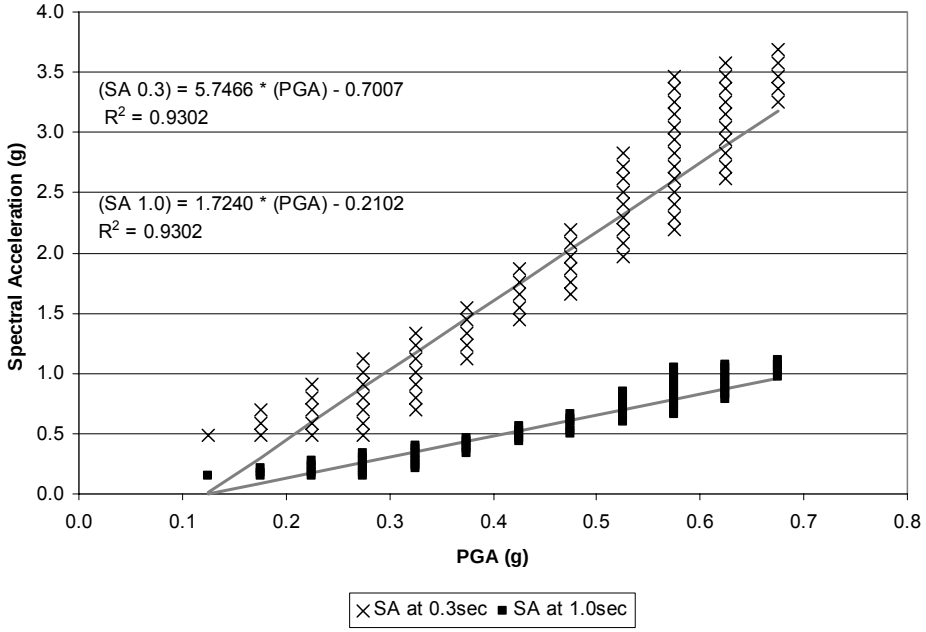

Figure 2-9 A Comparison of Peak Ground Acceleration and Spectral Acceleration Data from 1994 Northridge Earthquake, as Performed by Somerville, et al. (1995)

A similar examination of the USGS ground motion from Open File Report 94-197 was not performed because spectral acceleration data were not provided. Note that Mander's model is based on spectral acceleration. In various reports, the developers of the Mander model stated that they used USGS open file report data as well as information from the Somerville report to validate their model (Basöz and Kiremidjian, 1998; Basöz, and Mander, 1999). Based on this information, and confirmed by personal communication (Basöz, 2003), we have concluded that the original model was validated against spectral accelerations *converted* from peak ground acceleration data. However, as demonstrated above, these data - as well as information reflected in the AASHTO spectral shape - do not support the contention that there is a one-to-one correspondence between peak ground acceleration and spectral acceleration at 1.0 second for 1994 Northridge earthquake.

2.4 Ground Motion used in Validation Study

Throughout this report, the TriNet ShakeMap (March 1999) data are used. At the time this analysis was performed, this was the only digital data set publicly available with spectral accelerations at 1.0 second. The specific file that was used in this validation analysis was downloaded during 1999, and was current as of the initial runs in 2001. The TriNet data was distributed and processed by the EPEDAT loss estimation program. EPEDAT converts the raw ASCII file into a MapInfo geographic table. The ground shaking associated with the grids depicted in Figure 2-4 was then 'spatially joined' to the bridges in the study region through a point-in-polygon process. The ground shaking intensity for each bridge was then exported to Excel, where the site amplification factor was derived using the procedure described in Section 2.3.

The TriNet raw grid 'xyz format' contains the information needed to create the GIS file. The first line, or header file, provides key information on the event:

Name/CUSPID of event	For most events, this is an ID number, if an event is big enough to be named, such as "Northridge", this replaces the ID.
Mag	The Richter magnitude of the event
Epicentral lat	The latitude of the epicenter, datum unknown
Epicentral lon	The longitude of the epicenter, datum unknown
MMM DD YYYY	Date of event
HH:MM:SS timezone	Time of Event
W bound	West bounding longitude of event
S bound	South bounding latitude of event
E bound	East bounding longitude of event
N bound	North bounding latitude of event
Process time	When the file was processed
Location String	An optional description of the location, in this case, also Northridge

The header information from the TriNet file (1999) for the Northridge earthquake is:

```
Northridge 6.7 34.213 118.5357 JAN 17 1994 04:30:55 PST -119.175
33.775 -117.875 34.65 (Process time: Tue Mar 16 15:35:04 1999)
```

The header is followed by the attribute data:

Longitude of a given posting
Latitude of a given posting
Peak Ground Acceleration in % g
Peak Ground Velocity in cm/sec
Instrumental Intensity
Spectral acceleration at 0.3 s period, 5% damping in cm/sec
Spectral acceleration at 1.0 s period, 5% damping in cm/sec
Spectral acceleration at 3.0 s period, 5% damping in cm/sec

The reference datum used is the World Geodetic System 1984 (WGS-84). The increment and number of postings was not given in the header; these values were computed from the data.

2.5 Calculation of the Soil Amplification Factor

In general, surface ground motions at a site are estimated by applying soil amplification factors to bedrock ground motions. The effect of soil amplification is already included in published ground motion data, since surface ground motions are usually reported. However, to implement the REDARS methodology, a soil amplification factor is required to estimate the bridge damage state even though surface ground motion data are available. Furthermore, the TriNet methodology provides an estimate of the ground motion at the site using an arbitrary soil type, not at bedrock. Because of this, it is necessary to back-calculate the soil amplification factor

from the estimated surface ground motion. The reason for this step is to estimate the structural capacity of the bridge to given level of ground motion (See Appendix F of Werner 2000 for detailed capacity calculation). The following discussion explains the method used to estimate the Soil Amplification Factor (SAF) that corresponds to the estimated TriNet surface ground motion.

The surface ground motion is estimated by multiplying the bedrock shaking intensity by the soil amplification factor that corresponds to local soil type (Technical Report MCEER-00-0014). The soil amplification factor varies with soil type, as shown in Tables 2-2, and 2-3 for acceleration at 0.3 second and 1.0 second, respectively.

Table 2-2 Site Amplification Factors Used in HAZUS for 0.3 second (short period)

NEHRP Site Condition	Modified Peak Rock Acceleration, $(PRA)_B$				
	≤ 0.1 g	0.2 g	0.3 g	0.4 g	≥ 0.5 g
A	0.8	0.8	0.8	0.8	0.8
B	1.0	1.0	1.0	1.0	1.0
C	1.2	1.2	1.1	1.0	1.0
D	1.6	1.4	1.2	1.1	1.0
E	2.5	1.7	1.2	0.9	0.6

Table 2-3 Site Amplification Factors Used in HAZUS for 1.0 second (long period)

NEHRP Site Condition	Modified Peak Rock Acceleration, $(PRA)_B$				
	≤ 0.1 g	0.2 g	0.3 g	0.4 g	≥ 0.5 g
A	0.8	0.8	0.8	0.8	0.8
B	1.0	1.0	1.0	1.0	1.0
C	1.7	1.6	1.5	1.4	1.3
D	2.4	2.0	1.8	1.6	1.5
E	3.5	3.2	2.8	2.4	2.0

Since SAF is a function of the bedrock ground motion, the surface ground motion, y, at the site can be represented as follows:

$$y = SAF \times Peak\ Rock\ Acceleration \tag{3}$$
$$= \left[y_2 - \frac{y_1 - y_2}{x_1 - x_2} \cdot (x_2 - x) \right] \cdot x ,$$

where, x is peak rock acceleration (= peak ground acceleration at bedrock), x_1, x_2 are the lower and upper bounds of the PGA bin ($x_1 \leq x < x_2$) in Table 2-2, for the short-period case (0.3 second), and Table 2-3 for long-period case (1.0 second). Note that y_1, y_2 correspond to x_1, x_2, respectively in the tables. The bracket in the equation, [ ] represents a linear interpolation of the SAF according to the table. By solving the quadratic equation, peak rock accelerations are obtained, and by applying it to the tables we calculate the corresponding SAF.

For example, if a bridge built on top of soil type E experiences 0.91g of surface ground motion (e.g., long period, 1.0 second), the product of the peak rock acceleration and the SAF should generate a surface ground motion of 0.91g. By replacing the unknown SAF using linear interpolation, the equality is as follows:

$$0.91 = \left[y_2 - \frac{y_1 - y_2}{x_1 - x_2} \cdot (x_2 - x) \right] \cdot x$$

$$\frac{y_1 - y_2}{x_1 - x_2} \cdot x^2 + \left[y_2 - \frac{y_1 - y_2}{x_1 - x_2} \cdot x_2 \right] \cdot x - 0.91 = 0$$

$$a \cdot x^2 + b \cdot x + c = 0, \text{ where} \qquad (4)$$

$$a = \frac{y_1 - y_2}{x_1 - x_2},\ b = y_2 - \frac{y_1 - y_2}{x_1 - x_2} \cdot x_2,\ c = -0.91$$

The upper and lower peak rock acceleration values in each bin determine the coefficients of Equation (4). For example, in Table 2-4, the fourth column pertains to peak rock accelerations ranging from 0.3g to 0.4g, and the coefficients of Equation (4), according to the bin are 4, -4, and -0.91 for a, b, and c, respectively. Solving the equation, we get a bedrock motion that should lie within the peak rock acceleration bin. In this example, a bedrock motion of 0.35g in the bin of 0.3~0.4g is the only relevant solution, as all the other solutions of the peak rock accelerations (see Table 2-4) are beyond the corresponding bins. Once we solve Equation (4) and obtain the bedrock motion, we can calculate the SAF. In this example, the SAF is calculated as 2.6 (0.91 / 0.35). This SAF estimation method is used throughout the analysis.

Table 2-4 Sample Calculation of Bedrock Motion from Surface Motion Data

	Peak Bedrock Ground Acceleration					
PGA Bin	≤ 0.1 g	0.1~0.2 g	0.2~0.3 g	**0.3~0.4 g**	0.4~0.5 g	≥ 0.5g
x_1	0.0	0.1	0.2	0.3	0.4	0.5
x_2	0.1	0.2	0.3	0.4	0.5	1
y_1	3.5	3.5	3.2	2.8	2.4	2
y_2	3.5	3.2	2.8	2.4	2	2
a	0.0	3	4	4	4	0
b	-3.5	-3.8	-4	-4	-4	-2
c	-0.91	-0.91	-0.91	-0.91	-0.91	-0.91
Estimated PRA	0.26	0.946	0.65	0.65	0.65	0.455
	-	0.32	0.35	**0.35**	0.35	-

In summary, this section summarized the Northridge earthquake ground motion data used in this study to validate the bridge damage functions. As discussed, there are several versions of these data available. For purposes of our validation, however, we used the TriNet data of March, 1999.

SECTION 3
BRIDGE FRAGILITY MODEL

3.1 Introduction

This section describes the REDARS bridge fragility model, and compares its results to bridge damage states observed following the 1999 Northridge earthquake. In this section, the REDARS and Mander's theoretical models are examined separately to identify any possible discrepancy in implementation. The section includes the following sections:

- In Section 3.2, the theoretical Mander's model is briefly reviewed, and compared to REDARS through a controlled experiment. Since real-life data includes a lot of variation, the controlled experiment shows this comparison absent of these data uncertainties or variations.
- In Section 3.3 Mander's model is compared to REDARS once again, but observed ground motion data based on TriNet (March 1999) is applied to the models in this section.
- Section 3.4 documents the validation exercise in full, comparing results from the REDARS model with fragility curves derived from the observation data. There should be discrepancy of REDARS bridge fragility from observation generated, and where available, this is discussed.
- In Section 3.5, REDARS is tested with a linear scale factor to ground motion input to test the sensitivity to the perturbed ground motion input.
- Section 3.6 summaries this section.

A bridge fragility model estimates the damage state of a bridge for a given level of ground motion. A set of fragility curves portrays the aggregated probabilities of being damaged to certain damage states (or higher) for sample bridges within the study area. Since REDARS was developed for region-wide application of the bridge fragility model, validations via fragility curves is more relevant than comparison of individual damage states. In this study, the following sets of bridge fragility curves are generated from a sample of 940 bridges in the Los Angeles study area:

- REDARS model: Mean value of fragility, calculated by applying REDARS SRA method presented in Appendix A to generate multiple simulations for each bridge.

- Mander model: Theory-based curves. The model was originally validated with respect to the Loma Prieta and Northridge earthquakes, and serves as an independent check for REDARS results.

- Observation: A set of fragility curves developed for REDARS validation purposes, using observed damage states and TriNet spectral acceleration at 1.0 second intervals.

As mentioned in Section 2, it is important to note that the evaluation of bridge fragility was performed using a custom version of the model. The central US ground motion model employed by the original pre-beta version of REDARS is not applicable to study sites in the western US. Consequently, testing the model performance for the 1994 Northridge scenario requires external ground motion data. Difficulties inputting this external ground motion dataset required the use of an externally programmed version of the SRA method (hereafter termed the 'REDARS model'). Again, TriNet ground motion data released in March, 1999 is used through out the analysis.

3.2 Experimental Comparison Between REDARS and the Mander Models

This section provides a brief overview of the theoretical background of Mander's bridge fragility model. It is then compared to REDARS through a controlled experiment. The purpose of this experimental comparison is to verify if Mander's theoretical model was implemented correctly in REDARS.

3.2.1 Theoretical Background

The REDARS bridge fragility model is based on the Rapid Pushover method (Dutta and Mander, 1998), which was modified by Basöz, and Mander (1999) to ensure compatibility with the National Bridge Inventory (NBI) database and HAZUS 99. The rapid pushover method is a probabilistic model of bridge fragility for a given spectral acceleration.

Equation (5) is a generalized form that represents the probability of damage for any bridge structure. Spectral acceleration (SA) is x, the probability of being in damage state i (d_i) or higher, follows a log-normal distribution (Φ) over spectral acceleration (SA), with a dispersion factor β, and median PGA value (A_i) that corresponds to damage state i. The median PGA value represents the probability of damage (or resistance capacity) for different bridge types at a given level of ground shaking. Elsewhere, Dutta and Mander (1998) employ the Rapid Pushover model to estimate the strength of a bridge, by considering its structural characteristics.

Median PGA, A_i was validated (but not calibrated) by the developers of the Mander model using observed damage states and ground motion levels for the 1994 Northridge and 1989 Loma Prieta earthquakes (see Basöz and Mander, 1999).

$$P(d_i \mid SA = x) = \Phi\left(\frac{1}{\beta} \cdot \ln\left(\frac{x}{\overline{A_i} \cdot K_{3d} \cdot K_{skew} / SAF}\right)\right) \tag{5}$$

where β is the constant dispersion factor

$\overline{A_i}$ is the standard median PGA for damage state i and corresponding bridge structure.

K_{3d}, K_{skew} are coefficients for 3-dimentional effect and skew effect

SAF is the on-site soil amplification factor

x is spectral acceleration normalized to gravitational acceleration

3.2.2 Experiments to Compare REDARS and Mander Models

To compare and contrast the response pattern resulting from the REDARS and Mander fragility curves, theoretical curves for a sample bridge were computed under controlled conditions. These fragility curves *should* be identical, since they are both based on Equation (5). However, differences may arise because the Mander model is basically a stochastic model to estimate the probability of damage for a given bridge structure under on-site conditions, and produces continuous cumulative probability density curves. REDARS instead estimates the damage state for individual bridges in a pseudo-stochastic way by incorporating a random variable. Therefore, the purpose of this test is to verify if REDARS follows the probability distribution given by Equation (5). To compare these, bridge damage states from REDARS are converted to a probability distribution.

For comparison, the most common bridge type is selected from the 940 sample bridge data (see Table 3-1), which is using the following parameters:

- Bridge type = 2 (conventionally designed, multi-span bridge)
- Soil type = B (bedrock)
- Median PGA values assumed according to the bridge type = 0.35g for minor damage, 0.42g for moderate damage, 0.50g for major damage, and 0.74g for collapse.

The Mander model was applied, with the given parameters, to develop fragility curves over continuous spectral acceleration input. The REDARS model was also applied 2^{16} (65,535) times to a bridge with the same parameters over continuous spectral acceleration input, and then damage probabilities were calculated for each of the spectral acceleration bins.

Overlaying the resulting REDARS and Mander fragility curves for damage state 5 (collapsed) in Figure 3-1, reveals a number of discrepancies. When the ground motion (spectral acceleration) is higher than 0.3g, the two curves differ by a margin of 12.6%. Minor differences are evident in curvature and the inflection locations (location along the curve where the second derivative is equal to zero). These variations are due to differences in the implementation of uncertainty.

As shown in Equation (5), Mander fragility behaves as a cumulative lognormal distribution. However, based on the implemented REDARS SRA (Appendix A), REDARS produces a distribution that can be best described as a normal-exponential distribution. More precisely, Step 10 of the implementation process in Appendix A modifies the bridge spectral capacity to a random variable *X*. The exponent of *X*, which follows standard normal distribution, modifies the capacity as follows:

$$\begin{aligned} \textit{Capacity } C_i'' &= \exp\left(\ln(C_i') + 0.35 \cdot X\right) \\ &= C_i' \cdot \exp\left(N(0, 0.35)\right) \end{aligned} \tag{6}$$

where C'_i = site-specific median PGA (A_i * K_{3D} * K_{skew}),
X = random variable $N(0,1)$

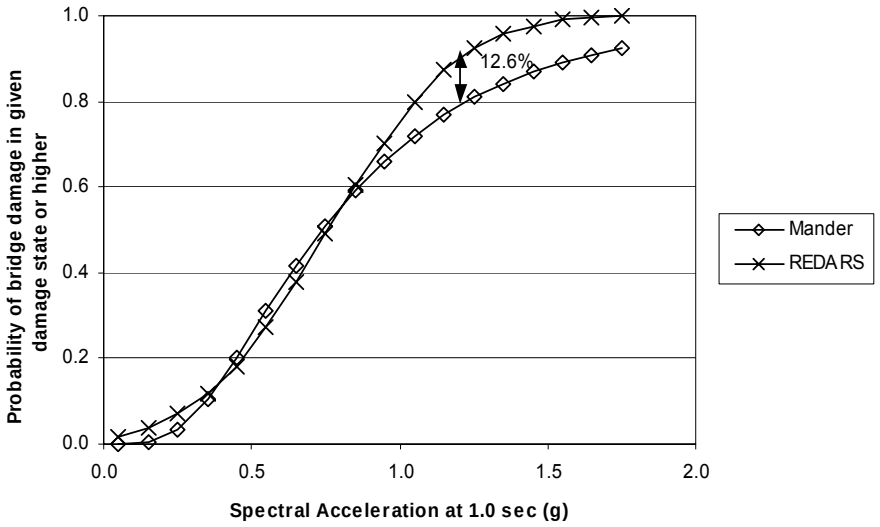

Figure 3-1 Graphical Comparison Between REDARS and Mander Fragility Curves (Bgroup2, Soil 5, DS5)

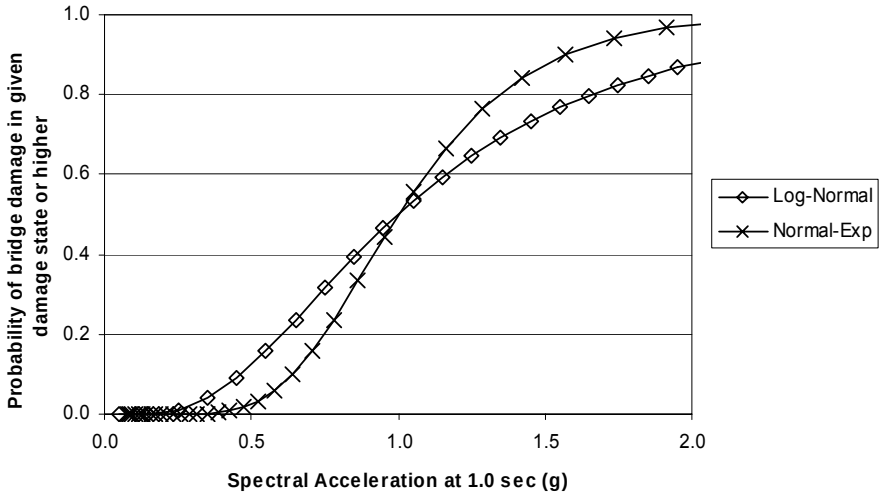

Figure 3-2 Log-Normal (Mander model) and Exponential of Normal (REDARS Model) Probability Distributions

Plotting lognormal and normal-exponential distribution curves in Figure 3-2 depicts these differences, and exaggerates the offset in distribution between the Mander and REDARS fragility curves.

In addition to variation in distribution, the REDARS model shows steeper fragility curves. Steepness of probability distribution is related to the measure of uncertainty (random) effects in the probability calculation. As an extreme case, if no uncertainty is implemented, REDARS would estimate either no damage, or damage from all the bridges depending on the ground motion. In this example case, fragility curves would be distributed stepwise. The probability

discontinuously jumps from 0 to 1 at the point that spectral acceleration is the same as the median PGA, and the slope (steepness) of the curve is infinite. In general, a stochastic event that has less uncertainty, has steep distribution, and the fragility curve generated from REDARS is the case. The uncertainty factor of 0.35 in Equation (6) might be responsible for the differences illustrated in Figure 3-1.

A simple sensitivity test reveals that increasing the uncertainty factor from 0.35 to 0.60 produces a set of fragility curves that is almost identical to the Mander fragility curves. Figure 3-3 shows the area surrounded by Mander and REDARS fragility curves. The area is reduced as the uncertainty factor approaches to 0.6. This suggests that the shape of the REDARS curve is particularly sensitive to the uncertainty factor, and that an uncertainty factor of 0.60 might produce an optimal fit with the Mander result.

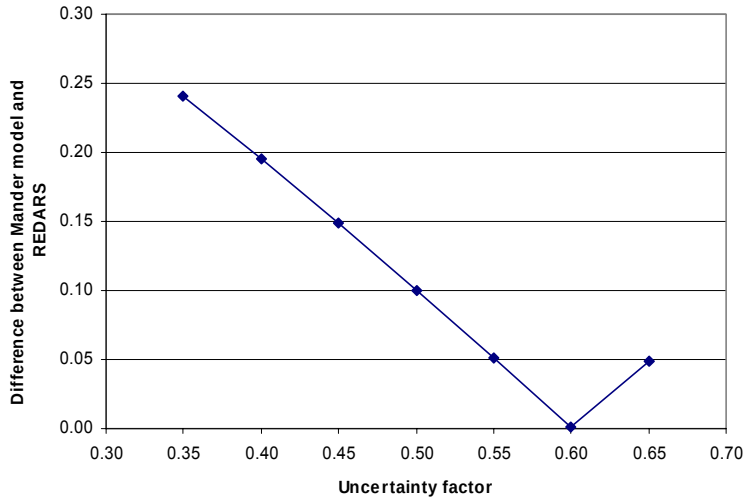

Figure 3-3 Area Between Mander and REDARS Fragility Curves

3.3. Comparison between REDARS and Mander Models Using TriNet (March, 1999) Observed Ground Motion Data

In the previous section, the REDARS fragility model was compared to Mander's in controlled experiments (with only one bridge type). This section provides a detailed comparison between the REDARS model and the Mander model developed from 940 sample bridge data in the Los Angeles area with TriNet ground motion data (March 1999) from the 1994 Northridge earthquake.

The following sections present detailed procedures involved in the development of fragility curves, first using the REDARS model, and second, through an empirical approach employing a locally calibrated version of the Pushover Method (Equation 5), termed the Mander model. A comparison is drawn between fragility curves developed using the Mander and REDARS model, which based on the same Northridge datasets, should theoretically produce the same response.

3.3.1 Development of Fragility from the REDARS Model

The custom Excel spreadsheet-based REDARS SRA methodology was used to develop a set of fragility curves for the 940 bridges within the Los Angeles study area. A set of 217 simulations (an arbitrarily selected number) were performed based on the TriNet (March, 1999) ground motion data for the Northridge earthquake, resulting in 217 estimations of bridge damage state for each bridge. For each spectral acceleration bin, the number of structures recording damage states 1 to 5 was counted. The probability of damage for a spectral acceleration bin and a particular damage state was then calculated as the ratio of the number of damaged bridges in a damage state to the total number of bridges in the bin. The mean probability of damage (by damage state and spectral acceleration bins) for the 217 simulations was used to generate the fragility curves. Figure 3-4 shows the fragility curves developed from the REDARS model.

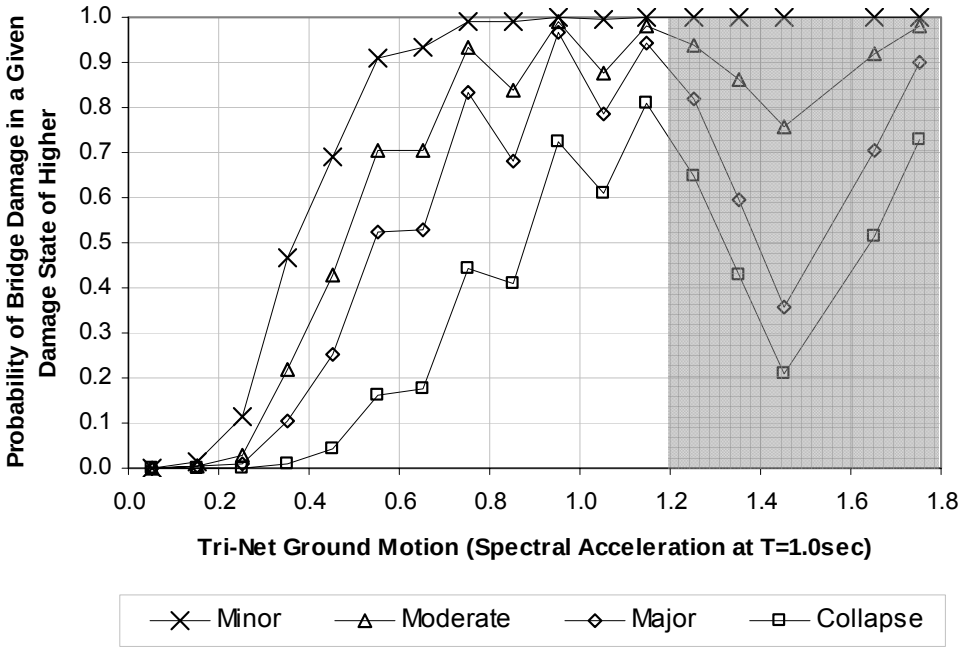

Figure 3-4 REDARS Fragility Curve for Bridges in Study Area

The REDARS fragility curves exhibit an irregular form over the full range of spectral acceleration values. Uncertainty in the ground motion data contributes to this irregularity, together with the geographically uneven distribution of bridges, bridge types, and soil. In order to compare results from the REDARS and Mander approaches (in Section 3.3.4), REDARS output for a subset of the 940 bridges were fitted to continuous curves. This subset included bridges with a spectral acceleration less than 1.2g, therefore 109 structures exposed to spectral accelerations greater than 1.2g were excluded (shaded area in Figure 3-4). Of the possible simplistic curves such as polynomial or exponential, the logistic form in Equation (7) offered a best fit. While the logistic function closely presents sigmoid curve of cumulative lognormal

distribution, other functions were found to distort the original distribution characteristics and generate lower correlation coefficients.

$$\bar{y} = \frac{1}{1 + \exp(\bar{\alpha} + \bar{\beta} \cdot x)} \tag{7}$$

where x is spectral acceleration normalized to the gravitational acceleration g,
$\bar{\alpha}, \bar{\beta}$ are estimated coefficients from the curve fitting process.

It is important to note that the purpose of curve-fitting using a form other than log-normal distribution is not to recalibrate REDARS fragility onto the logistic model, but to display the difference from the continuous curves generated by the Mander model. Since these functions are particularly sensitive in terms of inflection point location, where the convex part of a curve changes to concave, it is easy to visually compare the two sets of fragility curves by overlaying them.

3.3.2 Development of Mander Fragility Curves

The same sample bridges that were simulated for the REDARS fragility model were also used to compute Mander fragility curves, based on the empirical model developed by Dutta and Mander (1998) following the Northridge earthquake.

Based on the median PGA that was validated by Basöz and Mander (1999), fragility curves of five different damage states were generated for each of the 940 sample bridges. Table 3-1 categorizes the different design characteristics of the bridges in the study area, with a corresponding median PGA value, A_i for each damage state. For a given spectral acceleration x, the probability of being in (or higher) than a given damage state i, is calculated according to Equation (5). These curves were then aggregated by damage state, using the mean probability values in each of spectral acceleration bins. Figure 3-5 shows developed fragility curves from Mander model.

Table 3-1 Bridge Type Composition and Corresponding Median PGA

Design specification	Bridge group	Number of bridges In sample	Median PGA*			
			DS2	DS3	DS4	DS5
Conventional	1	297	0.33	0.46	0.56	0.83
	2	409	0.35	0.42	0.50	0.74
Seismic	1	50	0.45	0.76	1.05	1.53
	2	7	0.54	0.88	1.22	1.45
	3	9	0.91	0.91	1.05	1.38
	4	60	0.91	0.91	1.05	1.38
	5	105	0.80	0.90	1.10	1.60
	6	3	0.60	0.80	1.00	1.60

*Source: Stu Werner et al. (2000) 189-190

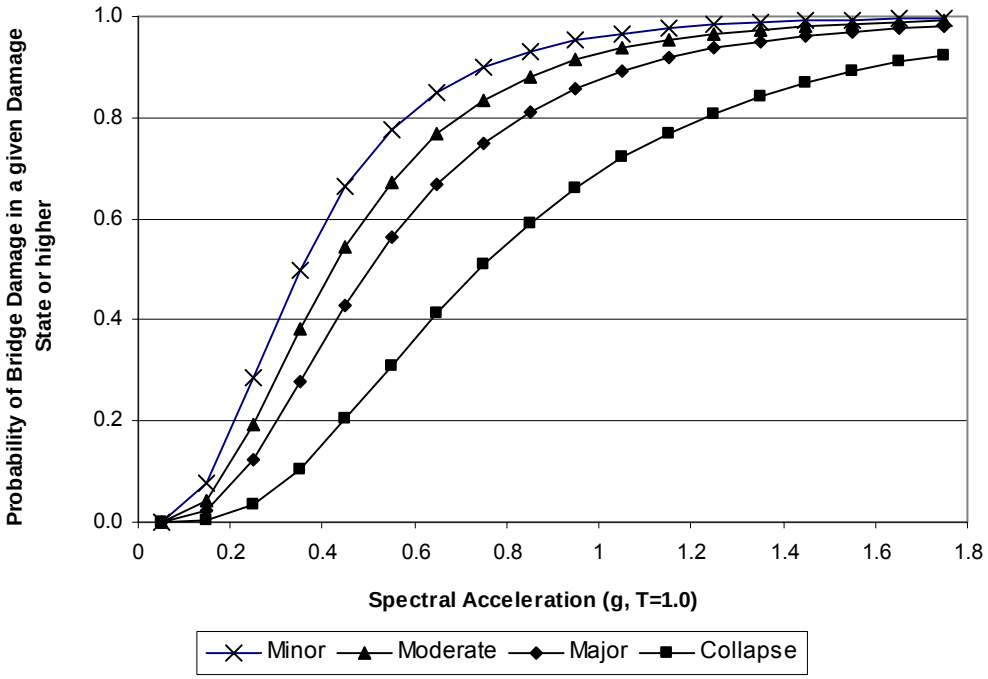

Figure 3-5 Mander Fragility Curves for 940 Bridges in the Study Area

3.3.3 Comparative Analysis

This section compares the bridge damage curves generated by the REDARS and Mander models above. The Mander model is validated with data from the Northridge and the Loma Prieta earthquakes. Providing the methodological procedures employed by REDARS are accurate and reliable, results should correspond closely with those from the empirically based Mander approach.

The offset between the Mander and REDARS fragility ranges from ± 30% of the cumulative probability (fitted using a logistic curve). As shown in Figure 3-6, the difference between the curves for DS 2 (Minor) is less than ± 10%. However, for collapsed bridges (DS 5), REDARS estimates a 30% higher probability than the Mander model. This implies REDARS is likely to overestimate the number of damaged bridges, or damage states for higher levels of ground shaking.

The experimental comparison in Section 3.2 is consistent to this finding of overestimation with higher level of ground motion. A steeper distribution of damage probability can be interpreted as indicating more damaged bridges. Statistical comparison on similarity between the curves is not relevant because it is obvious that the mathematical presentations of the fragility are not identical (lognormal and logistic curves). Also, returning to the methodological procedures employed by the Mander and REDARS approaches, the former method generates the probability of bridge damage, while the latter estimates individual bridge damage states, which are subsequently converted to a probability value. In spite of the obvious discrepancies, the two sets of curves still show the difference that has been established through Figure 3-1, and 3-2. In addition, as shown by Figure 3-3, a low uncertainty factor might be responsible for the difference.

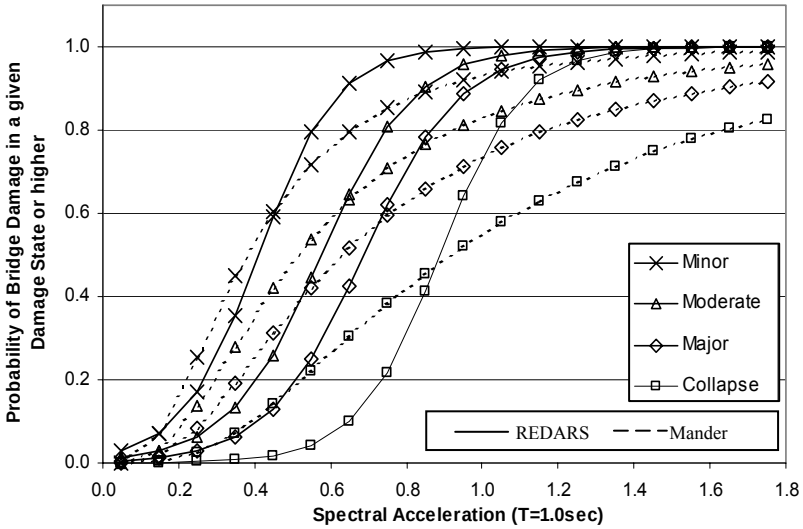

Figure 3-6 Comparison of the REDARS and Mander Fragility Curves Developed Based on TriNet (March, 1999)

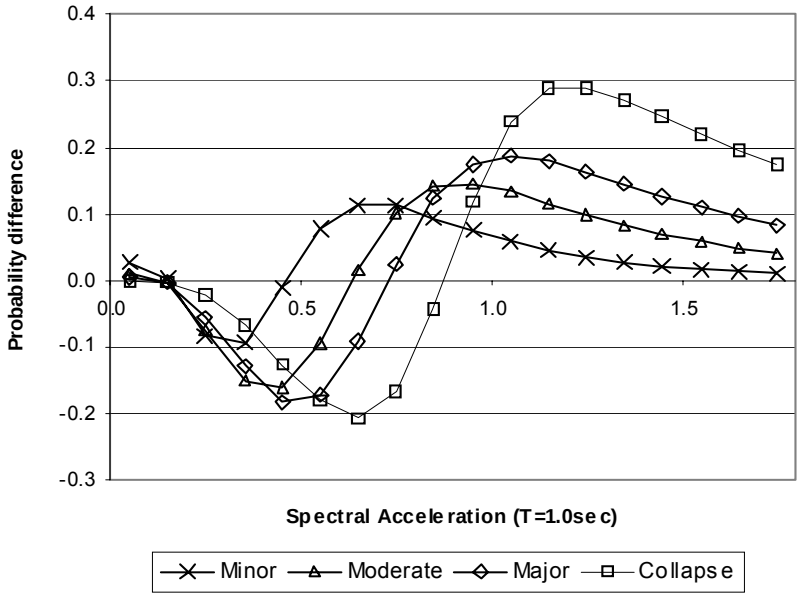

Figure 3-7 Cumulative Probability Difference Between the REDARS and Mander Fragility Curves Developed Based on TriNet (March 1999)

3.4 Comparison between REDARS and Observation

This section validates the REDARS bridge fragility model, with observed data. The locations of the 940 sample bridges are compared with the observations in Section 3.4.1. Then fragility curves from the observed data and REDARS model are compared. Methodological issues relating to the development of observation-based fragility curves are discussed in Section 3.4.2. The respective fragility curves are then compared in Section 3.4.3, to determine consistencies and differences between the sets of results. Section 3.4.4 offers some discussion of the discrepancies between the curves.

3.4.1 Comparison between the REDARS Deterministic Model with Observation

In REDARS, the deterministic analysis method was applied with the TriNet ground motion data (March, 1999) for the 1994 Northridge earthquake using 940 sample bridges in the Los Angeles area. Since no uncertainty effect is considered, the result from a deterministic analysis represents a mean value of the probability of bridge damage.

The results from the deterministic analysis indicate that REDARS overestimates bridge damage states, not only with regard to the frequency of damaged structures, but also in terms of the severity of damage. 190 of the bridges included in this study were actually damaged during the 1994 Northridge earthquake. However, the REDARS methodology predicts damage to 365

structures. While only seven bridges collapsed following the Northridge earthquake, REDARS estimates a much higher occurrence of 105. As shown in Figure 3-11a, REDARS further estimates that all bridges within the study area would sustain at least minor damage for ground shaking levels of 0.8g spectral acceleration at 1.0 second intervals (SA1.0). During the actual event, similar bridge damage states were observed at much higher levels of shaking: most bridges that experienced more than 1.5g at SA1.0 level sustained at least minor damage.

Table 3-2 REDARS Estimated and Observed Number of Damaged Bridges from 1994 Northridge Earthquake

	DS2 Minor	DS3 Moderate	DS4 Major	DS5 Collapse	Total Damaged Bridges
REDARS result (Deterministic)	91	72	98	102	363
Observation	70	78	35	7	190

Figure 3-8c, d draws a visual comparison between results from the REDARS model and observations of bridge damage, from which the following observations can be made:

- Bridges around I-10 and I-405 intersection are categorized as severely damaged in both the REDARS and the observed data. Although this location is relatively far from the epicenter, local conditions such soil type were effective in the REDARS estimation process.

- Second, severely damaged bridges were widely distributed following the Northridge earthquake. Together with two concentrated damage locations around intersection of I-405 and I-10, and around the intersections of I-405, SR-118, and I-5 (see Figure 3-8a), REDARS predicts severe bridge damage (damage state DS 4 or higher) at several other intersections, including: the I-5 and SR-134; and US101 and SR-170.

- Lastly, the REDARS predictions include most of the bridges where damage was observed. However, the predicted number is much higher than observed.

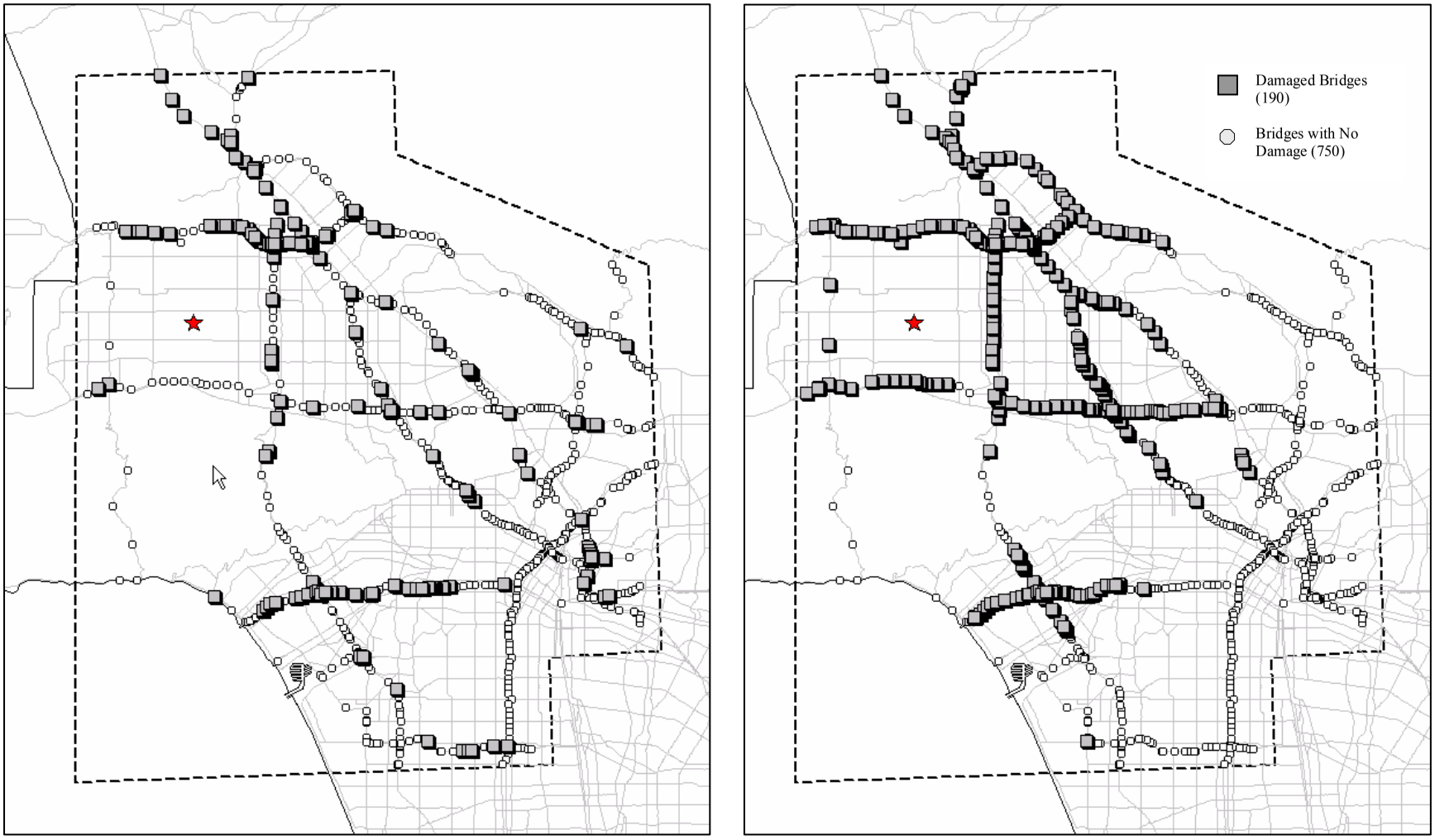

a) Observed Damage in Northridge **b) REDARS Estimated Damage (TriNet data)**

Figure 3-8 Comparison Between Observed and Estimated Damage Due to Ground Shaking

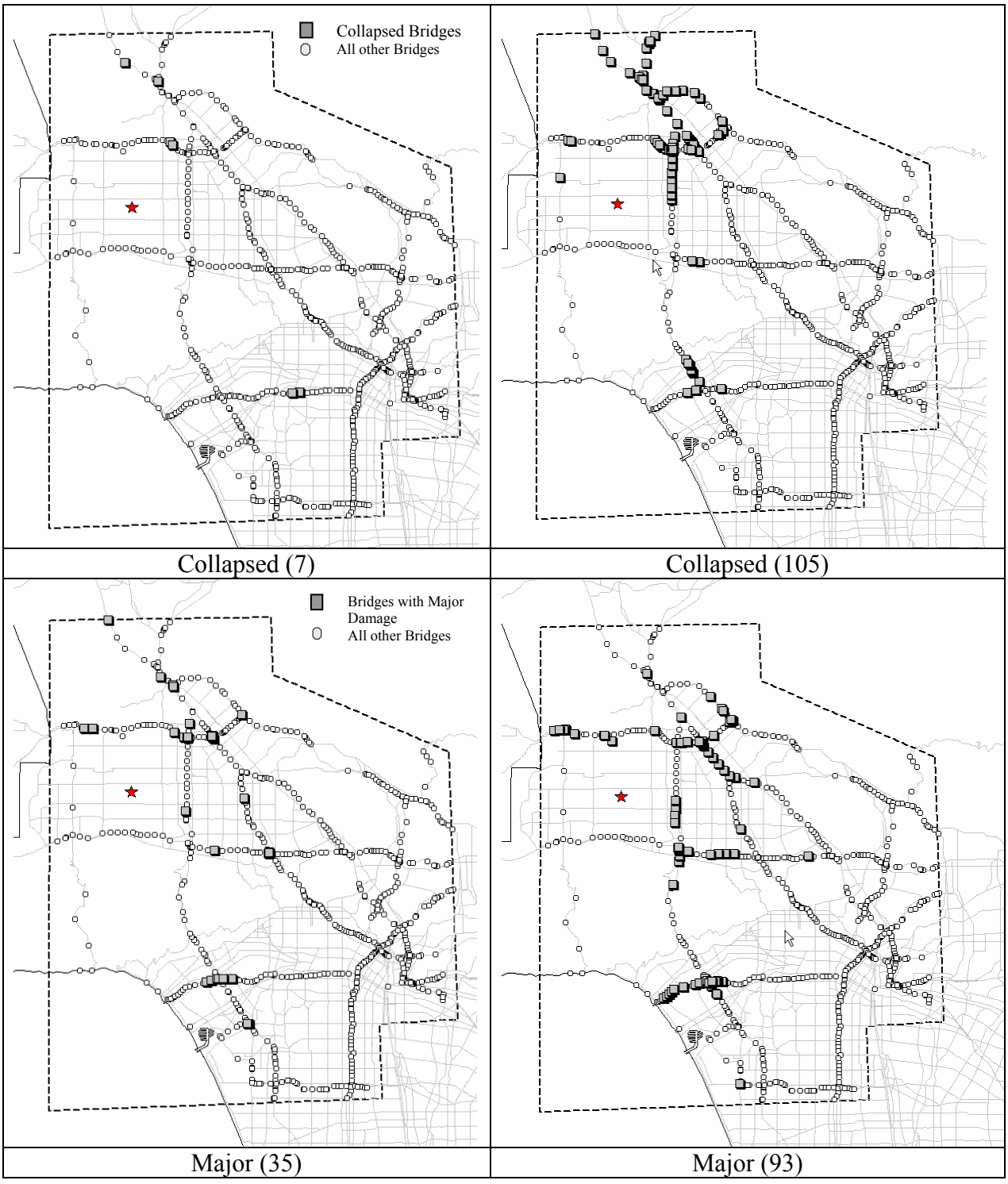

c) Observed Damage in Northridge **d) REDARS estimated Damage (TriNet data)**

Figure 3-8 Comparison Between Observed and Estimated Damage Due to Ground Shaking (continued)

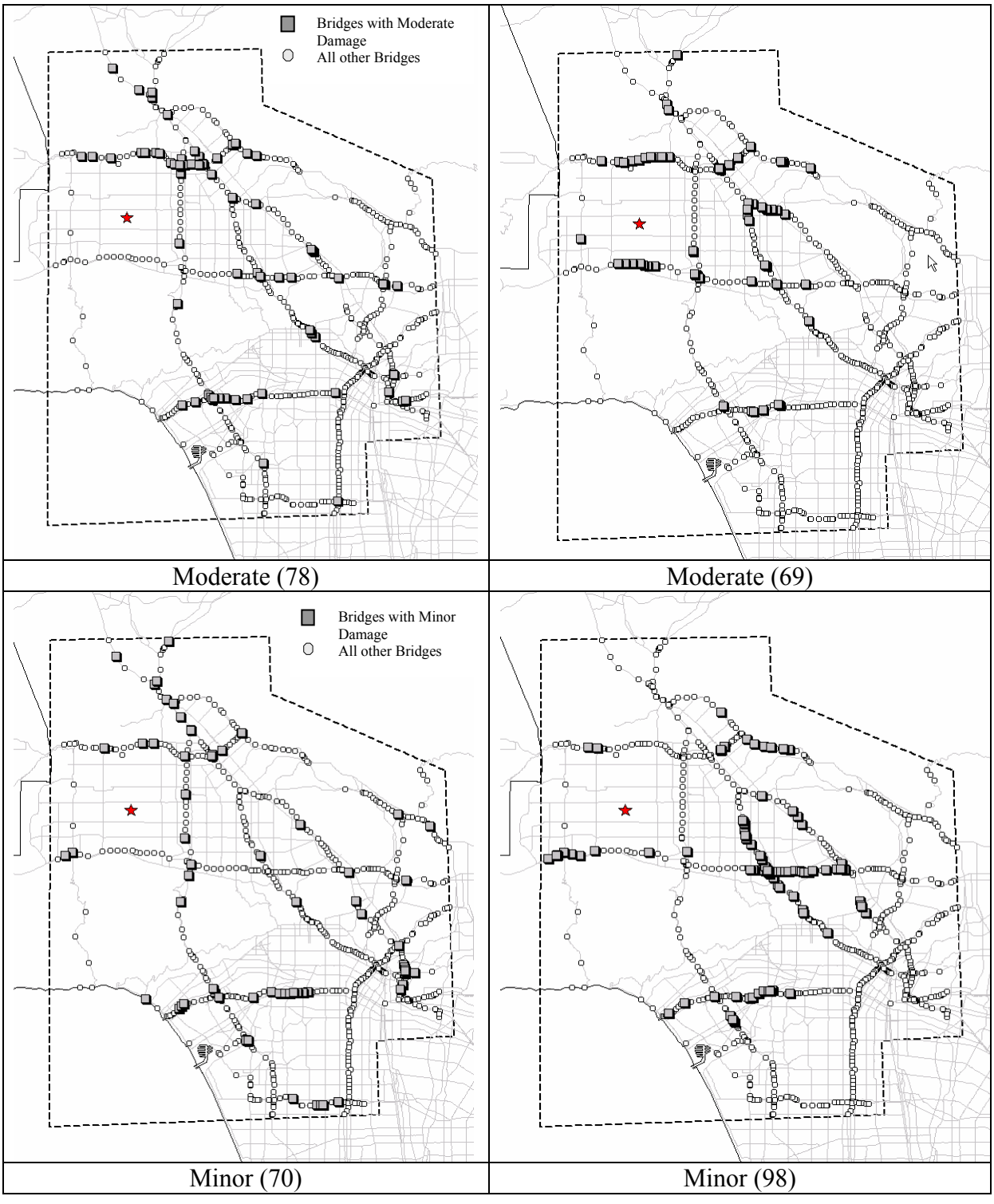

c) Observed Damage in Northridge **d) REDARS estimated Damage (TriNet data)**

Figure 3-8 Comparison Between Observed and Estimated Damage Due to Ground Shaking (continued)

3.4.2 Observation-based Fragility Curves

A set of observation-based fragility curves were developed for the 940 bridges within the Los Angeles study area, using bridge damage states recorded following the 1994 Northridge earthquake, together with corresponding ground motion measurements estimated for each site.

Damage state observations were gathered by field inspection. Initially, Caltrans' Post Earthquake Inspection Team (PEQUIT) evaluated the damage state for 2,021 Caltrans-maintained bridges in Los Angeles and Orange Counties. The research team of this validation study then re-evaluated this list of damage states, based on additional information from aerial photos and Caltrans biweekly traffic state reports. As shown in Table 3-3, most differences between the PEQUIT and Research Team findings relate to 26 structures that lacked a formally assigned damage state. In addition, four bridges classified with 'Major' damage (DS 4) were reassigned as 'Collapsed' (DS 5)[3]. Based on the re-evaluated bridge damage states, and TriNet (March, 1999) ground motion data, a set of fragility curves were developed, as shown Figure 3-9.

Table 3-3 Assignment of Bridge Damage States by Caltrans, and the Research Team

Damage State	Caltrans Evaluated	Research Team Evaluated	Database used for this study
Collapsed (DS5)	6	10	7
Major (DS4)	47	43	35
Moderate (DS3)	84	104	78
Minor (DS2)	95	101	70
Unassigned	26	0	0
Total damaged	258		190
Total bridges evaluated	2021		940

[3] A full evaluation of bridge damage states is presented by Basöz and Kiremidijian (1998).

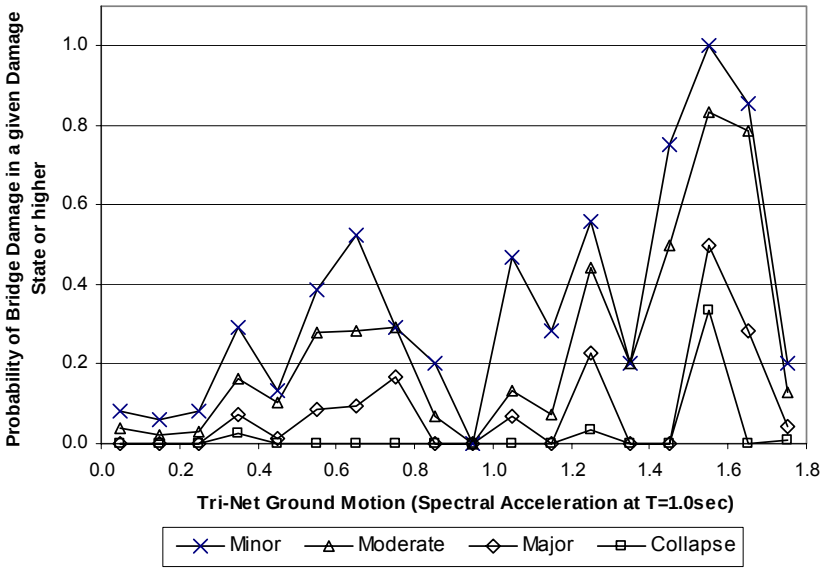

Figure 3-9 Observed Fragility Curves from 1994 Northridge Earthquake

3.4.3 Comparison of the Fragility Curves

As shown in the comparison between the theoretical model and REDARS fragility curves (Sections 3.2 and 3.3), minor differences are evident between their probability distributions. According to the developed fragility curves based on observed damage states, however, REDARS fragility curves are much higher across all ground motion levels, when compared to the observed data.

A rigorous statistical comparison between observation-based and REDARS generated fragility curves is not necessary, because the two sets of fragility curves are drastically different. From the graphical comparison in Figure 3-11, when ground motion is less then 0.6g, the observed fragility does not exceed 0.5 in any damage state. In contrast, REDARS estimates that more than 80% of the bridges will have at least minor damage when SA 1.0 is greater than 0.4g. In general, the observed fragility is lower than 2-standard deviations below the mean fragility estimates for REDARS when SA 1.0 is higher than 0.4g.

There are several possible explanations for this overestimation, including randomness of the bridge samples. For example, overestimation may reflect the close proximity between the study area (as well as the sample bridges) and epicenter of the 1994 Northridge earthquake. Figure 3-10 shows the distribution of bridges falling within each level of ground motion for the 940 sample bridges. According the figure, the majority of these structures were exposed to less than 0.3g of spectral acceleration, and more than 45% (430 out of 940) of bridges were also exposed to ground shaking equal to 0.4g or higher as well. While the higher level of ground motion would lead to a higher number of damaged bridges, there is no reason to believe that the mean estimation of fragility, which is dependent upon the probability of damage given ground motion, would be affected by proximity to the epicenter. Selection of a study area with bridges near the epicenter is not a probable cause of the overestimation of fragility by REDARS.

Errors in development of the bridge database or ground motion input might lead to the significant discrepancy between model result and observation. However, both databases are based on similar data sources. Theoretical models and the observed fragility curves were developed based on the same data sets. If errors in the data affect the REDARS results, they would also effect the Mander model. Therefore, the fragility curves should be comparable. The next section further explores the REDARS overestimation of bridge damage as compared to observed data.

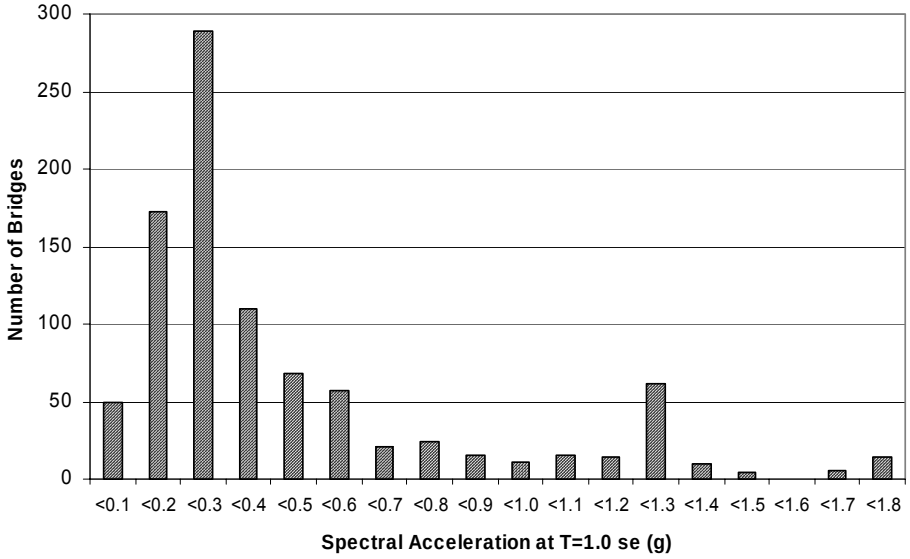

Figure 3-10 Number of Bridges Categorized by Ground Motion Produced for the Northridge Earthquake

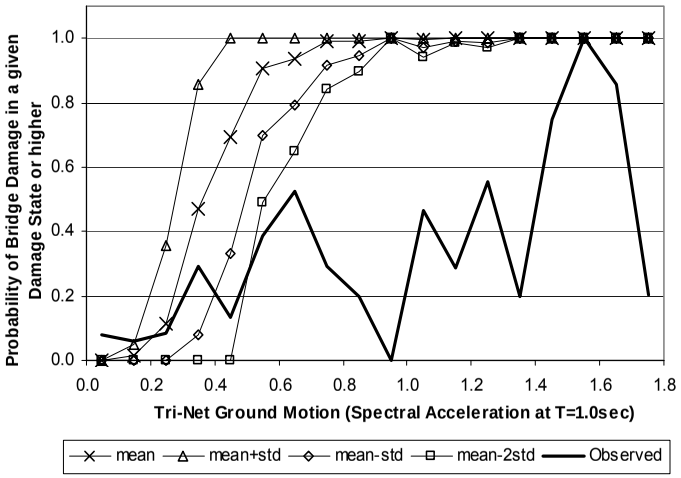

a) Minor Damage

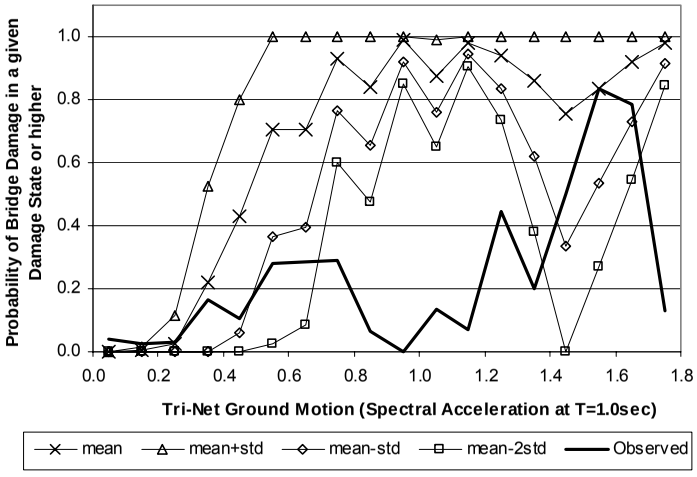

b) Moderate Damage

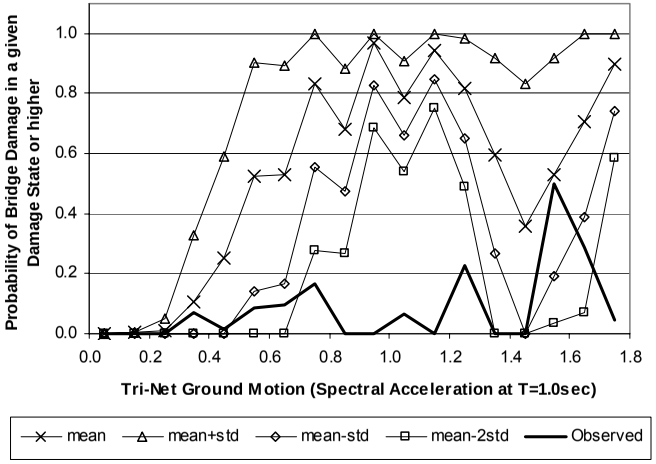

c) Major Damage

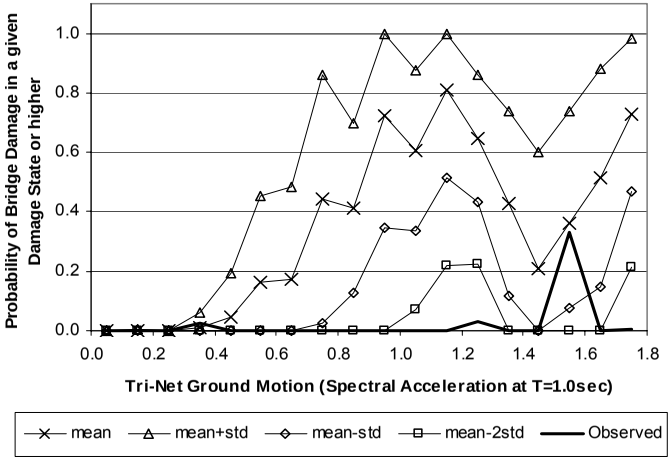

d) Collapsed Bridges

Figure 3-11 Observed Fragility Curves and Standard Errors of REDARS Fragility Curves

3.4.4 Discussion on Possible Reasons of REDARS's Overestimation

This section explores several possible reasons that might explain the significant overestimation in REDARS, including uncertainties that were not included in the development of median PGA values, uncertainty of ground motion data, and the effect of retrofitted bridges.

Uncertainties Associated with Median PGA

The median PGA value represents the capacity of a bridge to resist damage from spectral acceleration. In the REDARS SRA methodology, the median PGA is the most important factor in deciding the structure capacity. It was derived based on a series of factors that involve varying degrees of uncertainty by Dutta and Mander (1998). Uncertainties surrounding the following factors may have a significant effect on the estimation of median PGA values, and thus on the REDARS results. However, these uncertainties could not be readily incorporated into the bridge fragility model.

- Displacement of bridge structure observed in the Northridge and Loma Prieta earthquakes
- Construction quality control, such as material strength
- Soil amplification factor
- American Association of State Highway and Transportation Officials (AASHTO) spectral response shape

The relationship between damage states and structural strength is based on observations of displacement exhibited by structural components of the bridges. Depending on the structural type, various measurements are used to develop the bridge fragility model, such as vertical displacement of decks and deformation angles. From the observed damage states, 1.2 meters was assumed as a representative displacement value (Basöz and Mander, 1999). However, a range of values are possible, and it is unclear whether the dispersion factor in the Mander model includes displacement-related uncertainty.

Although material strength is assumed to be deterministic in the Mander model, material strength might be uncertain depending on construction quality control and should be modeled probabilistically. As reviewed in comparative analyses in section 3.3, the overestimation in REDARS might be due to a less uncertainty factor (steep distributions of REDARS fragility curves).

Although the type of soil associated with a given bridge site has a deterministic value, the amplification factor (SAF) may be stochastic. The probabilistic analysis of REDARS incorporates a standard deviation for the amplification factors, according to the time after shaking, and soil type. However, the use of published ground motion data for SAF calculation fails to consider any SAF-related uncertainty.

At a fundamental level, spectral shape is another source of uncertainty. According to the push-over method (Basöz and Mander, 1999), there is slight time gap between earthquake and structure damage, normally 0.3 second (short-period), or 1.0 second (long-period). Spectral acceleration is changing over these time periods. The spectral shape represents the time-variant acceleration, and is established from observed ground motion information[4], using a curve fitting technique. Although it is based on best-fit curves, estimation errors are a source of uncertainty.

Uncertainty in Ground Motion Input

As reviewed in Section 2, several sets of ground motion data have been generated for the 1994 Northridge earthquake. Some of these are distinct to each other significantly, indicating that the ground motion data is highly uncertain. Publicly available ground motion data sets (in our case, TriNet-March 1999, TriNet-December 2002, Somerville (1995), USGS- Borcherdt) are often given as contour maps, which were estimated by applying recorded station data to attenuation models. Hence, the contour values should be associated with estimation errors across over the region.

It is also true that differences in ground motion data have a significant effect on the results from bridge fragility as shown in Figure 3-12. Two sets of bridge fragility curves are shown for Southern California[5]. These were developed from USGS Open file report 94-197, and TriNet peak ground acceleration measure, (March, 1999). Fragility curves based on the USGS open file report shows that the probability of being damaged (minor or severe) is about 0.78 when PGA is 0.9~1.0 g. For the same PGA, the TriNet ground motion shows that the fragility is about 1.0. It can be restated such as "all bridges would be damaged when TriNet PGA is 0.9~1.0 g." Knowing that even the publicly available data sets show totally different curves, it may not be possible to have similar fragility by estimation using any kind of data. In other words, without knowing which ground motion data is valid to the model, it may not be possible to recover the observed fragility using the model. More detailed REDARS response for distinct ground motion data is provided in Section 3.6.

[4] For example, see "Seismograms from the Interactive Deaggregation Web page", *http://eqint1.cr.usgs.gov/eq/html/Stochastic_Seismgram_Theory.html*

[5] In Figure 3-9, the observed fragility is based on spectral acceleration at 1.0 second in g, while Figure 3-12 is based on PGA

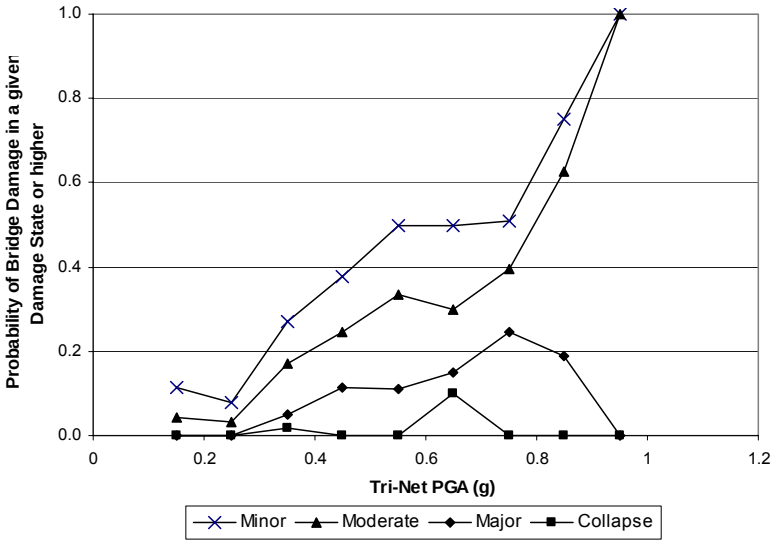

a) Fragility Curves Based on TriNet PGA (March, 1999)

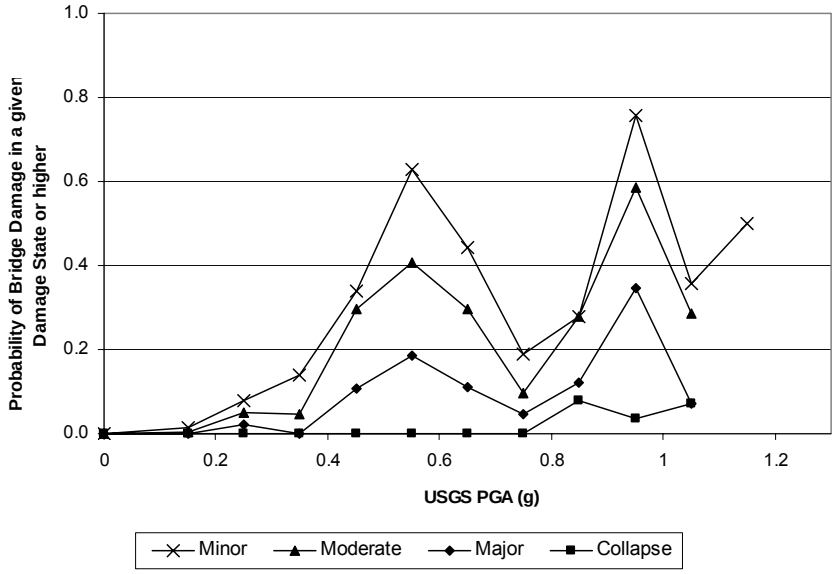

b) Fragility curves based on USGS PGA (ofr-94-197)

Figure 3-12 Differences in Multi-Span Bridge Fragility, Computed Using USGS and TriNet Ground Motion (March 1999)

Effect of Retrofitting Bridges

This section investigates whether overestimation of bridge damage by the REDARS fragility model may be attributed to differences in performance between the retrofitted and the non-retrofitted bridges in the study area. As seen in Table 3-1, median PGA values are given according to bridge's structural type, and design specifications -conventional design and seismic

design[6], but no distinction is given between retrofitted and non-retrofitted in bridge performance (median PGA values). Thus in REDARS's estimation, fragility for retrofitted bridges is not different from that of bridges that have not been retrofitted. However, if there were observable differences between performance due to retrofitting, REDARS's lack of consideration to retrofitted bridge performance could be a reason of the overestimation.

Besides the design specification, the California Department of Transportation (Caltrans) began its Phase 1 Seismic Retrofit Program after the 1971 San Fernando Earthquake. Approximately 1,400 bridges out of a state inventory of 12,000 bridges were retrofitted. The Phase 2 Seismic Retrofit Program commenced after the 1989 Loma Prieta earthquake. In this case, 1,039 bridges were retrofitted, together with several toll bridges. As a result of the 1994 Northridge earthquake, a further 1,364 bridges were chosen for retrofitting. By June 1995, 530 of these had been retrofitted.

Of the 940 sample bridges that Caltrans maintained within the study area, 56 were retrofitted prior to the Northridge earthquake under Phase 2 of the Seismic Retrofit Program. Table 3-4 compares damage states for retrofitted versus non-retrofitted structures within this sample. The retrofit/non-retrofit classification is based on a report by Yashinsky *et al*. (1995). The frequency occurrence of each damage state was compiled from observations made by the project team as summarized in Table 3-3.

Table 3-4 Damage State Comparison for Retrofitted and Non-Retrofitted Bridges

	Damage States				Damaged	No Damage	Total
	Collapsed	Major	Moderate	Minor			
Retrofit	0 (0%)	1 (1.8%)	9 (16.1%)	6 (10.7%)	16 (28.6%)	40 (71.4%)	**56** (100%)
No-Retrofit	7 (0.8%)	34 (3.8%)	69 (7.8%)	64 (7.2%)	174 (19.7%)	710 (80.3%)	**884** (100%)
Total	7 (0.7%)	35 (3.7%)	78 (8.3%)	70 (7.4%)	190 (20.2%)	750 (79.8%)	**940** (100%)

From Table 3-4 there is an insignificant difference between the percentages of damaged structures categorized as retrofitted (28.6%) and non-retrofitted (19.7%). This result is similar to the percentages recorded for bridges exhibiting 'No Damage' following the Northridge earthquake. 71.4% of the retrofitted bridges (40/56) were classified as 'No Damage.' For non-retrofitted bridge, the figure is 80.3% (710/940).

[6] In California bridges have been designed seismic standard since 1975.

One finding that should be noted from Table 3-4 is that, although the percentage difference is minor, damage states of retrofitted bridges are much lower than their counterparts. While the percentage of severely damaged bridges (major damage and collapsed) in non-retrofitted bridges is about 4.6%, less than 2% of retrofitted bridges were severely damaged from 1994 Northridge earthquake. In the same line, no retrofitted bridges collapsed.

At present, the REDARS program does not distinguish between retrofitted and non-retrofitted structures. Given the similar performance of bridges following the Northridge earthquake, irrespective of retrofitting, it is unlikely that failure to consider this variable in the REDARS model is totally responsible for the overestimation of the bridge damage states.

3.5 Application of a Ground Motion Scale Factor

In previous sections, the REDARS model was compared with observation from the 1994 Northridge earthquake, and the model overestimated the number of bridges damaged. As possible reasons of overestimation, uncertainty related to median PGA, ground motion input, and the effect of retrofitting were reviewed.

This section provides results from a simple sensitivity test of bridge fragility model to ground motion input. To rectify questions related to the uncertainty affecting median PGA values, an in-depth study might require vast efforts and ingenious statistical analyses. In this validation study, instead of study on uncertainties, effects of ground motion input are analyzed under the given condition of REDARS's overestimation.

This test analyzes the response of the REDARS generated bridge damage states to a linear stimulus. The TriNet ground motion data (SA) is modified by applying an incremental scale factor ranging between 0.1 and 1.5. Thus, all the surface ground motion level (demand ground motion) varies proportionally according to the scale factor. The REDARS model was applied to the modified ground motion data by the scale factor, and the number of damaged bridges in each damage state was counted.

In general, linear response of a system to linear stimulus presents stability of the system. If REDARS responds linearly to the scale factor, the number of damaged bridges will correlate strictly to the scale factor. In this case, the scale factor can be calibrated so that the REDARS estimation exactly matches observation without increasing the complexity of the model.

The trend in Figure 3-13 indicates that the REDARS response to a linear scale factors is stable. The simple regression coefficients for the curves in Figure 3-13 are 0.9898 (F=1258.44), 0.9900 (F=1292.50), 0.9816 (F=692.48), and 0.9453 (F=224.83), for damage states 2, 3, 4 and 5, respectively. Based on these high R^2 and F values, REDARS results behave linearly in response to a linear ground motion scale factor. Thus, it may be inferred that the quality of REDARS results primarily depends on the quality of ground motion data.

The results in Figure 3-13 indicate that when the scale factor is in the range of 0.5-0.6, the REDARS model estimates the number of damaged bridges to be equal to the number of observed damaged bridges. However, it fails to replicate the distribution of damage states. Table 3-5

compares the number of damaged bridges by damage state. When a scale factor of 0.56 is applied to the TriNet ground motion data, REDARS estimates 190 bridges as damaged, which is the same as the number of bridges observed damaged. However, a majority of bridges were observed as DS 3 (78 bridges), whereas REDARS estimates a minority to be DS3 (only 31 bridges). For all other damage states, REDARS predictions are consistently higher than observed.

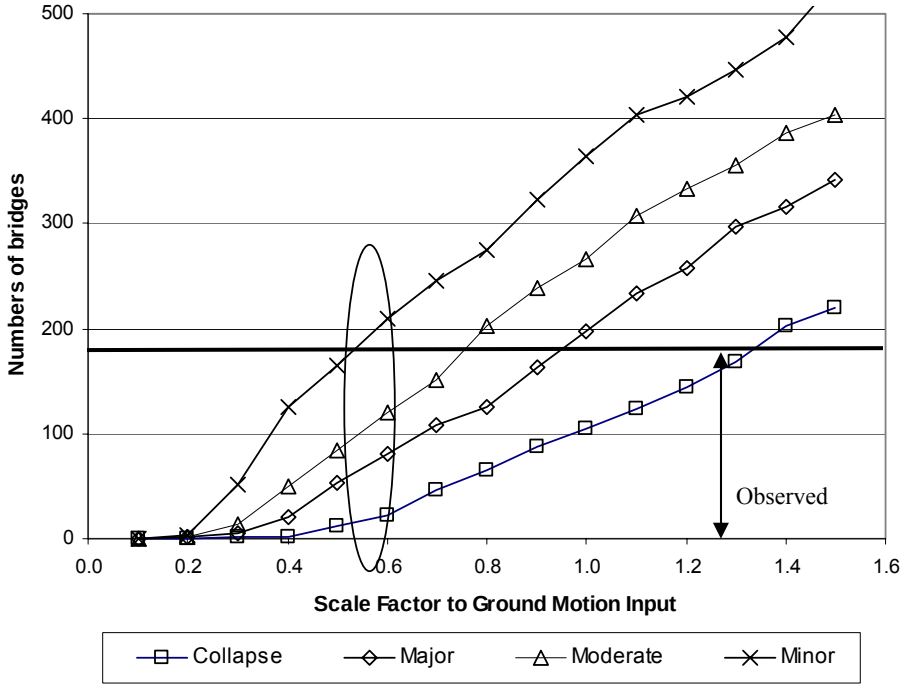

Figure 3-13 Changes in the Predicted Number of Damaged Bridges with Variations in Ground Motion Scale Factor.

Table 3-5 Number of Damaged Bridges by Damage State

	DS2	DS3	DS4	DS5	Total Damaged Bridges
Model result (Factor=1.0)	91	72	98	102	363
Model result (Factor=0.56)	86	30	56	18	190
Observed	70	78	35	7	190
Ratio	1.23	0.38	1.60	2.57	1.00

3.6 Summary

In this section, the REDARS SRA methodology, Mander's theoretical model, and observations are compared with respect to bridge fragility under given ground motions. A controlled comparison of theoretical distributions between REDARS with Mander's model reveals that REDARS estimates bridge damage following a distribution that can be best described with a "normal-exponential" distribution, while Mander's theoretical model follows lognormal distribution. Also, REDARS was implemented with less uncertainty factor so that its fragility curves are steeper than the Mander model. These findings are also identified from the comparison between REDARS and Mander model using 1994 Northridge earthquake data.

Comparison of REDARS to observed fragility curves expose significant discrepancies between the two sets of fragility curves, with REDARS showing significant overestimation. Several reasons can be found, including the limited effect of uncertainty factors to median PGA values, and changes to the ground motion data. The effect of retrofitted bridges in the overestimation is not significant. REDARS demonstrates its stability to a linear scale factor to ground motion input, and results matched the number of bridges with a scale factor of 0.5 - 0.6.

SECTION 4
THE TRAFFIC STATE MODEL

4.1 Introduction

This section reviews the REDARS traffic state model, and includes the following sections:

- Section 4.2 reviews the traffic state model implemented in REDARS.
- Section 4.3 compares the REDARS model against observed conditions.
- Section 4.4 summarizes the information in the section.

The traffic state model estimates the number of operating lanes on bridges after an earthquake. These estimates are based on two factors:

- Severity of damage.
- Number of designed lanes.

Bridges that have not collapsed (less than DS 5) may have operable lanes, even immediately after an earthquake, and the number of available lanes would gradually increase to full capacity over time. In REDARS, a look-up table converts damage state estimates to the residual capacity (functional capacity remaining on damaged bridges) for specific time-periods after the earthquake.

Traffic capacity measures the maximum number of cars allowed to traverse a bridge within a unit time (usually one hour). Bridge traffic capacity depends on two factors:

- Design specification of the road and bridge.
- Number of lanes.

The design specification determines the possible driving speed on the road by limiting gradient, curvature, and width per lane. Since the gradient and curvature are unchanged for a damaged bridge, the damage state is presented by number of lanes operating after an earthquake. Thus, the *number of operating (retained) lanes* and *remaining (operating) functionality* refer to the same physical entity of remaining ratio of capacity after earthquake. *Capacity loss*, on the other hand, refers to the reduction of its functionality.

Following the convention from the previous section, the *REDARS model* refers to estimated traffic states by applying REDARS SRA methodology, while *observation* refers to the number of closed bridges over the days after the 1994 Northridge earthquake. Since REDARS estimates traffic states as a number of operating lanes, the observation shows that bridges were rather operated in full or closed with no functionality.

4.2 Review the Traffic State Model in REDARS

In the current traffic state model, bridges with damage state 2 (DS2) or higher may be fully or partially closed for at least 7 days, depending on the number of lanes in each direction. REDARS uses a simple model to implement this relationship. Table 4-1 is the lookup table used in the model. For example, if a bridge has a damage state 3 (moderate) and has four traffic lanes, it would retain 75% of the original capacity with one lane out of four closed at 7 days after the earthquake.

Table 4-1 Remaining Functionality Over Varying Time-Periods

Damage States	Number of Designed Lanes	Capacity		
		7 days	60 days	150 days
1 (None)	N/A	1	1	1
2 (Minor)	N/A	1	1	1
3 (Moderate)	1	0	1	1
	2	1/2	1	1
	3	2/3	2/3	1
	4	3/4	1	1
	5	4/5	4/5	1
4 (Major)	1	0	0	1
	2	1/2	1/2	1
	3	1/3	1/3	1
	4	2/4	3/4	1
	5	2/5	3/5	1
5 (Collapsed)	1	0	0	1
	2	0	0	1/2
	3	0	1/3	2/3
	4	0	1/4	3/4
	5	0	0	4/5

As shown in Figure 4-1b, and d, a bridge designed with more lanes will not have fewer remaining lanes than others under the same damage state. For example, a bridge designed with five lanes in each direction would have four lanes at 7 days, and 60 days after the earthquake if the bridge were moderately damaged. And, its retained number of lanes is the same or higher than those of any other bridges that were designed with fewer than five lanes (the case of damage state 3, moderate, Figure 4-1b).

Estimating the number of retained lanes depends on the perspective of the model, and whether it favors safety or efficiency of the transportation system. For example, closing bridges until they are completely repaired provides maximum safety while sacrificing network efficiency. In this case, only two traffic states are possible - open and closed. On the other hand, a model can be applied to estimate number of lanes in continuous measurement, although physically not possible, such as 0.3 lanes. The method implemented in REDARS is in between these two methods. REDARS estimates bridge functionality to be quasi-continuous so that the number of lanes is always an integer value. For each time period of 7 days, 60 days, and 150 days after an earthquake, a bridge can have from 0 to 5 lanes according to the severity of damage and number of designed lanes.

(a) Operating functionality (damage state 3)

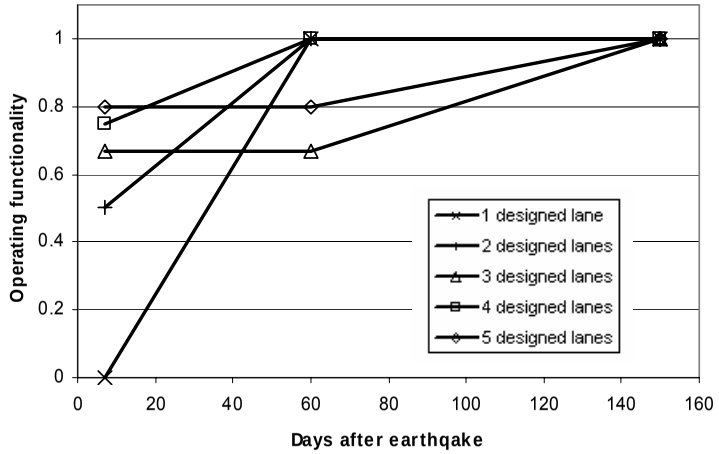

(b) Number of operating lanes (damage state 3)

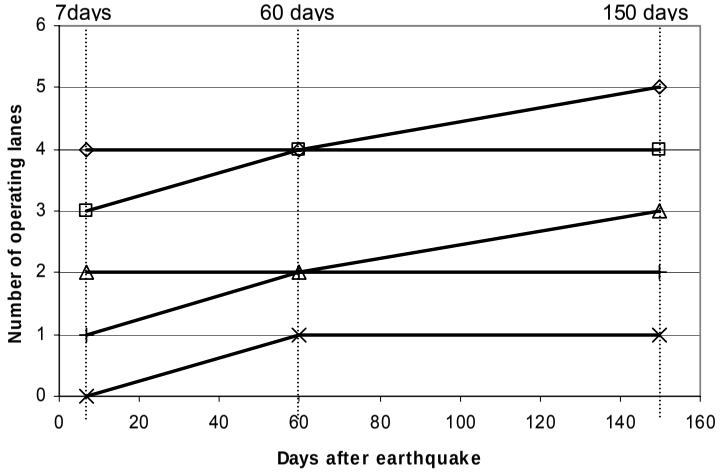

(c) Operating functionality (damage state 4)

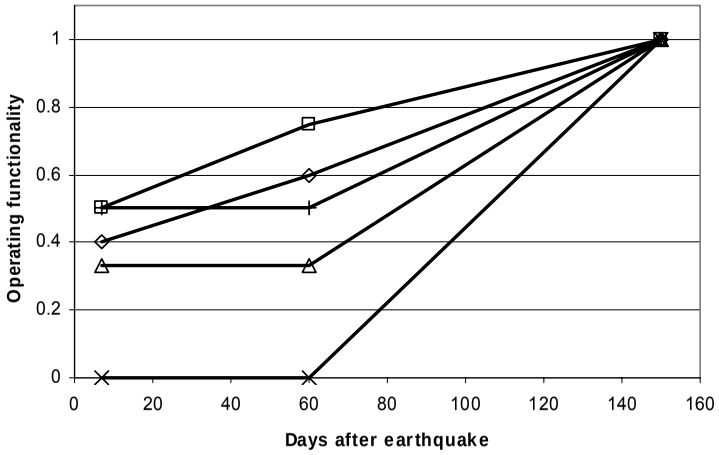

(d) Number of operating lanes (damage state 4)

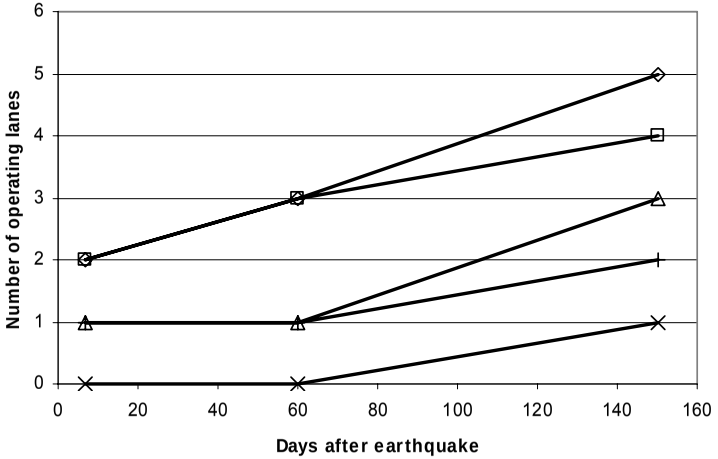

Figure 4-1 Operating Functionality and Number of Lanes by Damage States

4.3 Comparison between REDARS Model and Observation

As discussed in Section 1, this study validates REDARS methodology by comparing results from each of its component models to observations. Since the traffic model simply translates bridge damage states to its traffic states, the overestimation from the bridge fragility model should provide an effective estimate of traffic states. This section contains two sections:

- The traffic state model in REDARS is reviewed by running the model using only observed bridge damage state data. This isolates the traffic state model from errors generated by previous component model.
- The traffic states estimated by using REDARS methodology (including bridge fragility model) are compared to observation.

4.3.1 Estimation of Traffic State by REDARS using Observed Bridge Damage States

The REDARS traffic state model estimates that fewer than 13% (120 out of 940 bridge) would be operating at less than original capacity 7 days after the earthquake (point a on Figure 4-2), and fewer than 5% of the bridges would experience capacity reduction more than half (point b). Seven bridges (0.7% of 940 bridges) would be severely damaged, and not be fully recovered even five months later (points c and d). The following section compares these estimates to observed conditions.

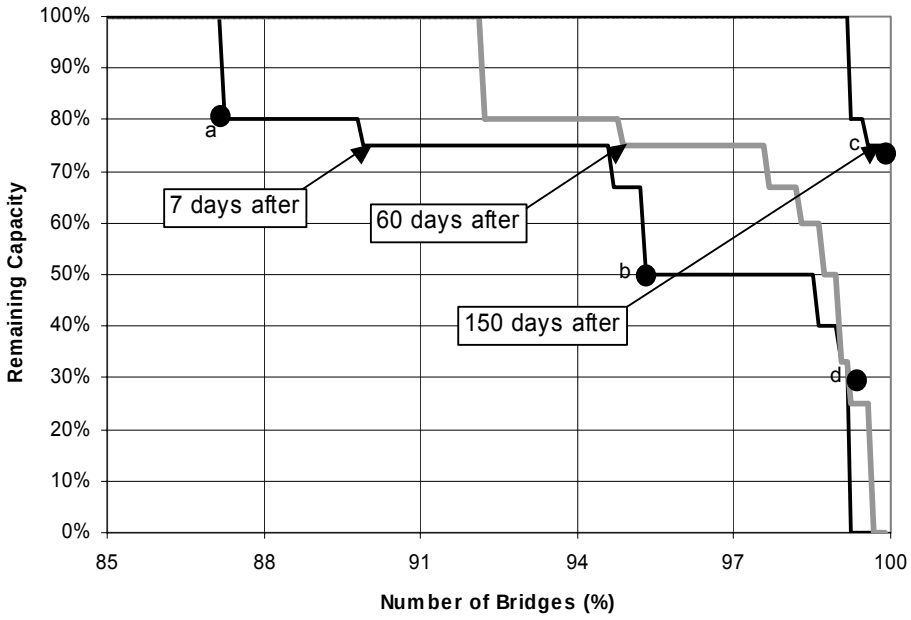

Figure 4-2 Traffic Remaining Capacity Over Various Time Periods Estimated Based on Observed Bridge Fragility

Following the Northridge earthquake, damaged bridges in Los Angeles County did not remain closed for very long. Figure 4-3 shows the percentage of damaged bridges in the study area,

together with their duration of closure. Approximately 60 % of the damaged bridges (118 of 190) remained closed for fewer than 5 days, while inspections and minor repairs were completed. 80% of the bridges (154 of 190) were closed for fewer than 15 days. Only 4% of the bridges (7 of 190) were closed for more than one month.

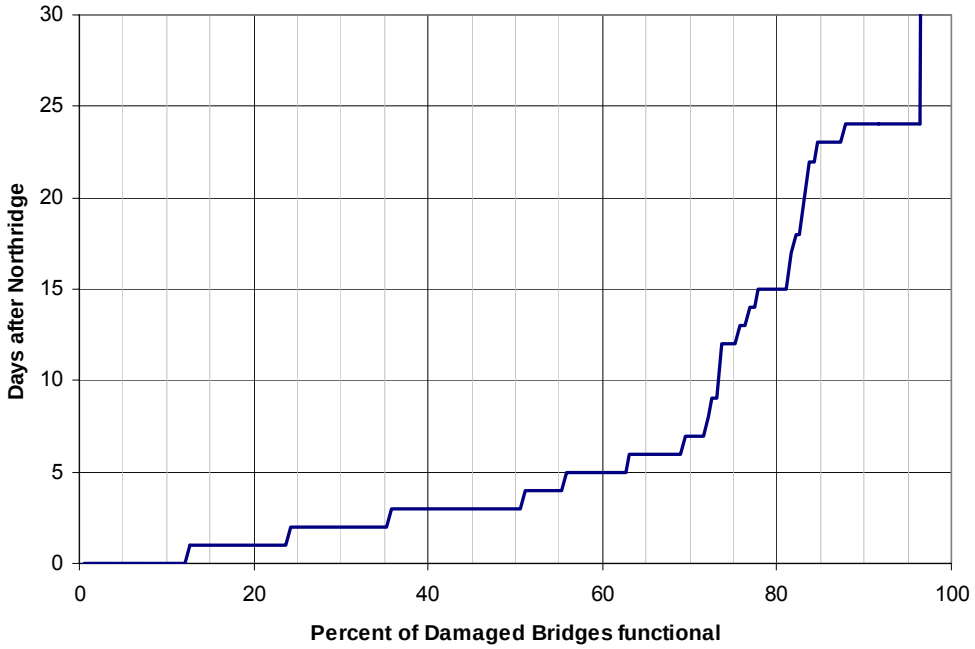

Figure 4-3 Observed Duration of Link Closure for Bridges in the Los Angeles Study Area, Following the 1994 Northridge Earthquake

Theses observations are based on the duration of bridge closures, while REDARS estimates are based on bridge functionality throughout the recovery period. Thus the two sets of traffic states may not be comparable directly. However, it can be inferred that, based on findings from observations and estimation, REDARS slightly underestimates traffic states. For example, while observation shows that 118 bridges were closed five days after the earthquake, REDARS estimates about same number of bridges would experience partial or full loss of functionality.

4.3.2 Comparison between REDARS Methodology and Observation

Figure 4-4 shows REDARS estimates for the remaining bridge capacity 7, 60 and 150 days after an earthquake. REDARS SRA methodology (bridge fragility model and traffic state model) was applied to the Northridge earthquake through TriNet March 1997, and the figure was developed based on the mean value of the 217 simulations (see Section 3.3.2), REDARS estimates that approximately 65% of bridges would have more than 90% of their original capacity in the 7 days after an earthquake (point a). After the same lapse of time, 9.6% of structures (91 out of 940 bridges) would have less than 20% of their original capacity (point b). REDARS estimates that even two months (60 days) after the earthquake, 10% of bridges would have less than 40% of

their design capacity (point c) available and 40% of bridges would not fully be recovered even five months (150 days) later.

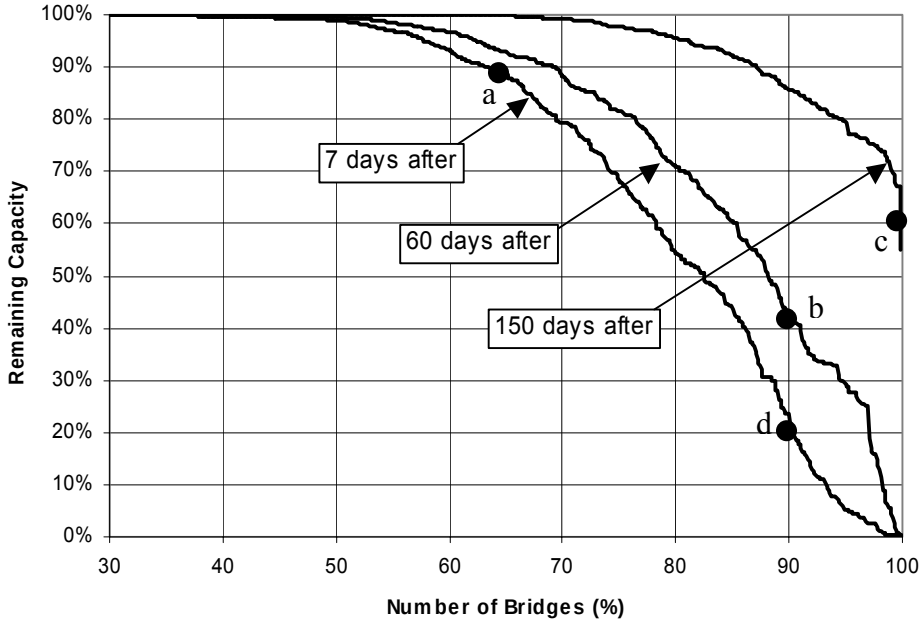

Figure 4-4 Remaining Capacity Over Various Time Periods Estimated Based on REDARS's Bridge Fragility Estimation

As a systematic model, REDARS SRA methodology overestimates the closure duration for bridges damaged by the Northridge earthquake when TriNet March 1997 is used. The disparity between predicted and actual duration is particularly pronounced after 60 days. Furthermore, the REDARS SRA model suggests that remaining capacity on the damaged bridges is similar after 7 and 60 days have elapsed, which is clearly unrealistic. In reality, recovery durations often have substantial variations due to the location and relative importance of a given structure.

This overestimation is primarily due to effects of bridge fragility model. While isolated estimates from the bridge fragility model predict that fewer than 13% of bridges would have a loss of functionality in 7 days after the earthquake, REDARS estimates that more than 50% of the bridges would be damaged after the same 7 days. The locations of bridges with capacity reduction are also primarily those estimated by the fragility model, as shown in Figure 4-5.

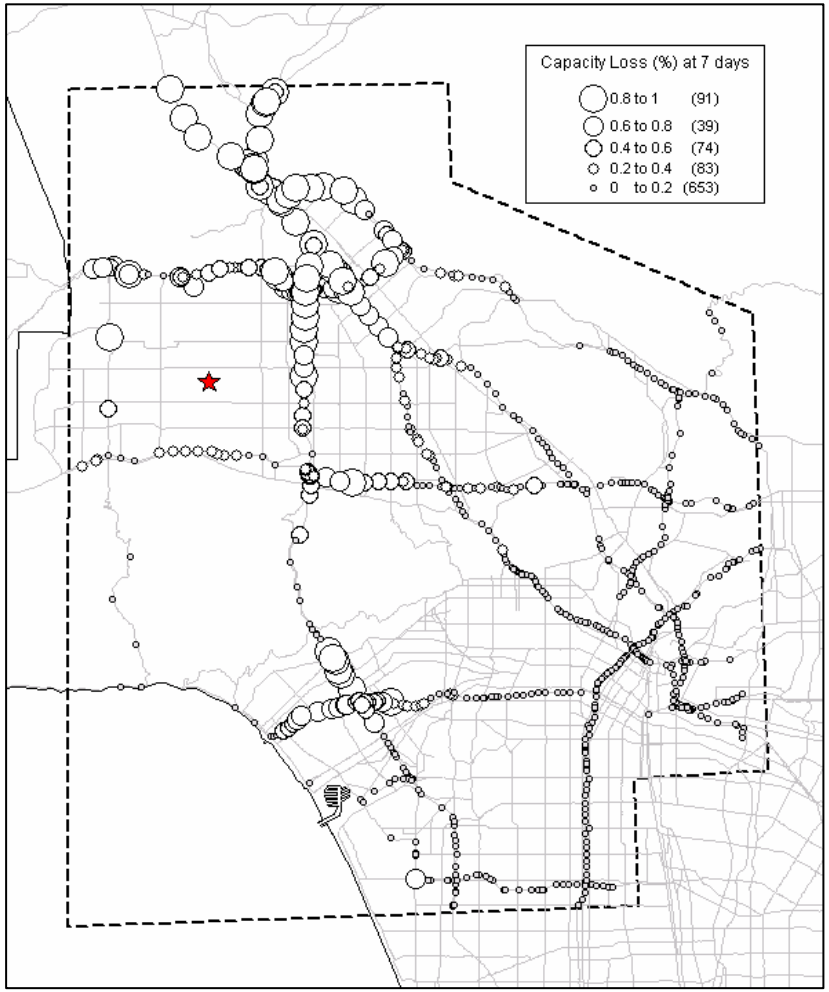

a) Capacity Loss at 7 days after the event

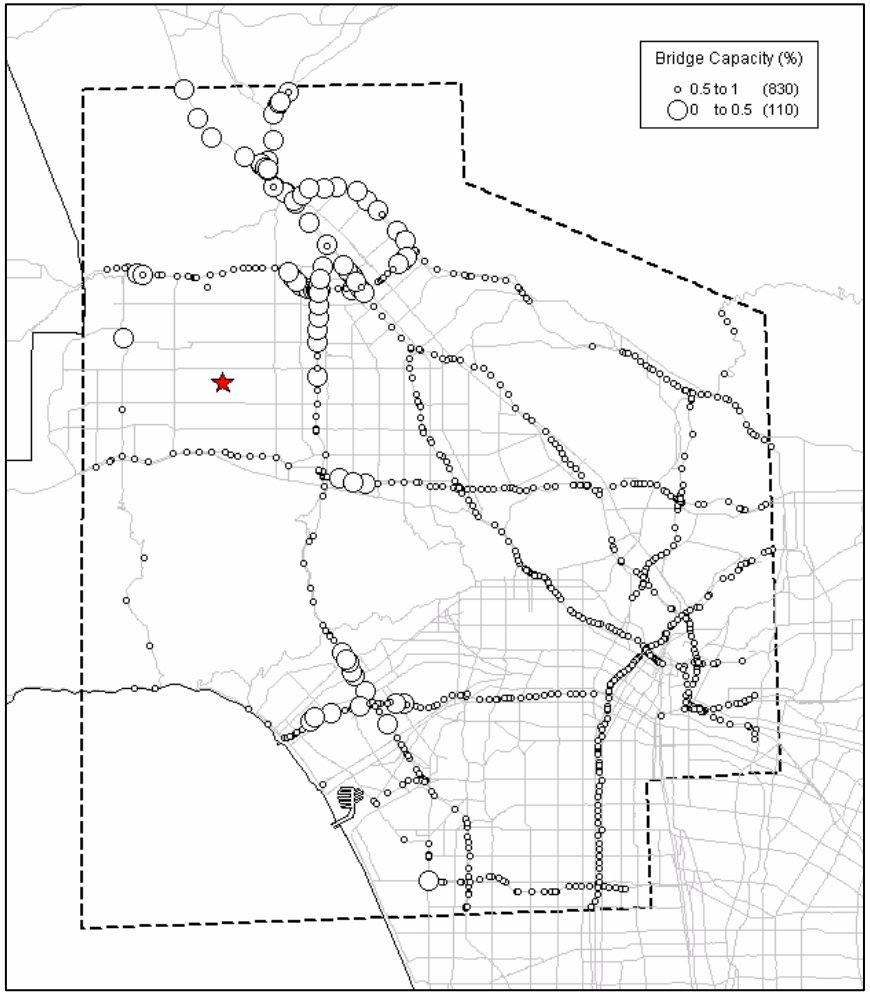

b) Bridges with more than 50% of Capacity 60 days after the event

Figure 4-5 Traffic States (Capacity remaining) Generated from REDARS

4.4 Summary

This section examined the REDARS traffic state model, which estimates remaining traffic functionality on bridges according to the severity of damage and number of designed lanes on the bridge.

If observed bridge damage states were applied to traffic state model, the model slightly underestimates the loss in functionality, while the result was highly overestimated when the REDARS bridge fragility model was applied.

Judging the quality of the REDARS traffic state model by comparison with observed Northridge earthquake data may not be relevant because of the extremely wide variation in the duration of bridge closures. In the case of high-priority Los Angeles bridges, for example, repairs were expedited by awarding bonuses to the contractors for reduced repair time after the Northridge earthquake. In contrast, some of the damaged structures from 1989 Loma Prieta earthquake never have been repaired, and the local government developed the alternative routes instead. Given these wide variations in actual recovery durations, establishing a thorough and robust traffic state model should be based on various cases.

SECTION 5
TRANSPORTATION NETWORK MODEL

5.1 Introduction

This section assesses the REDARS transportation network model and investigates the influence of network interruption in transportation network analysis due to a seismic event on model results. A transportation model, or network model estimates equilibrium states of link traffic volume and congested travel time given travel demand information (origin-destination requirements), and network configuration. Damaged bridges reduce link functionality on the bridges. The reduction in link functionality (capacity and speed) is presented in a network configuration. Networks with reduced capacity induce higher costs to the given travel demand than under pre-earthquake conditions.

The application of a network model to earthquake situations might present contradictions. Most transportation models analyze routes, volumes and congestion within an equilibrium framework, which assumes drivers are rational and have perfect information about the transportation system. However, under abrupt reduction of capacity such as after an earthquake, travelers may not have enough information to choose the best alternative. The principal effects of network interruption from earthquake events are:

- *Capacity reduction.* Damaged bridges lose their designed capacities, which reduce route capacity.
- *Reduced/disrupted demand.* Reductions in route capacity can cause a decrease in user demand. Drivers may choose not to travel until the system stabilizes, and they might not travel if the travel cost is extremely high. In addition, drivers may change their destination to avoid the impacted area.
- *Changes in route choice.* Localized capacity reduction can cause areas of concentrated congestion as drivers use alternate routes to reduce their travel time.
- *Lack of route information to drivers*. Drivers do not have enough time to try alternatives provided under a disaster situation and may not be provided with sufficient information regarding new or alternative routes.

This section presents the first known validation study for the application of an equilibrium model to an earthquake damaged transportation network. Drivers may not have enough information and time to select best routes to travel, and thus it is not clear if the equilibrium model is suitable to use. The assumption that driver's choices are rational after an earthquake may contribute to the discrepancy between observed and predicted traffic conditions. However, recent studies sponsored by several earthquake research centers have applied equilibrium models to earthquake damaged transportation networks without validating the equilibrium model.

The following sections describe the REDARS transportation network model, and compare the results to observed traffic patterns:

- Section 5.2 provides an initial review of the user equilibrium traffic assignment model using "toy" network data.
- Section 5.3 presents a validation study, focused on changes of traffic demand to alternate routes when the capacity of a link is reduced.
- Section 5.4 presents a comparison between transportation network model results and observed system-wide traffic patterns.
- Section 5.5 compares REDARS estimates with observed traffic patterns in a subregion around places of severe bridge damage.
- Section 5.6 discusses network model effects when inaccurate or incorrect network data are used.
- Section 5.7 briefly summarizes the comparison between the REDARS transportation network model and observed conditions.

5.2 User Equilibrium Traffic Assignment Model

The REDARS transportation network model is based on the user equilibrium (UE) traffic assignment paradigm. REDARS alternatively employs an Associative Memory (AM) Matrix to analyze transportation systems based on a trained stimulus-response system using user equilibrium traffic assignment model.

A fundamental assumption in transportation planning is that traffic conditions are stable, with similar conditions each weekday, at the same time of day. The user equilibrium model best applies where the users have full knowledge of the system, and have sufficient buffers (in terms of time and information) to accommodate changes by self-adjustment. However, sudden system changes, such as those caused by a severe earthquake can create a system for which users cannot plan in advance.

Route travel times are used to establish equilibrium in a transportation system. In a highway network system, it is possible to use a variety of routes to travel between two zones. In general, the route with the least travel time (or cost) is preferred. However, congestion may make another route more desirable. In an equilibrium state, the commonly-used routes have lower travel times than unused ones. This is the first principal of network equilibrium, as stated by Wardrop (1952), and it is built-into the User Equilibrium Traffic Assignment model.

The mathematical form of the model is a nonlinear optimization problem with non-negativity, and flow conservation constraints. The first order condition of the optimization of link travel time meets Wardrop's first principal (Sheffi, 1985 Chapter 5).

$$\max\ z(\mathbf{x}) = \sum_a \int_0^{x_a} t_a(w)\ \ dw \tag{8}$$

subject to:

$$\sum_k f_k^{rs} = q_{rs} \qquad \forall r,s \tag{9}$$

$$f_k^{rs} \geq 0 \qquad \forall k, r, s \tag{10}$$

$$x_a = \sum_{rs}\sum_k f_k^{rs} \cdot \delta_{a,k}^{rs} \qquad \forall a \tag{11}$$

t_a : link performance function of link a.
f_k^{rs} : flow on path k connecting OD pair r-s.
q_{rs}: trip rate between OD pair r-s.
x_a : flow on link a.
$\delta_{a,k}^{rs}$: 1 if link a is on path k between OD pair r-s, otherwise 0.

Several algorithms were developed to solve the optimization problem for a large transportation network, such as column generation algorithm, packet-switching algorithm, and fixed-point algorithm. REDARS employs the Frank-Wolfe algorithm, which uses six steps (Steps 0 through 5) to solve transportation network problem, as follows:

0. Initialization.
Find an initial feasible flow pattern $\{x_a^n\}$. Set n:=1.

1. Update link travel time
Set $t_a^n = t_a\left(x_a^n\right) \forall a$.

2. Find auxiliary link volume by all-or-nothing assignment

$$y_a^n = \sum_{rs}\sum_k g_k^{rs^n} \cdot \delta_{a,k}^{rs} \quad \forall a$$

3. Find best Moving Step
Solve following system for α.

$$\min z(\alpha) \sum_a \int_0^{x_a^n + \alpha\left(y_a^n - x_a^n\right)} t_a(w)dw \text{, subject to } 0 \leq \alpha \leq 1$$

4. Flow Update

$$x_a^{n+1} = x_a^n + \alpha_n\left(y_a^n - x_a^n\right)$$

5. Convergence Test
If following inequality holds for very small κ, terminate.
Otherwise, set n:=n+1 and go back to step 1.

$$\sum_a \frac{\left|t_a^n - t_a^{n-1}\right|}{t_a^n} \leq \kappa \text{, and } \alpha_n \leq \kappa$$

Calculating the first feasible solution in Step 0, and the auxiliary solution in Step 2 requires building paths between the zones. The user equilibrium model employs the Dijkstra algorithm, one of the most efficient path-building algorithms. Despite the efficiency of the algorithm, the model has a prohibitively long running time, primarily because of the large network size (many links and nodes), number of zones, and iterations to converge. It takes approximately 5 hours for three time-periods of 217 system states (651 cases) developed from the bridge fragility model (Section 3.4.2).

Link travel time is a function of the link capacity, design speed, and traffic volume on the link. REDARS employs the BPR (Bureau of Public Road) function, as link performance function t_a. The mathematical form is, $t_a = t_a^0 \cdot \left(1 + 0.15 \cdot \{x_a / C_a\}^4\right)$ where t_a^0 is free flow travel time, x_a link volume, and C_a capacity. When a bridge is damaged, and retains only partial functionality, link travel time follows the Greenshield flow-speed relationship (Greenshields 1935, recited from Sheffi, 1985 Chapter 13). As shown in Figure 5-1, flow is a quadratic function of speed. When the capacity is reduced to 50%, the original design speed is also reduced by 50% (see the dotted curve in Figure 5-1).

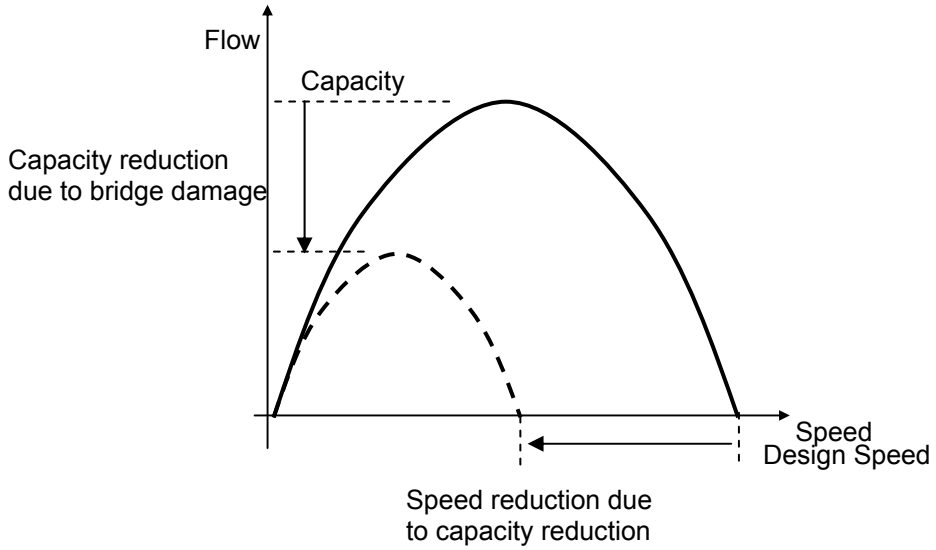

Figure 5-1 The Greenshield Flow-Speed Relationship

5.3 Evaluation Using a Toy Network

This section describes a "toy network," which demonstrates a theoretical evaluation of the UE traffic assignment model. This test shows the response of the UE model to a forced reduction of link capacity.

5.3.1 Synopsis of the Toy Test

A "toy network" tests the REDARS transportation network model to assess the dependability of its results. This test corroborates the reciprocal effect of typical capacity reduction of a link to system traffic volume. For a given travel demand, the UE model readjusts the equilibrium condition for a new network configuration.

Figure 5-2 shows the toy transportation network model. It consists of 6 zones, 28 nodes, and 78 directional links. The network replicates part of a typical urban network, with freeways and local road segments. Link attributes, such as the number of lanes and design speed, are assigned typical values. 63,000 vehicles, in passenger car equivalents (PCE), pass through the links between zones A and B during a three-hour daytime period. Minor demands also generate and terminate in each of the four remaining zones from each of the corners. Links connecting zone A with zone B through the middle of the network are assumed to be freeways with four lanes each direction and a capacity of 2000 PCE/Hour per lane.

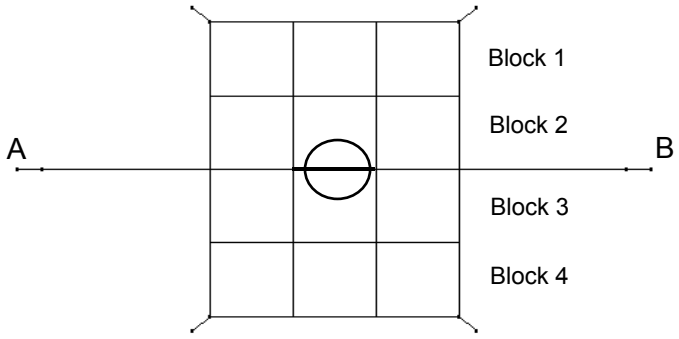

Figure 5-2 Toy Network

Each block represents four vertical links (eight directional links) in the network. Traffic volumes in each block measure the degree of detour. Given the travel demand between zones A and B (63,000), disconnecting a horizontal link leads to volume changes in the vertical links. To test the network, the state of the circled links was changed from 1.0 (fully functional) to 0.0 (fully closed), in 0.2 increments. The system costs and traffic volume of the surrounding network were recorded at each increment.

5.3.2 Toy Test Results

In a transportation network, travel demands compete for a fixed supply of network capacity. Congested travel time is the equivalent of the market price (or equilibrium), at which travel demand meets network capacity. When the network capacity is reduced, congestion is higher for a given demand, leading to longer travel times.

The validation results consist of traffic volume changes and system-wide travel costs (see Table 5-1) for each link state. The system-wide travel cost represents the total time for all travel demand to be met (cumulative sum for all links of volume multiplied by travel time). The

system-wide travel cost and the average zone-to-zone travel time increases as the capacity of the circled link falls. In this test, link system states 0.2 and 0.0 generate identical system costs and the travel times, reflecting an identical distribution of travel demand to alternative routes for both of these link system states.

Table 5-1 Toy Network Response to a Link Capacity Reduction

Link State	System Cost (PCU*Minute)	Average Zone-to-Zone Travel Time (Minutes)
1.0	1,512.997	1.415
0.8	1,518.133	1.416
0.6	1,521.063	1.417
0.4	1,521.485	1.419
0.2	1,523.680	1.422
0.0	1,523.680	1.422

For the baseline situation, the circled link in Figure 5-2 serves as the major route between zones A and B. As the capacity of the circled link falls after an earthquake, traffic flow between A and B gradually moves to alternate routes adjacent to the circled link. Figure 5-3 shows the link volumes in each of the network configurations, with line thickness indicating volume on the link. As this link capacity drops, traffic volume on the adjacent links increases.

As detouring traffic takes immediately adjacent routes, volume in the vertical links of blocks 2 and 3 increases proportionally to the circled link's diminished capacity, as shown in Figure 5-4. However, no volume changes are observed farther away, in blocks 1 and 4. The congestion increment due to the closure of the circled link in Figure 5-2 does not exceed the additional travel cost of crossing four additional (two upwards, two downwards) vertical links to reach links in block 1 or 4. Additionally, the detour traffic volume on the vertical links in block 2 and 3 is more than three times higher than the baseline traffic volume, with increment ratios of 3.33, and 6.01, respectively. These ratios are exceptionally high and may not be an acceptable representation of a realistic highway network. In an actual highway network, the observed traffic volume cannot exceed network capacity. In the toy network, traffic volume can exceed capacity, and volume will not divert to the outer links until travel time increases unrealistically. The next sections provide real-world validations, comparing model predictions with observed traffic conditions following the Northridge earthquake.

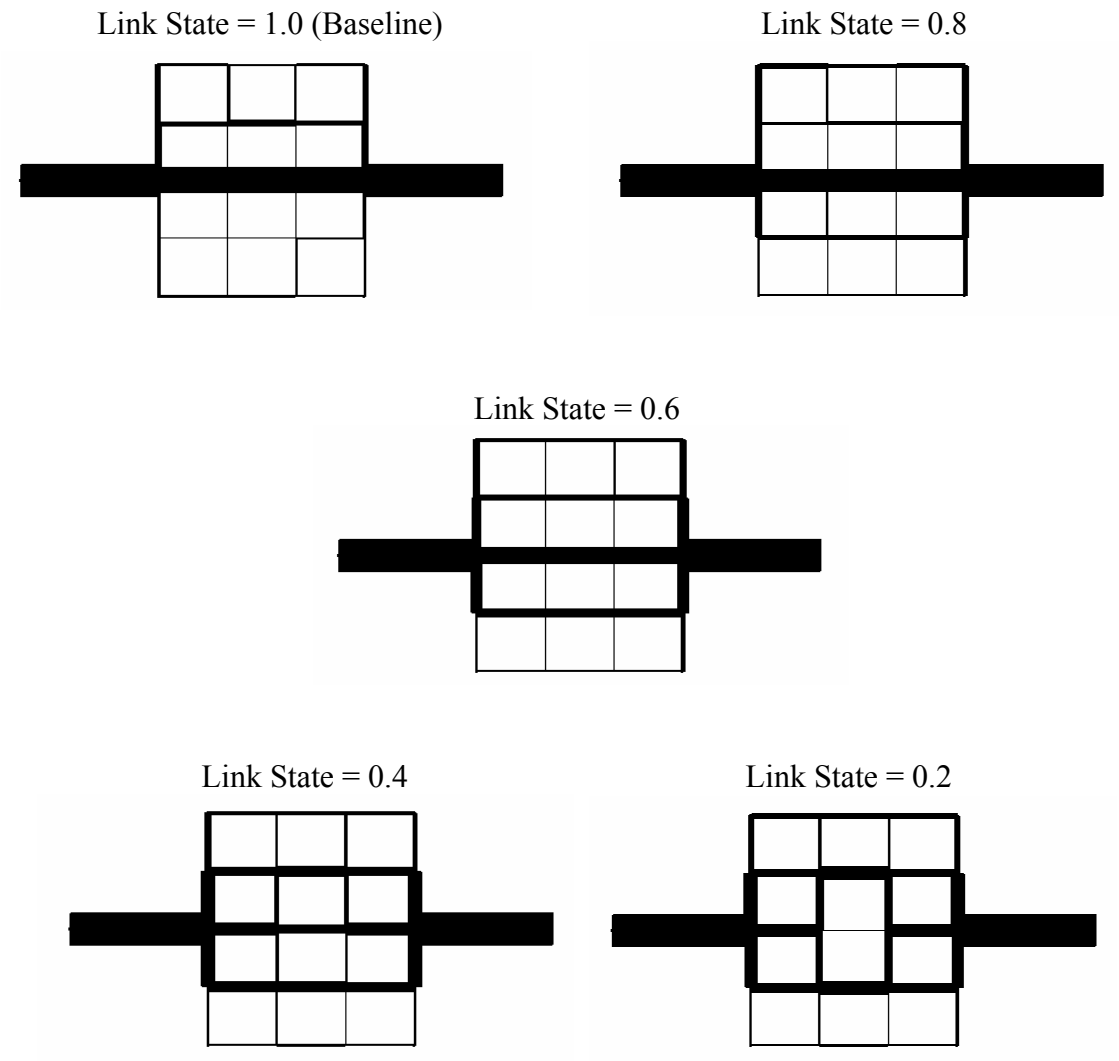

Figure 5-3 Link Volumes Changes by a Reduction in Link Capacity

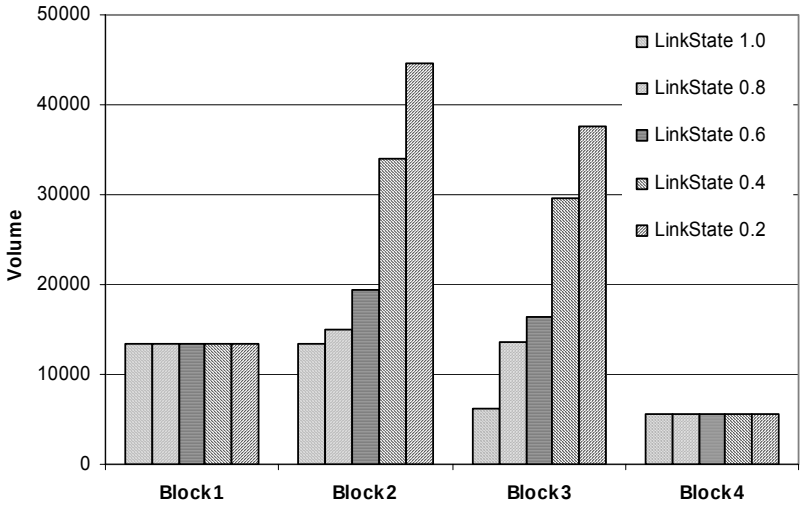

Figure 5-4 Vertical Volume Changes in Toy Network

5.4 Comparison of Estimated and Observed System-wide Freeway Volumes

This section compares REDARS user equilibrium traffic assignment model estimations with traffic data recorded immediately after the 1994 Northridge earthquake. Traffic volumes on freeways are compared with the REDARS prediction. Freeways account for more than 90% of vehicle-miles traveled (VMT) in Southern California (Cho, et al. 1999). As such, the majority of travel cost increment between pre- and post-earthquake conditions should be due to freeway traffic conditions. Since a highly detailed transportation network for Southern California was applied to UE model in REDARS (see Section 4.4.1), the effects of closed links to changes in route choice on freeways, as well as local streets are included in the estimated volumes on freeway segments. Therefore, although the comparison would be made for only freeway volumes, it is equivalent to a system-wide comparison. Section 5.5 presents a comparison of traffic volumes on local streets near the one of the collapsed sites.

5.4.1 Estimation of Freeway Traffic Volume using UE

Transportation network and trip demand data (Origin-Destination) for REDARS is provided by SCAG (Southern California Association of Governments). Figure 5-5 shows the extent of SCAG transportation network data. The data covers Los Angeles, Orange, and Ventura counties, and parts of Riverside, and San Bernardino counties with 22,444 links representing freeways, arterials and collectors. There are 7,787 nodes including 1,534 traffic analysis zone centroids.

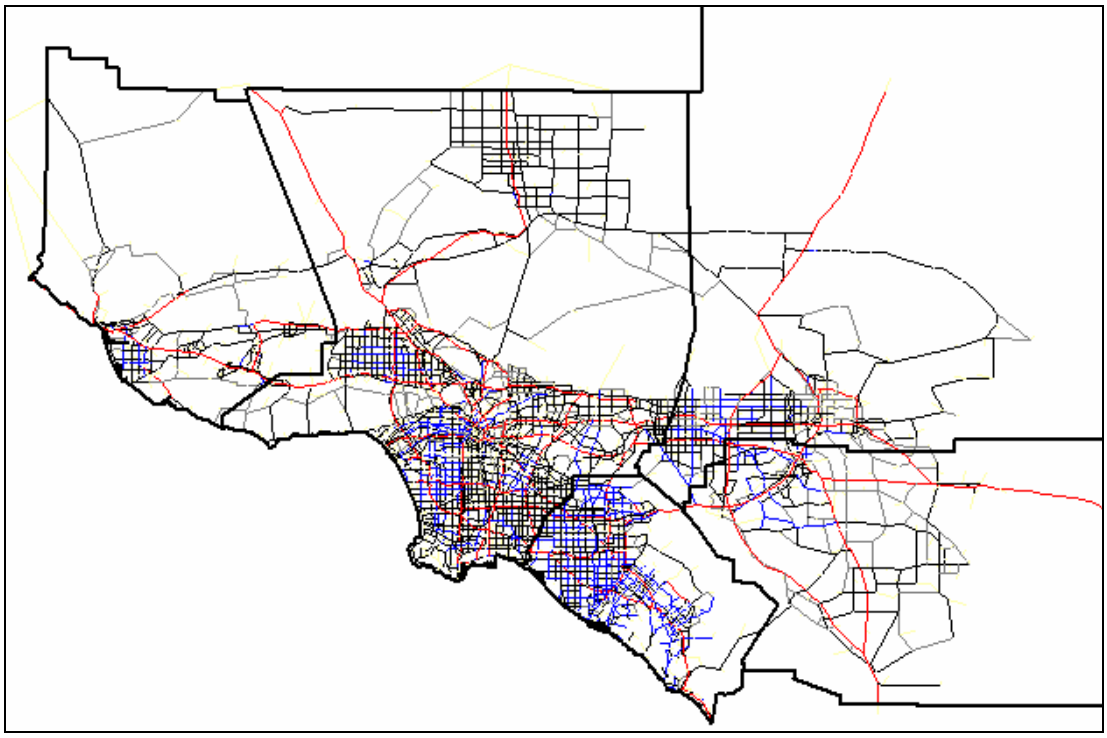

Figure 5-5 Transportation Network Data Applied to Estimate Freeway Traffic Volume Before and After 1994 Northridge Earthquake

For the purposes of this analysis, SCAG and OD data are converted to three-hour averages. Since the observed volume is for 24 hour periods, and REDARS results are for three hour periods, a direct 1:1 comparison of the observed volume and estimated volume is not possible. Linear correlation coefficients (R2) were used to quantify the degree of similarity between the REDARS results and actual traffic counts.

5.4.2 Observed Freeway Traffic Volumes

Vehicle traffic volumes for the ten locations in Figure 5-5 were counted for the 24 hours immediately following the 1994 Northridge. Comparable traffic volumes were obtained for the same locations one-year before. As shown in Table 5-2, freeway volumes range between 100,000 and 400,000 vehicles per day under normal traffic conditions. The earthquake and resulting bridge damage severely impacted these traffic volumes, which dropped to between 2,000 and 300,000. In Table 5-2 reduced volumes were observed for all freeway segments except segment G. Part of the reason for this discrepancy may be because a complete accounting of traffic (pre-earthquake) on the I-105 was not available due to its recent completion just before the earthquake.

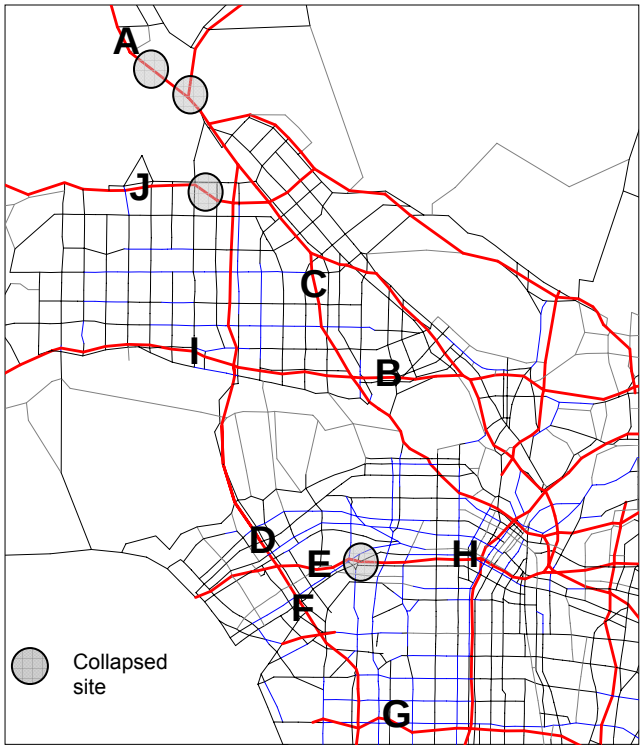

Source: Caltrans (1995), ibid, p44.

Figure 5-6 Volume Count Locations (Circles represent collapsed bridge sites)

Table 5-2 Freeway Traffic Volumes Before and After the Northridge Earthquake (AADT)

Location		Pre-earthquake volume (Jan. 1993)	Post-earthquake volume (Jan. 1994)
A	I-5 on North of SR-14	129,000	2,000
B	SR-143 East of SR-101/SR-170 Junction	212,000	202,000
C	SR-170 North of SR-101 (Southbound only)	145,000	120,000
D	I-405 North of I-10	333,000	265,000
E	I-10 East of I-405	262,000	55,000
F	I-405 South of I-10	312,000	265,000
G	I-105 East of I-405	177,000	200,000
H	I-10 West of I-110	388,000	200,000
I	SR-101 West of I-405	318,000	315,000
J	SR-118 West of I-405	121,000	40,000

Source: Caltrans (1995), Northridge Earthquake Recovery Report

5.4.3 Comparison of Freeway Traffic Volumes

For the pre-earthquake condition, the results in Figure 5-7 indicate that REDARS predicts with accuracy of more than 93% of the observations (R^2=0.9314). The coefficient should not be assumed to be 1, due to the different units of volume measurements (24- versus 3-hour volumes). Immediately after the earthquake, approximately 80% of the volume is predicted by the user equilibrium model. In either case, the REDARS traffic volume estimates closely match the observed traffic counts.

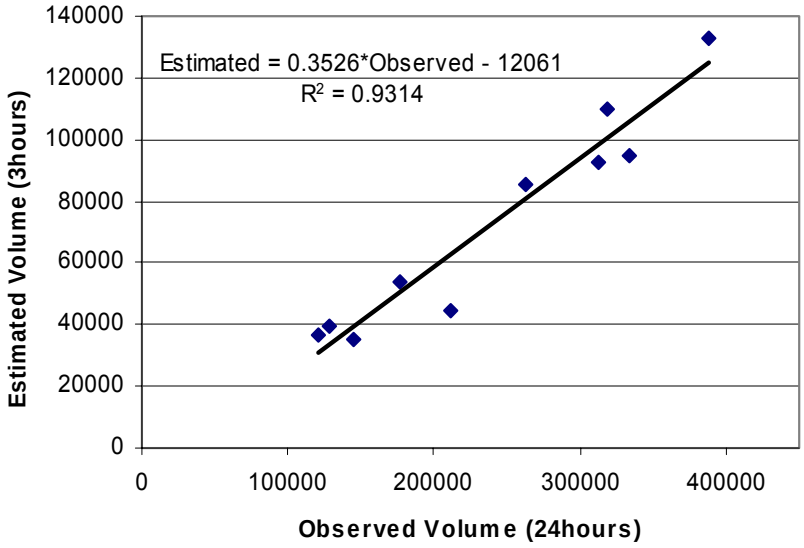

a) Before earthquake

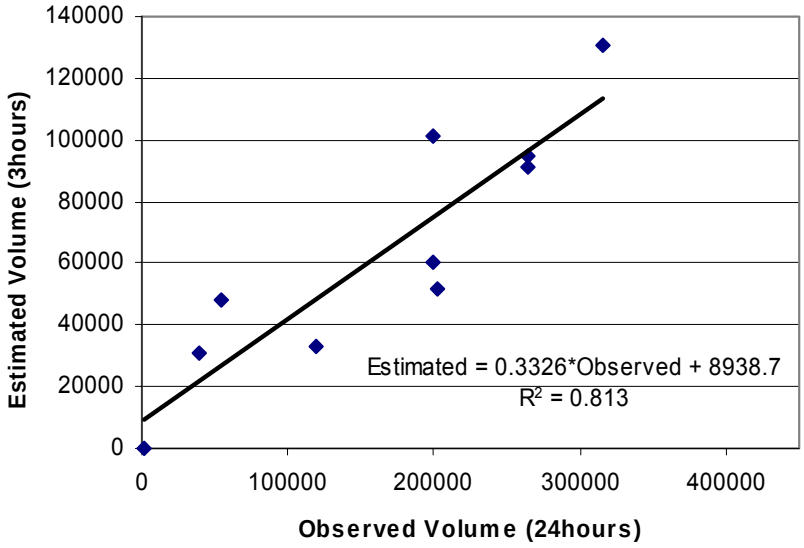

b) After earthquake

Figure 5-7 Comparison of Freeway Volumes

Even though the model uses three-hour time blocks instead daily traffic volume, the ratio of pre-earthquake to post-earthquake traffic volume should be identical to a similar ratio based on traffic volume observations, and directly comparable. The response of drivers to abruptly reduced network capacity leads to changes of route choice, and thus to a variation of link traffic volume between before and after earthquake conditions. If the UE model in REDARS adequately simulates the drivers' behavior, the estimated ratio of pre-earthquake and post-earthquake volume change should be identical.

The model estimates a higher increment in post-earthquake traffic volume than was actually observed. The graphical representation of estimated compared to observed volume-change ratio in Figure 5-8 shows that, in most cases, the estimated ratio lies above the 45-degree line. In reality, freeway volumes changed from 20-115%, with an average of 73%, between the baseline condition and after the Northridge earthquake. In contrast, REDARS estimates the percentage of post-earthquake volume to pre-earthquake volume to be between 55-120%, with a 95% average.

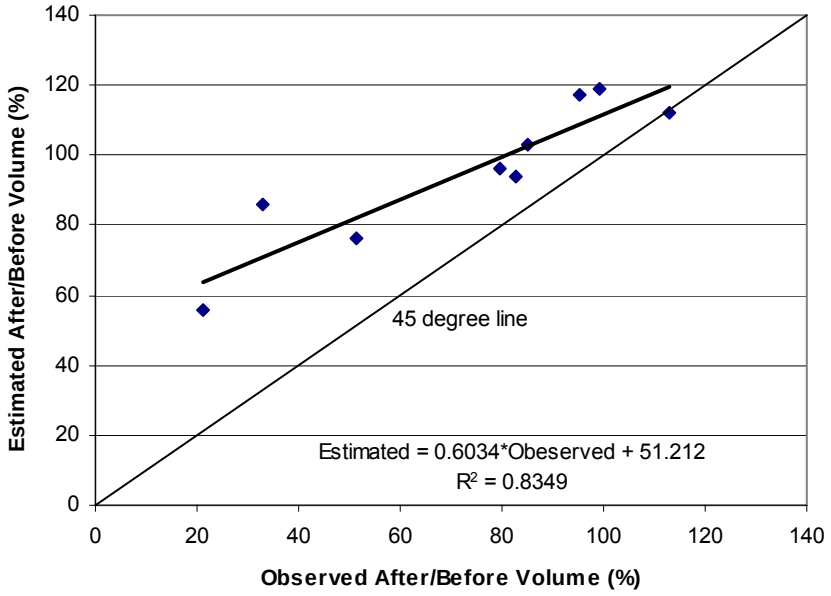

Figure 5-8 Comparison of REDARS and Observed Traffic Volume Ratios (Post-Earthquake/Pre-Earthquake)

For the entire system, REDARS estimates are highly comparable to the observed volumes. However, REDARS overestimates post-earthquake volumes by approximately 30%. Since system costs depend on travel time, and the travel time is proportional to the 4th power of the volume-capacity ratio (BPR function, Section 4.2), a small overestimation in traffic volume within a reduced-capacity system generates a significant overestimation of the system cost.

5.5. Traffic Volume Comparison on Local Streets near Collapsed Bridges

While the system-wide network performance (compared with freeway volumes in Section 4.4) is important to economic losses, local traffic patterns are also an important concern in transportation network analysis under seismic conditions because of emergency plans for evacuation and detour routes. In this section, REDARS estimates were compared with observed traffic volumes on arterials for the La Cienega Blvd and Fairfax Ave area, where two bridge decks on both directions of the I-10 collapsed. This particular interstate is among the most traveled freeways within the Southern California transportation system. Consequently, the effect of damage on this link was considerable.

For this comparison, more detailed sub-regional transportation data was established based on Tiger street databases from the Census Bureau of the Department of Commerce. The lack of detailed transportation data is a problem for local level comparisons such as this. After the Northridge earthquake, Caltrans established two detour routes:

- A small collector road (Apple Street near the I-10 at Fairfax Ave., and Washington Blvd.)
- A service road (near I-5, and SR-14).

However, the SCAG regional network data, used for freeway volume comparison, is not sufficiently detailed to analyze local traffic, because collector roads are usually omitted. The final network data that was established is presented in the next subsection, followed by subsections that review traffic count data, and compare results.

5.5.1 Transportation Data

The network data for the transportation model comprises an area 1.5 miles to the west of downtown Los Angeles. This area, shown in Figure 5-9, is bordered by Wilshire Boulevard to the north, Jefferson Boulevard to the south, Robertson Boulevard to the west, and Crenshaw Boulevard to the east. The collapsed bridges on I-10 are located within the area. The circled area in Figure 5-9a was extracted and converted to the transportation network data shown in Figure 5-9b. The network comprises 52 zones (26 internal and 26 external zones), 549 nodes, and 1553 directional links. This subset network topology (relative locations of links) was derived from the 1998 Tiger street line data. Link attributes, such as design speed and capacity, are assigned according to the functional category and population density around the link. For example, links with function types 1, 2, 6, and 7 and design speeds 55 to 65 miles are assigned to the freeways (see Appendix B for details).

Travel demand information was extracted from the 1990 SCAG OD database. The OD matrices were used to develop an OD for the sub-regional transportation network within the study area. First, the person-trip OD data, organized by trip purpose, are merged into one daily vehicle trip matrix. From the daily person trip demand, a 3-hour representative matrix is developed on a daily basis, for the entire 1527-zone region. From the regional OD data, a new small OD matrix for the 52-zone subregion is created by applying the OD sub-setting method.

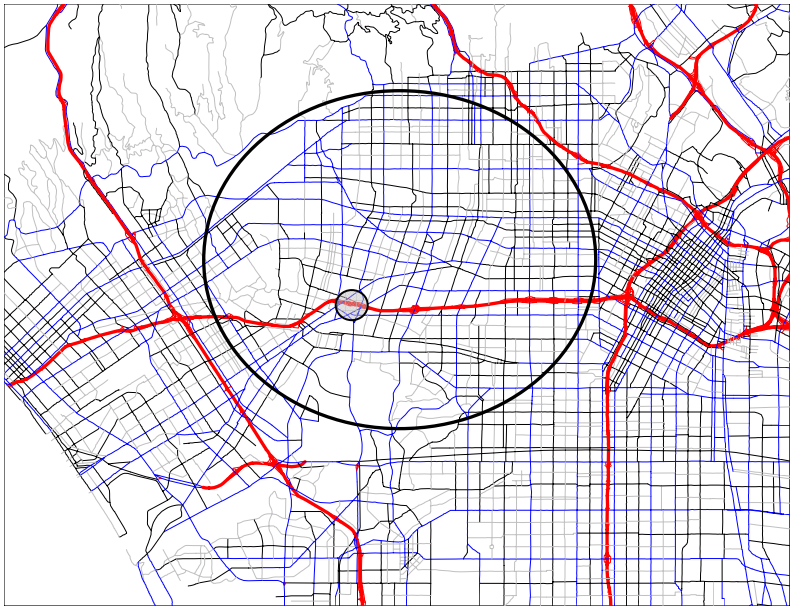

a) Study Area Depicted in the 1998 Tiger Street Map

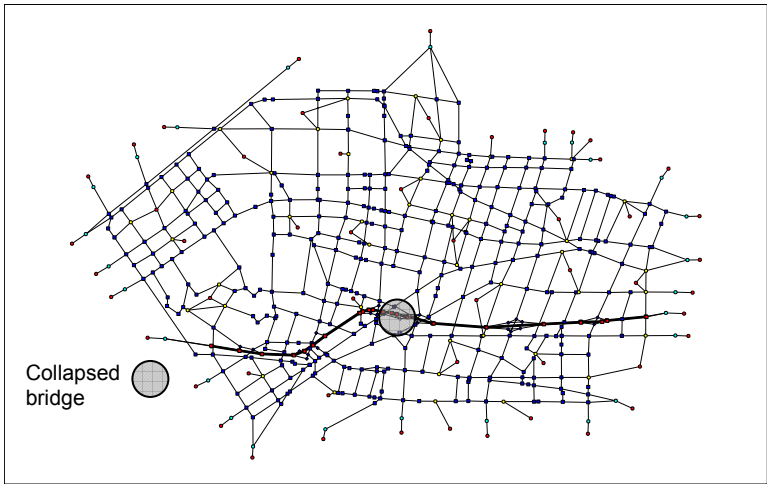

b) Network data

Figure 5-9 Network for the Analysis of Arterial Traffic

5.5.2 Count Data

Immediately after the 1994 Northridge earthquake, the Automated Traffic Surveillance and Control System (ATSCS) of City of Los Angeles Department of Transportation gathered arterial traffic volumes for 12 hours (January 18, 1994, from 7 AM to 7 PM). Table 5-3 shows pre-earthquake and post-earthquake traffic volumes on these arterials.

Table 5-3 Pre- and Post-Earthquake Arterial Traffic Volumes (Vicinity of I-10 at La Cienega Blvd)

Street	Segment	Pre-quake Volume	February Volume	Percent of Pre-quake
La Brea Ave	Jefferson to I-10	38,000	38,000	100%
	I-10 to Venice	35,000	36,000	103%
	Venice to Wilshire	35,000	33,000	94%
La Cienega Blvd	Jefferson to I-10	26,000	23,000	88%
	I-10 to Cadillac	54,000	54,000	100%
	Cadillac to Wilshire	29,000	26,000	90%
Robertson Blvd	I-10 to Washington	15,000	16,000	107%
	Washington to Cadillac	38,000	38,000	100%
	Cadillac to Pico	33,000	34,000	103%
	Pico to Wilshire	27,000	27,000	100%
Fairfax Ave	La Cienega to I-10	28,000	21,000	75%
	I-10 to Venice	31,000	22,000	71%
	Venice to Wilshire	17,000	17,000	100%
Washington Blvd	Crenshaw to La Brea	20,000	20,000	100%
	La Brea to Apple	16,000	14,000	88%
	Fairfax to La Cienega	13,000	26,000	200%
	West of La Cienega	15,000	13,000	87%
Adams Blvd	Washington to La Brea	13,000	15,000	115%
	La Brea to Crenshaw	18,000	18,000	100%
Jefferson Blvd	La Brea to La Cienega	17,000	31,000	182%
	West of La Cienega	17,000	31,000	182%
Venice Blvd	Crenshaw to La Brea	20,000	20,000	100%
	La Brea to Fairfax	26,000	26,000	100%
	Fairfax to I-10	27,000	26,000	96%
	South of I-10	41,000	39,000	95%
Pico Blvd	Crenshaw to La Brea	17,000	17,000	100%
	La Brea to La Cienega	21,000	22,000	105%
	La Cienega to Robertson	26,000	27,000	104%
Olympic Blvd	Crenshaw to La Brea	16,000	16,000	100%
	La Brea to La Cienega	28,000	29,000	104%
Cadillac Ave	Venice to La Cienega	19,000	19,000	100%
	La Cienega to Robertson	7,000	7,000	100%
Crenshaw Blvd	Jefferson to I-10	34,000	34,000	100%
	I-10 to Pico	27,000	26,000	96%
	Pico to Wilshire	24,000	24,000	100%
Apple St	Washington to Fairfax	13,000	12,000	92%

Source: Caltrans Northridge Earthquake Recovery Report, 1995, p102.
Pre-earthquake volume = monthly average of Oct. 1993
Post-earthquake volume (February volume) = counted on Jan. 18, 7am to 7 pm.

The most significant traffic volume difference corresponds with a segment of Washington Boulevard where a bridge collapsed. Traffic volumes between Fairfax Ave and La Cienega Blvd on Washington Blvd doubled. However, other segments of Washington Boulevard show a 87% decline in volume compared to the pre-earthquake volume. Increases in the volume are also found on the Jefferson Boulevard, which is two blocks south of I-10. Volumes on Robertson Blvd, Pico Blvd, Olympic Blvd, and Cadillac Ave increased slightly, or showed no significant change. Despite abrupt increases in traffic volumes for specific road segments near the collapsed site, these results indicate that, many corridors did not experience significant volume increase. In the absence of guided detours (which were not established until February 1, 1994), these counted volumes reflect drivers' initial response to an altered network.

5.5.3 Comparison of Local Traffic Volumes

Figure 5-10 summarizes the pre-earthquake and post-earthquake conditions of the observed and estimated traffic volumes. The user equilibrium model in REDARS estimates pre-earthquake traffic volumes with a linear trend against observed 12-hour traffic counts[7].

The R^2 value of 0.75 is surprisingly high considering the size of the network data. Precise link volume estimation requires a highly disaggregated zone system. Various combinations of zone pairs could generate results close to observed changes in link volume. In the SCAG transportation network shown in Figure 5-5 and Figure 5-6, the ratio of the number of links to the number of transportation analysis zones is 14. For the network used in this comparison, it is 29 (1,553/52). An amplified link to zone ratio implies that a greater number of routes connect the zones, and link volume is determined by a few interchanges between zone pairs. Considering this condition, 75% of accuracy is promising.

Unlike the pronounced linearity between baseline and pre-earthquake conditions, the REDARS model predicts only 45% (R2=0.4503) of the post-earthquake arterial volumes. As shown in Figure 5-10b, the low R^2 value[8] implies that additional random factors influence traffic volumes including uncertainty in whether drivers make trips and which routes they choose. REDARS cannot account for these factors.

The change in travel demand following the Northridge earthquake is a possible cause for the deviation between REDARS and observed values. As shown in Figure 5-7, the slopes of estimated and observed volume for both pre-earthquake and post-earthquake conditions on the freeway are stable at approximately 0.35. However, the slopes are 0.28 and 0.43 respectively for the arterial streets. This implies post-event volume was overestimated relative to pre-earthquake volume. One simple explanation for overestimation of post-earthquake volume is that the transportation model does not consider demand deformation due to a disaster or a reduced capacity. The following section further addresses the effect of reduced capacity.

[7] If the outlier point (volume from I-10 to Cadillac on La Cienega) is left out, the R^2 drops to 0.5986.
[8] If the two outlier-points are left out, the R^2 drops to 0.2846.

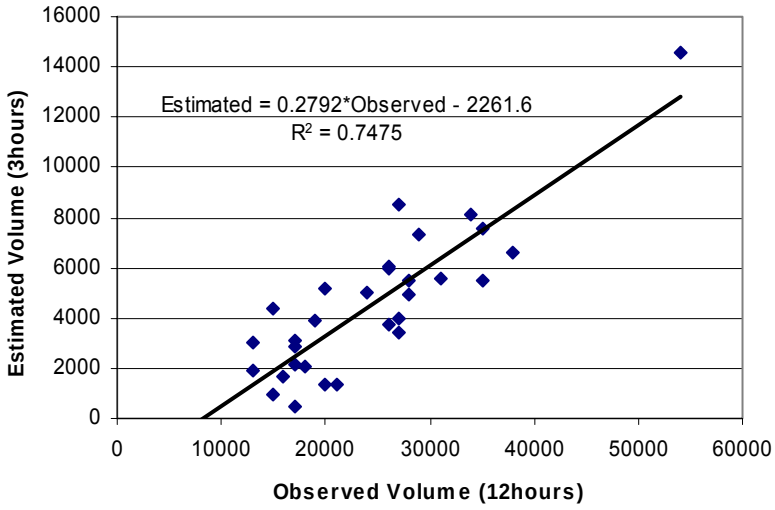

a) Before Earthquake Volume

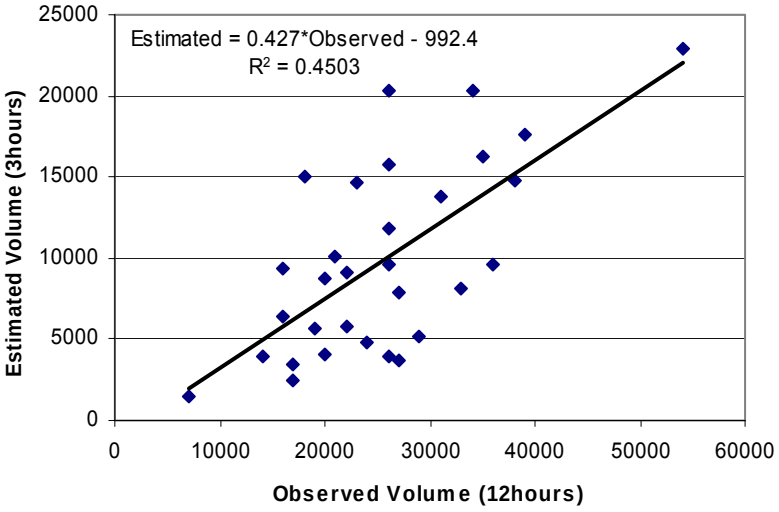

b) After Earthquake

Figure 5-10 Arterial Volume Comparison

5.5.4 Volume Change Ratios

To compare REDARS results with observed data, a ratio was calculated between volumes before and after the earthquake. In spite of the different time-base of these datasets, the estimated volume-change ratio should be comparable to the observed volume-change ratio. Volume-change ratios are depicted in two different ways by Figure 5-11. Figure 5-11a shows that the linear relationship between REDARS and observed volume-change ratios are not strong with $R^2 = 0.65$.

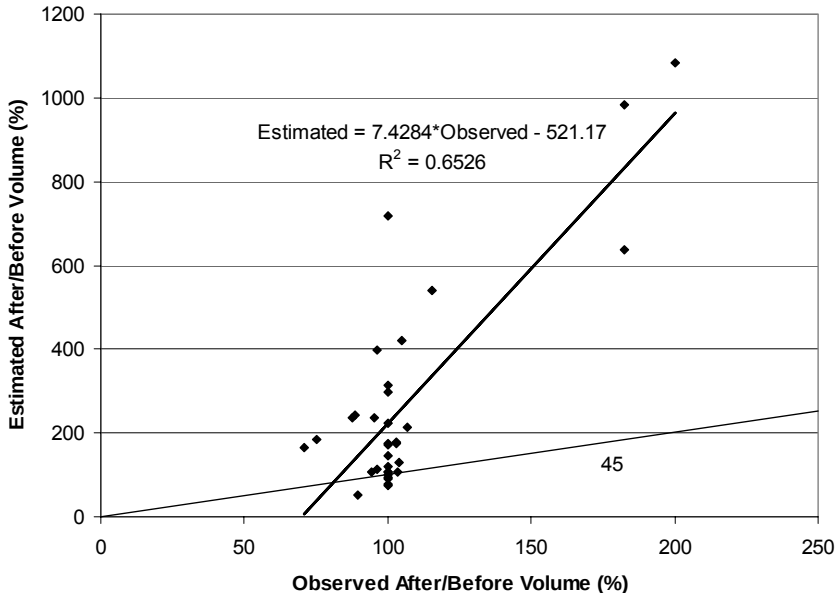

a) Linear Relationship Between Estimated and Observed Volume Change Ratios on Local Streets

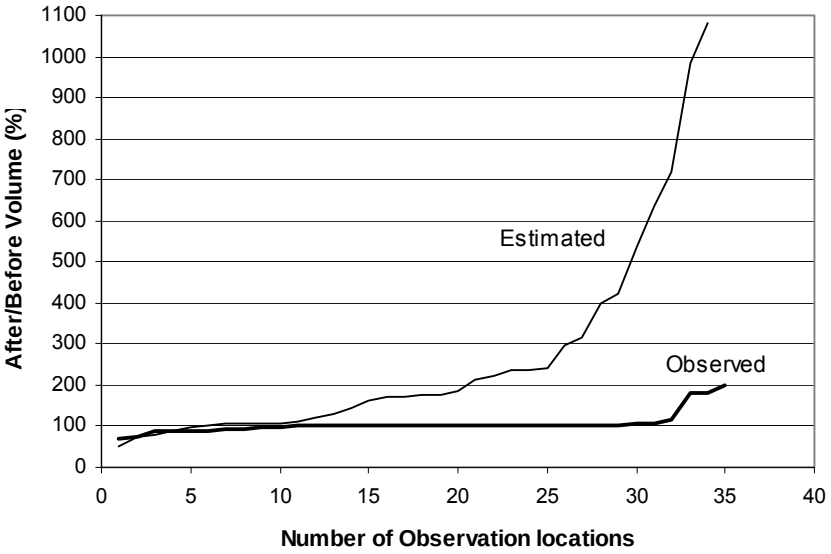

b) Number of Observation Locations and Volume-Change Ratio

Figure 5-11 Comparison of Estimated and Observed Volume Change Ratios on Local Streets

However, Figure 5-11b also indicates that the estimated volume-change ratio is consistently higher than the observed ratio. When compared with the pre-earthquake volume, only 33% of the locations observed had more than a ±10% change in observed traffic volume. Traffic volume counts at four locations increase up to 200% after the earthquake and volumes at six locations are

reduced compared with the pre-earthquake volume. From these results, REDARS estimates do not agree with observations. As Figure 5-11b indicates, REDARS generates only 12 post-earthquake link volumes that match the observed data to within 10%. The remaining link volume estimates are extremely high, ranging from 50 to 1,100% of the pre-quake traffic volume.

Unrealistic overestimation for post-earthquake volume was also noted during tests with the toy network. In Section 5.3, the toy network volume increment for links adjacent to the damaged segment is more than 300% of the pre-earthquake volume. Since the two estimations (with toy network and real-world network) agree with each other, tendency for overestimation for post-earthquake volume is consistent. In the observed data, the arterial traffic volumes actually remained very stable even though the bridges were collapsed.

A logical inference is that the system-wide reduction in total travel demand after an earthquake creates post-earthquake volume stability. A possible explanation for this reduction in the travel demand is reluctance to travel due to the increase in congestion levels. Driving ensues from various activities such as working and shopping. After a seismic event, the benefit from any given activity is uncertain and drivers lack information on road conditions, capacity, and increased travel times. If the uncertainty associated with travel cost exceeds the benefit from the activity, people might decide not to travel.

In the estimation of equilibrium traffic volume, the travel demand data (OD matrix) developed for the pre-earthquake condition is applied to the post-event network. REDARS assigns all demand to the network, regardless of whether the travel cost generated is realistic. REDARS should allocate demand to various alternatives, rather than concentrating demand on certain advantageous routes with reduced capacity. Overall, the volume estimated dramatically increases. In reality, this situation would not materialize, since demand cannot exceed capacity (although this can happen in the REDARS results) and drivers might postpone making trips under such high levels of congestion.

5.5.5 Effects of Detours on Results Deviations

Examining the pattern of estimated volume changes on specific routes reveals some important features of REDARS. From the observed data after the earthquake, traffic volumes on most routes decrease, while volumes on Olympic Blvd, Pico Blvd, Robertson Blvd, and Jefferson Blvd remain unchanged or increase insignificantly. According to this finding, drivers appeared to take longer detours to avoid the area surrounding the damaged location, causing the total system demand in the system to fall.

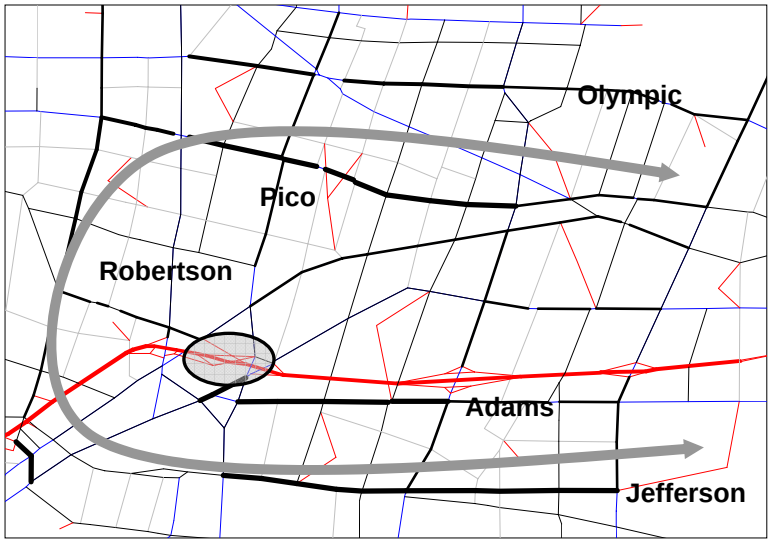

a) Observed Detour Route

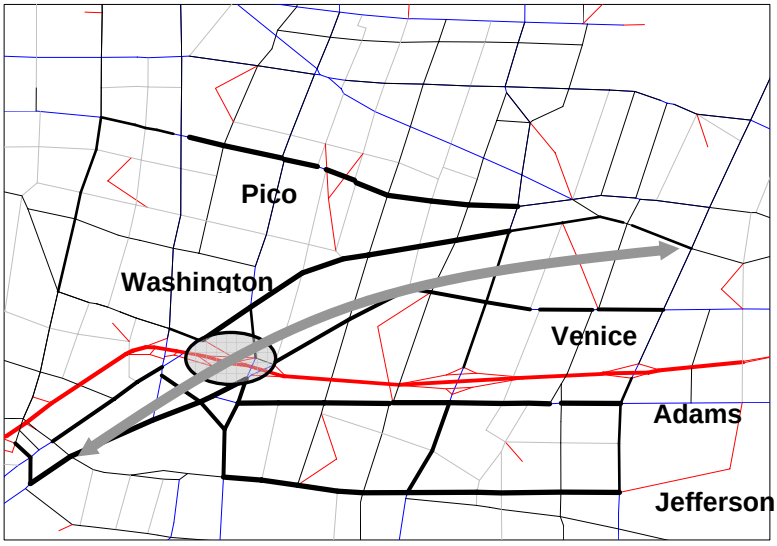

b) Model Estimated Detour Route

Figure 5-12 Travel Routes Following the Northridge Earthquake

In contrast, REDARS allocates the demand to localized or adjacent alternative routes to the closed route. Although REDARS estimated significant increases in the volumes on Jefferson Blvd, and Pico Blvd, the most apparent deviation of REDARS from the observed results is the rapid increase of volume on Washington and Venice Blvd. These are the two closest modeled corridors to the collapsed bridges and, as such, provide shorter travel times than the other routes.

The effects of this preferential route allocation were also observed in the toy network. The user equilibrium model works under the assumption that drivers have perfect information about the traffic situation, creating marginal changes in travel time when they change their route. Since

the observed data was recorded the day after the earthquake, drivers did not have time to adjust their routes due to condition. This discrepancy between the assumption that drivers have perfect information and reality may account for the difference between REDARS and observed traffic patterns. The inclination to avoid the damaged area is not modeled in the user equilibrium model of REDARS.

5.6. Effects of Inaccurate or Missing Network Attributes

In general, the reliability of modeling results improves with data accuracy. However, extremely accurate data is more expensive to produce or obtain. In general, transportation data are available from regional and federal agencies. Regional planning organizations develop network data for their own analytical purposes, which is of acceptable quality for REDARS. However, since there is not a standard format for transportation data exchange, compatibility problems may arise with respect to issues of accuracy, detail, and data format. Federal transportation data is also useful, as it provides extensive information for all US territories in a standard format. However, its compatibility with mathematical models, such as the one implemented in REDARS, is sometimes limited because network attributes required for analysis such as free flow speed and capacity may be absent. Additionally, this data needs to be formatted for modeling purposes, which is a costly process.

Knowledge on the effect of less accurate data on results is useful to validate the reliability of the analysis. To investigate the importance of accurate network data, the REDARS transportation network model was tested using modified network data with respect to missing links, and incorrect attributes. Results from the model were then compared with observed conditions.

5.6.1. Network Scenarios

This section presents several test scenarios with modified transportation network data. The following six network scenarios are analyzed for comparison with the observed traffic volumes:

Scenario 1: Unique free-flow speed and capacity are assigned according to the Highway Performance Monitoring System (HPMS) link classifications.

Scenario 2: For all local streets (except centroid connectors and freeways), the same free flow speed (30mile/hour) and capacity (700 pce/lane) are assigned, regardless of the link classification.

Scenario 3: For all local streets except centroid connectors and freeways, randomly generated values are assigned with a uniform distribution. The ranges are 25-40 miles/hour for free flow speed, and 400-800 pce/lane for capacity.

Scenario 4: All collectors are taken out of the network provided that they do not directly link zone centroids to the network. The same link attributes are assigned as in scenario 1.

Scenario 5: All collectors are taken out of the network unless they do not disconnect zone centroids if removed. The same link attributes are assigned as in scenario 2.

Scenario 6: All collectors are taken out of the network, unless they do not change the connectivity of the zone centroids if removed. The same link attributes are assigned as in scenario 3.

Table 5-4 Link Attributes for Subset Network

Link Classification	Free flow speed (Miles/Hour)	Capacity (PCE/Lane)
Centroid connectors	20	10,000
Freeway	60	2,000
Ramp	40	600
Major arterial	35	800
Minor arterial	30	600
Collector	25	400

The principal difference between scenarios 1-3 and scenarios 4-6 is network size. In the first three scenarios, the network attributes such as free flow speed, and capacity are disturbed for 1,553 links. Link attributes are not always readily available from data sources, and the user might assume values. Scenarios 4-6 are simplified subsets from scenarios 1-3 where local collector roads have been eliminated. Collectors represent small roads in blocks, and usually have low capacity and free flow speeds. In the model, collectors may be removed to simplify the network unless eliminating the collectors affects zone-to-zone connectivity. Scenarios 4-6 have 1,293 links and the network connectivity is intact.

5.6.2 Results of Comparison for an Unsophisticated Network

Table 5-5 summarizes results for the six scenarios. The R^2 values reveal several regularities. First, R^2 values corresponding with the volume-change ratio in column C are consistently higher (for all scenarios) than the R^2 for post-earthquake volume estimations in column B. It may therefore be deduced that the model is not particularly sensitive to the complexity of network data.

The results also suggest that simplified networks perform better than more complex ones, with R^2 values for Scenarios 4-6 notably higher than for Scenarios 1-3. The only difference between these groupings is the exclusion of the collector links in Scenarios 4-6. For areas with plenty of redundant capacity, simplified networks might perform better.

Overall, differences in R^2 between the base network, (with finely tuned attributes), and the network with incomplete link attributes, are not significant for the pre-earthquake volumes (96%-71% of baseline estimation). For the post-earthquake volumes, R^2 for an unsophisticated network volume is similar to the base network (Scenarios 1, 4 Table 5-5). If this degree of difference can be generalized, predefined link attributes can be used, without the time consuming

editing of attribute values. These preliminary tests therefore suggest that for urbanized areas, REDARS performs better with simplified networks. This assertion is a subject for further testing.

Table 5-5 R^2 for Volumes from Unsophisticated and Observed Network Volumes

Scenario	R^2: Pre-earthquake volumes (A)	R^2: Post-earthquake volume (B)	R^2: Volume-Change Ratio of After/Before (C)
1	0.5998	0.3824	0.6051
2	0.5314	0.2468	0.5604
3	0.5916	0.3015	0.4193
4	0.6267	0.3906	0.6221
5	0.7200	0.3341	0.5682
6	0.6352	0.3780	0.4286
Base Network	0.7475	0.4503	0.6526

5.7 Summary

Tests with the toy network user equilibrium model generally corroborated REDARS estimates of route choice behavior under reduced network capacity. The model estimates the diversion of traffic after bridge collapse. However, the increment of traffic on routes immediately adjacent to the damaged bridge is highly overestimated.

REDARS results and observed data for system-wide freeway volumes were compared. The model estimates higher post-earthquake traffic volumes than were actually observed. The ratio of average estimated volume-change ratio to average observed volume-change ratio yielded an overestimation factor of 1.3 (0.955/0.734). The estimated volume-change ratios for local street level conditions are higher than for the freeways. Traffic volumes observed at 36 locations near the La Cienega-Washington intersection show an increase in volume of more than 200% compared with pre-earthquake traffic. For local roads, REDARS results in an overestimation for the entire study area of 2.5 (2.650 / 1.053) for the ratio of average estimated to observed volume change. The highest factor of overestimation for any one location was 5.5 (1108% / 200%).

REDARS highly overestimates post-earthquake traffic volumes, which were observed to be relatively stable. In a transportation system with reduced capacity, traffic volume can be stable when demand is reduced proportionately to the capacity reduction. However, REDARS uses a single travel demand for both of pre-earthquake and post-earthquake conditions. Estimated post-earthquake route choice behavior does not match observations. While drivers took longer detours to avoid areas surrounding collapsed bridge sites, REDARS assigned a significant portion of detours to links next to the closed route.

SECTION 6
ECONOMIC LOSS MODEL

6.1 Introduction

This section reviews and summarizes the REDARS economic loss model. When an earthquake occurs, increased traffic congestion levels within the network system increases travel costs. The difference between pre-earthquake and post-earthquake travel times has an associated social cost. The economic loss model aggregates and translates this indirect social cost into monetary terms. Economic loss thus becomes a function of the severity of damage, the duration of link closure, and the congestion level. Performance of the REDARS methodology as a whole (models of bridge fragility, traffic state, and network) may therefore be judged by comparing results generated by the economic loss model (in US$) with recorded losses from the Northridge earthquake.

The following sections discuss the economic loss model:

- Section 6.2 reviews the structure of the economic loss model
- Section 6.3 compares REDARS economic loss estimates with those of Caltrans for 1994 Northridge earthquake.
- Section 6.4 reviews the probability distribution of the economic loss, based on the simulations of 217 system states (see Section 3.3).

6.2 Model Structure

The increment in traffic delay relative to the baseline delay time is converted to a monetary cost using a two-stage process. First, the daily travel cost for a given number of days after the earthquake is calculated, based on the network-wide system delay. And, its increment from the pre-earthquake network delay is calculated. The positive daily travel costs are then aggregated over the duration of the system recovery to give an economic loss measure.

As shown in Equation (12), total daily travel cost in US$ (C_{TOT}) is the sum of passenger and freight travel costs, together with additional gasoline costs. The increment in the system-wide travel time (X_1) is the sum of increments in passenger and freight shipment travel time, which have incomparable values of time (VOT). For passenger trips in cars, vehicle occupancy (passenger per vehicle, X2) and gasoline consumption (X6) are also considered:

$$C_{TOT} = C_1+C_2+C_3 \quad (12)$$
$$C_1 = X_1 \times X_2 \times X_4$$
$$C_2 = X_1 \times (1\text{-}X_2) \times X_3 \times X_5$$
$$C_2 = X_1 \times X_6$$

X_1: increase in total system-wide travel time (in units of hours) over a 24-hour time period at a given time after the earthquake
X_2: proportion of truck traffic to total traffic

X_3: vehicle occupancy rate for automobile traffic
X_4: economic cost of delay for trucks
X_5: economic cost of delay for person
X_6: cost of excess fuel per hour

The economic loss model in REDARS calculates daily costs at time periods of 7, 60 and 150 days after the earthquake. Once the increment of daily travel costs from the pre-earthquake condition for the predefined time-periods are calculated, all the increments are aggregated into an economic loss. This aggregation procedure is not programmed into the pre-beta version of REDARS.

Figure 6-1 demonstrates how the total cost is equivalent to the area below the lines that connect the increment of daily travel costs of these three time periods. The increment of daily travel cost is assumed to remain constant between immediately after to 7 days from the earthquake. Extrapolating the line that connects the points of the 60 and 150 day travel costs to meet the X-axis gives a point in time when daily travel cost is equivalent to the pre-earthquake baseline cost, i.e., no increment of travel cost.

Since REDARS uses a three-point estimate, infinite economic loss is a possible result. This occurs when the daily travel costs for 60 and 150 days are equal. Since the extrapolated line then is parallel to the X-axis, the area below the line is infinite. To prevent the estimation of infinite economic losses, the duration of recovery is assumed limited to 500 days.

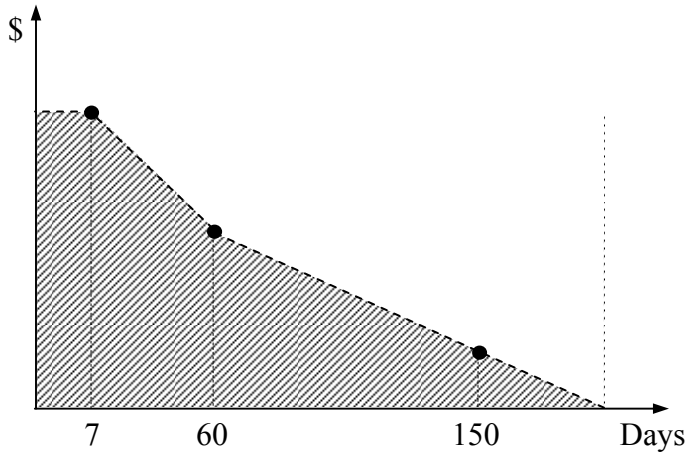

Figure 6-1 Economic Loss Over Increasing Time-Periods

6.3 Comparison of Economic Loss Estimations by REDARS and Caltrans

This section compares REDARS loss estimates to the Caltrans estimation for direct economic loss from transportation disruption due to 1994 Northridge earthquake. The Caltrans estimation is basically accounting for additional travel cost –as a result of the collapse of bridges around the following three locations:

- I-10 on La Cienega-Washington.

- Interchange between I-5 and SR-14.
- SR-118 on Gothic Ave - Bull Creek bridges.

While the Caltrans estimation was limited to those three collapsed areas, REDARS estimation considers the effects of system-wide bridge damage.

Based on the coefficients for converting the delay time to a dollar value suggested by Caltrans[9] and SCAG[10], REDARS estimates the total economic loss. Table 6-1 presents the related coefficients and their sources, and Table 6-2 shows the intermediate calculations.

Table 6-1 Coefficients and Data Sources for the Economic Model

Coefficients		Value	Source
X_2	Proportion of truck traffic	0.04	- 1997 Model Validation & Summary from SCAG - Heavy Duty Truck Model and VMT Estimation from SCAG.
X_3	Vehicle occupancy rate	1.46	1990 OD Survey from SCAG
X_4	VOT of a truck	$19.20	Northridge Earthquake Recovery Report, Caltrans (1994)
X_5	VOT of a person	$6.0	
X_6	Gasoline price per hour	$1.1	

In Table 6-2, column A shows the REDARS transportation model estimates. The REDARS economic loss model converts the system-wide travel time to economic values for each time period (column B), and calculates the difference from the baseline economic values (column C). The time before the transportation system would be fully recovered was estimated to be 158.94 days after the earthquake, according to the gradient between the variations of economic values for 60 days and 150 days. Based on the intermediate calculations, the model estimates $1,099,741,347 of direct economic loss (approximately $1.1 billion).

[9] Caltrans (1995), Northridge earthquake recovery report - Final comprehensive transportation analysis
[10] SCAG, 1997 Model Validation & Summary

Table 6-2 Calculation of Economic Loss in REDARS

	System-wide travel time (hours / day) (A)	Economic value of travel time ($1,000 /day) (B)	Variation of economic value from baseline ($1,000/day) (C)
Baseline	2,083,974	20,938	-
7 days after	4,398,674	44,194	23,256
60 days after	2,504,081	25,159	4,221
150 days after	2,121,926	21,319	381

The actual social cost to Los Angeles drivers was much lower than REDARS predicted. Caltrans estimated daily delay costs while detours were in place of $0.23 - $1 million for the three locations with collapsed bridges (on I-10, SR-118, and I-5/SR-14). By assuming that the delay cost is twice as much before the detours were established, and that route choice is based on the personal experiences of the drivers, the total delay cost is estimated to be $220 million (Table 6-3). Apart from the three collapsed bridge locations, Caltrans did not evaluate the economic impact due to less than severely damaged bridges that recovered quickly.

Table 6-3 Delay Cost Per Bridge Collapse After the Northridge Earthquake

Location	Days before Detour Opened	Days Detour used	Delay cost per days during detours used	Total delay cost up to the bridges reopened
I-10	11	70	$999,000	$91,908,000
I-5/SR-14	14	109 (I-5) 160 (SR-14)*	$436,000	$70,850,000
SR-118	0	228	$238,000	$54,264,000
Sum				$217,022,000*

Source: Caltrans (1995) Northridge Earthquake Recovery Report – Final Comprehensive Transportation Analysis

* Delay cost before detours were opened is assumed to be twice of the cost incurred once the detour was in use. For the period after I-5 was opened but the SR-14 detour was still in use, 50% delay costs were assumed.

The discrepancy between REDARS results and Caltrans loss estimates may in part reflect differences in coverage. While Caltrans focused on daily costs surrounding the three collapsed bridge locations, REDARS estimates network-wide economic loss. Although the effect of a link closure diminishes with network distance, the effect from collapsed bridges should not be discounted in this case because the three segments of closed links play very important roles in

operations, and their effects were system-wide. For example, the I-10 accommodates the heaviest daily traffic volume in Southern California, and the area around I-5 / SR-14 intersection provides very little redundancy. Thus, the effects of damage in both of these locations are significant throughout the network. Given that Caltrans estimates do not consider network-wide impacts, the $220 million of observed losses should arguably form the lower boundary for economic loss calculations.

REDARS does not consider several significant economic loss items that, on the basis of the Northridge earthquake, have a major impact on the indirect social cost. These include:

- Effects on production activity.
- Repair cost of bridges.

Production activity is affected by difficulties experienced in goods transportation. Higher transportation costs lead to increased input prices, and a reduction in output. The impact on production propagates across the economic system, due to strong industrial linkages between sectors. The repair cost of bridges qualifies as a social cost, because the highway system is a 'public good,' and its maintenance requires public revenue. However, repair subsidies from outside the region serve as a 'foreign investment,' that might have a positive effect on the regional economy.

6.4 Distribution of Economic Loss

As noted in section 3.2, 217 system states were developed using the REDARS bridge fragility model. These system states were analyzed sequentially in REDARS to calculate economic loss. This section provides further investigation into the distribution of the economic loss estimates.

Figure 6-2 shows the distribution of economic losses for the 1994 Northridge earthquake estimated by REDARS SRA methodology. The economic loss follows a stepped distribution, with each step of the curve near horizontal or flat. Economic losses range from $34 million to $1,735 million. 65% of the simulations have an economic loss of roughly $1,200 million (point a).

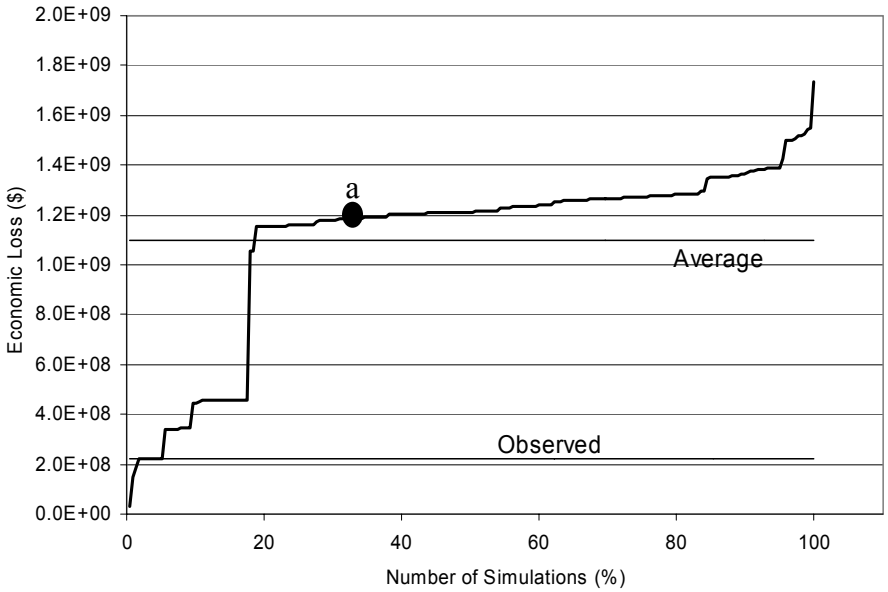

Figure 6-2 Distribution of Economic Losses Estimated for Northridge Earthquake

This stepped distribution corresponds with the profile of daily travel costs for each time period (see Figure 6-3), which is estimated by the transportation network model. Although the remaining bridge capacity has a continuous profile (see Figures 4-2 and 4-4), the transportation network model estimates discontinuous system cost increments.

Two explanations are possible for the discontinuity in system-wide travel time estimation, and as a result, the economic loss distribution.

First, the links and bridges have a one-to-many relationship. Therefore link capacity does not necessarily correspond directly to remaining bridge capacity. The link capacity is instead determined by the particular damaged bridge that has the smallest remaining capacity. Under such a condition, 'one more' bridge closure does not cause an additional reduction of link capacity.

Second, the effect of link closure on travel cost is nonlinear. Link usage differs according to the spatial concentration of demand. Freeways surrounding central business districts are used more than those in outlying areas. The effect of two link closures on travel cost is not twice that of one link closure. Closing an important, heavily utilized link may have a greater impact on the system cost than closing a redundant link.

If network configuration has an explicit relationship with the economic loss, categorizing the network configurations with respect to which important bridges are damaged, would simplify the seismic risk analysis procedure. Once causality between the economic loss value and the network configuration (or importance of links prior to the analysis) is established, the economic loss may be approximated, without running the time intensive traffic model.

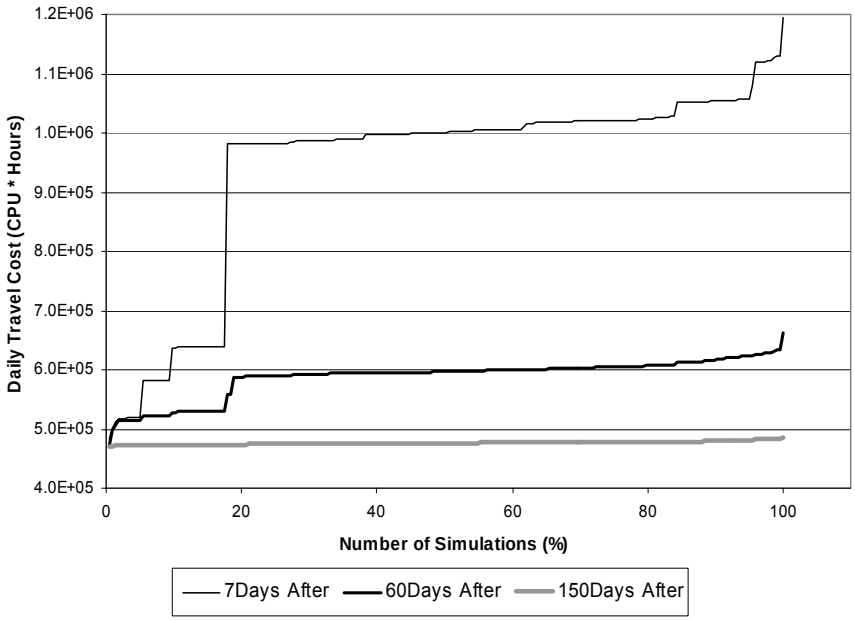

Figure 6-3 Distribution of Estimated Daily Travel Costs for Northridge Earthquake

Development of a probability distribution would be another way to simplify the analysis process. A cumulative probability distribution of the economic loss can be developed, based on the stepped economic loss distribution. Together with the aggregated economic loss, daily travel costs for each of the time-periods are converted to a probability distribution, using a form of sigmoid curve. For example, Figure 6-4 shows the cumulative probability distribution of the economic loss estimate, overlaid with a best-fit Logistic curve. Developing this type of probability distribution before running the transportation network model would simplify the REDARS economic loss estimation process.

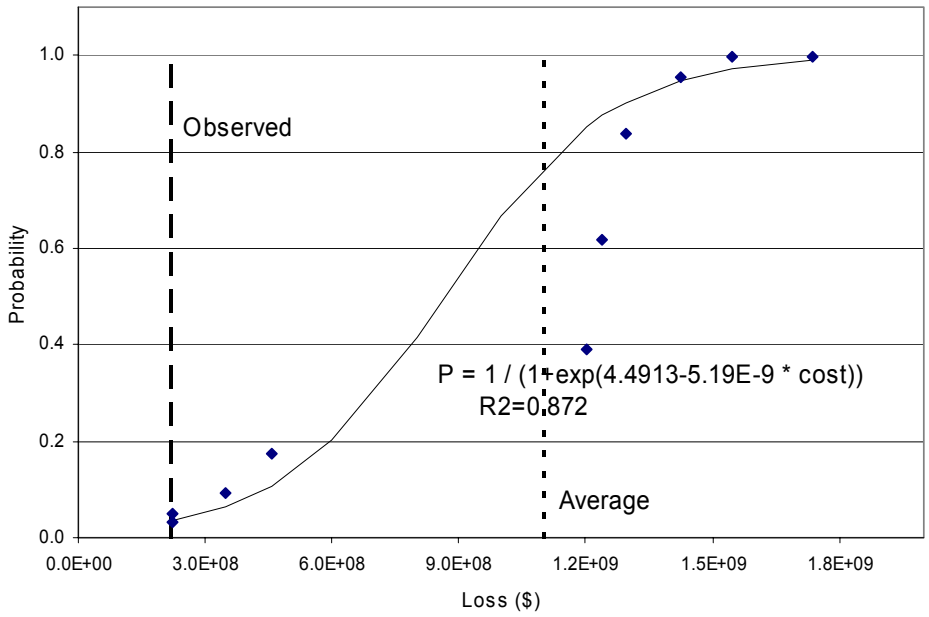

Figure 6-4 Cumulative Probability Distribution of Economic Loss for Los Angeles Transportation Network

6.5 Summary

In this section, the REDARS economic loss model was compared to the Caltrans estimation for 1994 Northridge earthquake. Using an identical set of coefficients, REDARS estimates $1.1 billion loss, while the Caltrans estimation is about $220 million. Since the Caltrans estimation focused on the additional detour costs around the three sites of collapsed bridges, its estimation should be regarded as a lower bound of economic loss from Northridge earthquake.

Estimated economic losses from stochastic analysis of REDARS are distributed in steps. Therefore, simulated network configurations can be categorized into each of the corresponding groups (or steps). This is due to the nonlinearity between bridge damage states, link functionality, and system-wide travel cost. Categorizing system states would support the possibility of a systematic approach to reduce computing time for estimating economic loss, without running the costly transportation analysis model for every network configuration.

SECTION 7
KEY FINDINGS AND RECOMMENDATIONS

7.1 Key Findings

The REDARS software program estimates the economic impact of earthquakes on transportation networks by evaluating damage to bridges and modeling subsequent impacts on traffic flow. The component models in REDARS:

- Estimate ground motion from a given earthquake.
- Calculate bridge damage states from the given ground motion.
- Convert the bridge damage states into traffic states.
- Analyze additional travel costs under damaged network configurations.
- Aggregate the increased travel cost into an economic value.

Each of these component models are reviewed and evaluated in the present study. The following sections summarize overall performance, as well as findings from each of component models.

7.1.1 Overall Performance of REDARS

In general, the results indicate that REDARS is a conservative tool for seismic risk analysis of transportation networks. Tests establish that REDARS responds stably and linearly to the variation of some input variables. REDARS estimates are higher than observed values with respect to the number of damaged bridges, duration of bridge closures, traffic volume on freeway and local streets, and most importantly, economic loss. Further study revealed that over-estimation of the severity of bridge damage propagated throughout the process.

Estimation errors from the bridge fragility, traffic state and transportation network models cumulatively influence the economic loss computed by REDARS. Figure 7-1 summarizes the performance. Twice the number of damaged bridges, longer bridge closure durations, and up to three times higher link traffic volume estimates, results in five times higher economic loss than actually occurred after the Northridge earthquake. In addressing this overestimation, the bridge fragility and transportation network models require further detailed review.

While the current structure of the traffic state model and economic loss model are simple—aggregating the delay costs produced by other model components—these two models were developed on the basis of concrete theories, and improvement of the component models might require serious debates. Due to the sequential structure of REDARS, bridge fragility and transportation network models are also important independently.

However, the results require careful interpretation because they are generated from only one particular event (the 1994 Northridge earthquake), in a single location (Southern California). The results may not be transferable to other locations or events with different characteristics (intensity).

Detailed findings are presented below for each model component, as computed using TriNet ground motion data (released on March 7, 1997).

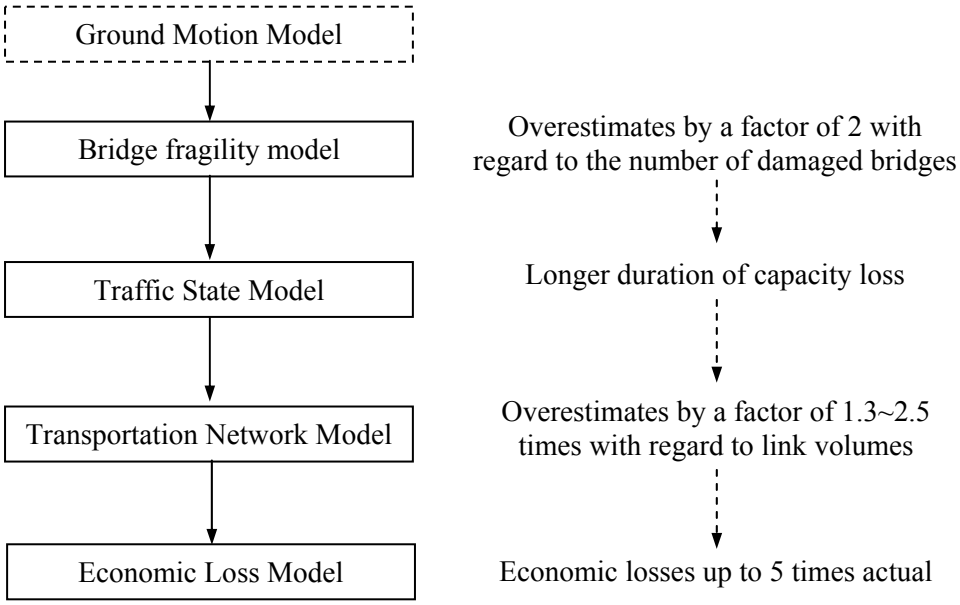

Figure 7-1 Overall Performance of REDARS

7.1.2 Bridge Fragility Model

- The fragility curves developed by REDARS are similar to Mander fragility curves. The difference in the inflection points is due to the low uncertainty for spectral capacity, and different probability distribution implemented in REDARS.

- REDARS estimates higher fragility than observations from the 1994 Northridge earthquake, in terms of the number of damaged bridges. The model estimates 363 damaged bridges out of 940 bridges, seven days after the earthquake. 190 out of the same 940 bridges were actually damaged immediately after the earthquake,

- Observation-based fragility curves are less than 2-standard deviation from the mean fragility estimated by the REDARS probabilistic analysis when ground motion input (spectral acceleration at 1.0 second) is higher than 0.4g. Therefore REDARS estimation of bridge fragility is significantly higher than reality, specifically when on-site ground motion is high.

- Model results are highly dependent on various uncertainties that are not considered in the methodology. These uncertainties include: the probability distribution of the observed displacements of the structural components; material strength for bridges; estimation errors of on-site ground motion, the soil amplification factor, and the AASHTO spectral response shape.

- The difference in the ground motion data for REDARS has a significant effect on results. Fragility curves based on TriNet PGA (released on March 7, 1997) do not match those based on USGS PGA (OFR-197-94).

- Lack of independent consideration of retrofitted bridge performance is one reason for the overestimation.

- When a scale factor is used to modify the ground motion input in REDARS, the estimated number of damaged bridges changes linearly to the factor. When the factor is 0.5 - 0.6, the predicted number of damaged bridges matches the number observed. Based on this finding, the bridge fragility model in REDARS overestimates the number of damaged bridges by a factor of two for the 1994 Northridge earthquake.

7.1.3 Traffic State Model

- For the Northridge scenario, REDARS estimates 10% of the 940 bridges will have less than 20% of their design capacity seven days after the earthquake. In addition, the residual capacity on the damaged bridges after 60 days is similar to that computed after seven days. This finding is unrealistic. In reality, observed recovery durations exhibit substantial variation.

- A possible reason is overestimation of damaged bridge frequency and the severity of damage by the bridge fragility model. Actually, to the observed bridge damage states, the traffic state model slightly underestimates the rate of reduction in bridge functionality. For example, only seven bridges (0.7% of 940 bridges) were estimated to be severely damaged for the first two months, and not fully recovered even five months later (point c and d), while in reality, 20% of 190 damaged bridges were closed more than 15 days after Northridge earthquake.

7.1.4 Transportation Network Model

- For the volumes on freeways in a region-wide transportation network, REDARS results and the counted volume are highly similar. The R^2 are 0.93, and 0.81 for pre- and post-earthquake network configurations respectively. Comparing volume-change ratios (post-earthquake volume: pre-earthquake volume), REDARS results show a linear relationship with actual observations.

- Observed traffic flows immediately after the Northridge earthquake show that traffic demand in the sub-regional network declined, and therefore the volumes on the intact local arterials exhibited little change, although no traffic was allowed on closed freeway links. However, REDARS uses identical travel demands for both pre- and post-earthquake network configurations, which is unrealistic.

- REDARS predicts that local link volume changes may exceed by 10 times the pre-earthquake volume, which is not possible in reality. These results are obtained because the model does not restrict link volume up to its capacity.

- REDARS results demonstrate that the links immediately adjacent to the collapsed bridge site have comparative advantages over the other links, in terms of travel time. Those links are estimated to be heavily used in a post-earthquake situation. Immediately after the Northridge earthquake, observations show that drivers took long detours to avoid collapsed bridge sites. This finding proves that the transportation model in REDARS does not correctly account for travelers' response to the earthquake-damaged network.

- Variations in the link attributes, such as free flow speed and capacity, do not have a significant impact on REDARS results. In general, performance of the transportation network model is more effective where the network comprises fewer links.

7.1.5 Economic Loss Model

- The economic loss model estimates $1.1 billion as the direct cost due to increased traffic congestion levels from the 1994 Northridge earthquake. Actual observations and data show the total cost to be $220 million.

- Estimated economic loss from damaged transportation network distributes with steps, in spite of the system states (bridge damage state), which distribute continuously. The step-wise distribution is due to nonlinearity between bridge damage state, link functionality, and system-wide travel cost. Based on this finding, all network configurations can be categorized into a limited number of groups for each economic loss step.

Table 7-1 summarizes the key findings from the components models.

Table 7-1 Summary of Key Findings

	How different from the observation	Why different	How sensitive to input
Bridge fragility model	o The model estimates 363 bridges damaged, while 190 bridges were damaged due to Northridge earthquake o Observed fragility is lower than 2-standard deviation from the mean fragility of the model result	o Uncertainties from - Observed displacements - Material strength - On-site ground motion - Estimation of soil amplification factors - AASHTO spectral response shape o Difference in ground motion data sources for calibration and validation of the model	o In terms of the number of damaged bridges, the model results are linearly sensitive to a scale factor applied to the ground motion input. o The model results match with observed data when the scale factor is 0.5~0.6
Traffic State Model	o The model estimates 91 bridges (9.6%) have less than 20% of the original capacity, while 7 bridges collapsed in reality immediately after the earthquake o Overall the duration of capacity reduction is longer than observation	o The model results cannot be generalized because of: - The lack of calibration data - Wide variation in terms of closure duration in the available data	o The model tested with observed bridge fragility to isolate the effect from bridge fragility model o Traffic states were slightly underestimated than observed.
Traffic Model	o Volume changes between pre and post earthquake conditions are overestimated by 30% for system wide freeway volumes, and 150% for the local street volume near a collapsed bridge site. o The model estimates the links adjacent to the closed bridge is the best alternative detour, while in reality, volume increments are observed in a wider area.	o The model does not take into account the reduction in travel demand o Route choice relies only on travel time.	o The model results are not so sensitive to unsophisticated network attributes such as the free flow speed, and the capacity when considering the pre and post-earthquake volume changes.
Economic Loss Model	o Model estimates 5 times higher social cost increment from the baseline condition	o In the model, the whole region was included in the travel cost calculation, while in reality, designated boundaries are considered around the collapsed bridges o Errors from other models affect this model results	N/A

7.2 Recommendations

To enhance the reliability and quality of the REDARS results, the component models require some improvement. Selected recommendations for future development and improvement, based on the key findings of this evaluation, are as follows:

- When publicly available ground motion data is used, various uncertainty factors need to be considered. The original methodology in REDARS considers several uncertainty factors throughout the procedure (uncertainties for attenuation of ground motion, soil amplification factors, and spectral capacity). However, if external ground motion data is used, the spectral capacity is the only uncertainty factor considered. The median PGA value estimated should be verified for this condition.

- Uncertainty factors in the bridge fragility model require further investigation. For example, it appears that the model is calibrated with the assumption that the available ground motion is deterministic. The fragility model can be refined by the consideration of stochastic characteristics from various observations.

- Designation of a ground motion data source in calibration and application of a bridge fragility model is required. Results from the bridge fragility model vary widely, depending on the ground motion data used. The development of a more flexible model should enable it to be used with various sources of ground motion data. However, in situations where such a model is not readily available, it would be recommended to designate a single source of ground motion data for the development, calibration, and application of the model.

- Results of the REDARS models are very specific to one event, in a particular location and are optimized by employing the data used during original model calibration. There are unified data sources available, such as the TriNet data, and the models using data sources other than those employed for calibration, should be recalibrated. Alternatively, there should be systemic methods for converting ground motion data from one source to match with a different source such as applying simple scaling factor.

- For the traffic state model, further research is required concerning the relationship between the importance of a link and the duration of bridge closure. Pre-earthquake traffic volume is an index to measure the importance of any particular link. Currently, the severity of damage and number of designed lanes are the parameters that determine the duration of bridge closure. However, it is reasonable to assume that if one link is more important than the others, repairs for the bridges on that particular link would be expedited.

- In the transportation network model, travel demand should be sensitive to the level of congestion. There was a reduction in the travel demand around collapsed bridge sites following the Northridge earthquake. Therefore the congestion levels did not change significantly though the system lost its capacity. However, in REDARS, one fixed demand (OD) is used in both the pre and post-earthquake networks. REDARS results generate an

unrealistic increment of link volumes in the post earthquake network. To produce realistic results, the model should account for the post-earthquake travel demand reduction.

- Investigation of a more realistic route choice model in the post earthquake network is required. For the Northridge case, wide and long detours were observed. Regardless of the additional travel time required for the longer detours, drivers chose to avoid collapsed bridge sites. The traffic model fails to demonstrate this behavior. Research is required concerning other types of path-finding algorithm that can account for such stochastic behavior.

- The transportation network model should be consistent with the other component models, in terms of running time. The bridge fragility and traffic state models take less than a few minutes to generate several hundred system state data files, while the transportation network model takes more than 8 hours to analyze them. This long and inconsistent running time can hinder the use of REDARS. Improving the algorithms and/or simplifying the procedures can reduce the running time.

- Categorization of the network configurations would be a way to simplify the seismic risk analysis procedure. The economic loss analysis from 217 simulations reveals that the distribution of the social costs can be grouped into fewer than ten categories. Once causality between the US$ value of economic loss and the network configuration, or importance of links prior to the analysis is established, economic loss could be estimated without running the time intensive traffic model.

- Other significant cost items need to be included in the earthquake economic loss model. Repair cost of damaged bridges, and business interruptions due to high transportation cost could prove top be important in the calculation of a thorough economic impact.

These findings and recommendations are specific to the 1994 Northridge earthquake and for southern California conditions. The validity of REDARS for other events and locations with different networks cannot be evaluated with any certainty. To generalize the findings, further investigations are required. These should include various network configurations, composition of soil types, different intensity and location of the earthquake events.

In addition to the generalization of the findings, parameter sensitivity analysis is required. Sensitivity tests for some of the component models are performed in the present study. Parameters are modified to investigate the effects on intermediate results for the component models. However, the degree to which each parameter affects the estimation of the economic loss remains uncertain. Unless the sequential structure of REDARS constituent models is revised, errors from each component will have a cumulative effect on the economic loss estimation. Each of the component models contributes to the existing differences between model results and actual observations. By investigating the combinatorial effects on the economic loss estimations, key parameters and their contributions to the results should be identified.

SECTION 8
REFERENCES

Basöz, N., and Kiremidjian, A.S., (1998), *Evaluation of Bridge Damage Data from the Loma Prieta and Northridge, California earthquakes*, Technical Report MCEER-98-0004.

Basöz, N., and Mander, J.B., (1999), *Enhancement of the Highway Transportation Lifeline Module in HAZUS*, Final Pre-Publication Draft.

Borcherdt, R. D., (1994) Estimates of site-dependent response spectra for design – methodology and justification, Earthquake Spectra, v. 10, pp. 617-653.

California Department of Transportation (Caltrans) (1994), *The Northridge Earthquake, Caltrans PEQUIT Report, Division of Structure*.

California Department of Transportation (Caltrans) (1995), *Northridge Earthquake Recovery Report - Final Comprehensive Transportation Analysis*, District 7, Division of Traffic Operations.

California Department of Transportation (Caltrans), *Northridge Earthquake Recovery Report - Weekly Transportation Report*, March 7 to July 8, 1994., District 7, Division of Traffic Operations.

California Department of Transportation (Caltrans), *Northridge Earthquake Recovery Report - Interim Transportation Report #1, #2, and #3*, January 17 to October 30, 1994, District 7, Division of Traffic Operations.

California Department of Transportation (Caltrans), *Northridge Earthquake Recovery Report - Home Interview Survey of Travelers Impacted by The Earthquake*, January 17 to October 30, 1994, District 7, Office of Operations.

California Department of Transportation (Caltrans), (1994), *Northridge Earthquake Recovery Report - Home Interview Survey of Travelers Impacted by The Earthquake*, District 7, Office of Operations.

California Department of Transportation (Caltrans), (1994), *Northridge Earthquake Recovery Report - Survey of Transit Riders of MetroLink Commuter Rail and Bus Routes*, District 7, Office of Operations.

California Department of Transportation (Caltrans), (1994), *Northridge Earthquake Recovery Report - Intercept Survey of Truck on Regional Travel Routes into Los Angeles*, District 7, Office of Operations.

California Department of Transportation (Caltrans), (1994), *Northridge Earthquake Recovery Report - Interstate 10 Recovery Report*, District 7, Office of Operations.

California Department of Transportation (Caltrans), (1994), *Northridge Earthquake Recovery Report - Follow-up Home Interview Survey of Travelers Impacted by the Earthquake*, District 7, Division of Traffic Operations.

Cho, S., Gordon, P., Moore, J.E. II, Richardson, H.W., Shinozuka, M., and Chang, S., (2001), Integrating transportation network and regional economic models to estimate the costs of a large urban earthquake, *Journal of Regional Science*, Vol.41, No. 1, pp.39-65.

Dutta, A., and Mander, J.B., (1998), *Capacity Design and Fatigue Analysis of Confined Concrete Columns*, Technical Report MCEER-98-0007.

Federal Emergency Management Agency (FEMA), (1997), *HAZUS99 - Natural Hazard Loss Estimation Methodology*, Chapter 4 (Potential Earth Science Hazards Methods), 7 (Direct Physical Damage To Transportation System).

Federal Highway Administration, National Bridge Inventory database, *http://www.fhwa.dot.gov/bridge/nbi.htm*

Federal Highway Administration, National Highway Planning Network, *http://www.fhwa.dot.gov/planning/nhpn*

Federal Highway Administration, Highway Performance Monitoring System Network, *http://www.fhwa.dot.gov/ohim/hpmspage.htm*

Friedland, I., Mayers, R., Bruneau, M., (2001), Recommended Changes to the AASHTO Specifications for the Seismic Design of Highway Bridges (NCHRP Project 12-49). http://mceer.buffalo.edu/publications/resaccom/0001/rpa_pdfs/05freidland_final.pdf

Greenshields, B., (1935), "A Study of Traffic Capacity", *Proceedings of the Highway Research Board*, Volume 14, pp. 448-477.

Joyner, W., Boore, D., (1988), Measurement, Characteristics and Prediction of Strong Ground Motion, State-of-the-Art Report, Proceedings, *Specialty Conference on Earthquake Engineering and Soil Dynamics II – Recent Advances in Ground Motion Evaluation*, ASCE, Park City, Utah, pp.43-102.

Joyner, W., Boore, D., and Fumal, T., (1997), Equations for Estimating Horizontal Response Spectra and Peak Acceleration from Western North American Earthquakes: A Summary of Recent Work, *Seismological Research Letters*, Vol.68, January/February.

Mander, J.B., Dutta, A., and Kim, J.H., (1998), *Fatigue Analysis of Unconfined Concrete Columns*, Technical Report MCEER-98-0009.

Park, S. and Ellrick, S., (1998) Predictions of shear wave velocities in southern California using surface geology, **88**, 677-685.

Sheffi, Y., (1985), *Urban Transportation Networks: Equilibrium Analysis with Mathematical Programming Methods*, Prentice Hall, Englewood Cliffs NJ.

Somerville, P., Saikia, C., Wald, D., and Grave, R., (1996) "Implications of the Northridge Earthquake for Strong Ground Motions from Thrust Faults." BSSA Vol. 86, No. 1B (Feb) S115-S125.

Southern California Association of Governments (SCAG), (1991), *1990 OD Survey Findings*.

Southern California Association of Governments (SCAG), (1997), *1997 Model Validation & Summery - Regional Transportation Model.*

Southern California Association of Governments (SCAG), (1998), *Heavy Duty Truck Model and VMT Estimation*.

TriNet shake map, http://www.trinet.org

USGS, "Seismograms from the Interactive Deaggregation Web page", http://eqint1.cr.usgs.gov/eq/html/Stochastic_Seismgram_Theory.html

USGS, Maps of peak horizontal and vertical accelerations recorded for the Northridge, California, earthquake of January 17, 1994 and general geology of the epicentral region, compiled by C.M. Wentworth, R.D. Borcherdt, R.K. Mark, and D.M. Boore, http://wrgis.wr.usgs.gov/open-file/ofr94-197/

Walton, J.S., Cho, S., Werner, S.D., Moore, J.E. II, and Taylor, C.E., (2000), *User Manual, REDARS 1.0 - A Computer Program For Evaluation of Risks From Earthquake Damage To Roadway Systems*, MCEER.

Wardrop, J., (1952), "Some Theoretical Aspects of Road Traffic Research", *Proceedings of Institute of Civil Engineering*, Volume 1, Number 2, pp 325-378.

Werner, S.D., Taylor, C E., Moore, J.E. II, Walton, J.S., and Cho, S., (2000), *A Risk-Based Methodology for Assessing the Seismic Performance of Highway Systems*, Technical Report MCEER-00-0014.

Yashinsky, M., Hipley, P., and Nguyen, Q., (1995), *The Performance of Bridge Seismic Retrofits During the Northridge Earthquake*, Caltrans Office of Earthquake Engineering.

APPENDIX A
CALCULATION STEPS FOR REDARS FRAGILITY MODEL

The project team reprogrammed the bridge fragility model of REDARS methodology in Microsoft Excel. This was done to use external ground motion data from the Northridge earthquake, instead validating REDARS with a ground motion attenuation model for the mid-west United States. This appendix provides detailed procedures implemented in the spreadsheets. This independent implementation of REDARS SRA methodology from its developers should be verified.

Incorporating the REDARS methodology into a spreadsheet involved the 13 steps outlined below, which are documented in full by REDARS Technical Report (MCEER-00-0014). Several departures from the exact procedure should be noted. Steps relating to calculation of the demand surface motion (on-site ground motion) are either omitted (Steps 1, 2 and 11), or replaced (Steps 3 and 4) using observed TriNet ground motion data and mathematical calculations to convert bedrock to surface motion.

Step 1. Calculate bridge distance from the earthquake epicenter (in kilometers)

$$R = \sqrt{\left\{\left(x_e - x_b\right)^2 + \left(y_e - y_b\right)^2\right\}} / 1000$$

- x_e, y_e : coordinates of epicenter in meters
- x_b, y_b : coordinates of bridge in meters

- Coordinates are State plane in meter
- Assumed 10km in depth for the Central US
- Note: this step is not used for the Northridge earthquake

Step 2. Calculate deterministic bedrock motion

$$\ln Y = C_1 + C_2 \cdot M_w + C_3 \cdot \ln\left(\sqrt{R^2 + H^2} + 0.06 \cdot \exp\left[0.7 \cdot M_w\right]\right) + C_4 \sqrt{R^2 + H^2}$$

- Y = Bedrock spectral acceleration at each of times of 0.0, 0.3, and 1.0 second
- C_1 to C_4 =Regression coefficients of Table 27 in Werner et al. (2000)
- M_w = Moment magnitude of earthquake
- R = Distance from earthquake source to bridge site, including minimum source-site distance for NEHRP soil types D and E
- H = Focal depth of earthquake, assumed to be 10km for CUS
- Note: for the Northridge earthquake scenario, TriNet ground motion data for surface shaking is converted to bedrock motion, using the Soil Amplification Factor (see Section 3.3)

Step 3. Calculate soil amplification factors

$$\ln(SAF) = a \cdot Y(T = t) + b$$

- SAF = Deterministic estimate of the site amplification factor
- a,b = Regression coefficients of Table 30 in Werner *et al*. (2000)
- $Y\ (T=t)$ = Sample acceleration calculated in step 2
- Note: for the Northridge earthquake scenario, amplification factors are used according to NEHRP soil type, defined in Table 4-10, HAZUS 99

Step 4. Calculate demand surface motion

$$Y'' = Y \cdot SAF$$

- Y'': Deterministic ground surface motion
- Y : Deterministic bedrock motion calculated in Step 2
- SAF: Deterministic soil amplification factor calculated in Step 3
- Note: for the Northridge scenario this Step is replaced by using the TriNet ground motion data

Step 5. Calculate median PGA for standard bridges by damage state

- Group bridge structure type based on following parameters, as defined by Table 36 and 37 in Werner *et al*.(2000)
  - NBI class
  - Applied design standard according to built year and location
  - Seismic design if built after 1990 outside of California, or 1975 in California
  - Damage state
- For the bridges where damage state 2 is governed by short period (0.3 second), median PGA values are multiplied by –1 for simple identification.

Step 6. Convert median PGA to Spectral Acceleration Capacity

$C(0.3)_{i,m} = -2.5 * PGA_{i,m}$ (if short periods govern, thus $PGA_{i,m}<0$)
$C(1.0)_{i,m} = PGA_{i,m}$ (if long periods govern)

- $C(0.3)_{i,m}$: Short period spectral capacity of bridge m for damage state i.
- $C(1.0)_{i,m}$: long period spectral capacity of bridge m for damage state i.

Step 7. Calculate bridge skewness coefficient, K_{skew}

$K_{skew} = \sqrt{\sin(Angle/\pi)}$ was applied according to *HAZUS* 99.

- 136 from 940 bridges in the Los Angeles bridge database were used in the validation study Skew angle of 99 was replaced with 90 (no skew)

Step 8. Calculate 3-dimensional effect coefficient, K_{3d}

- Calculated K_{3d} value based on Table 38 in Werner *et al.* (2000)

Step 9. Calculate on site bridge capacity

- For damage state 3,4,5,& 2 governed by longer period
  $C'(1.0)_{i,m} = K_{skew} \cdot K_{3d} \cdot C(1.0)_{i,m}$

- For damage state 2 governed by short period
  $C'(0.3)_{i,m} = C(0.3)_{i,m}$

- K_{skew} : Skewness coefficient calculated in step 7
- K_{3d} : 3-dimensional effect coefficient calculated in step 8

Step 10. Incorporate uncertainty in capacity spectral calculation

- damage state 3,4,5,& 2 governed by longer period
  $Q_{i,m} = \ln\left(C(1.0)_{i,m}\right) + 0.35X$

- for damage state 2 governed by short period
  $Q_{i,m} = \ln\left(C(0.3)_{i,m}\right) + 0.35X$

- $Q_{i,m}$: Spectral capacity with uncertainty
- X: Random variable developed based on the procedure explained in F.2.7.2 Werner *et al*. (2000)

Step 11. Modify bedrock motions at 0.3 second and 1.0 second and corresponding soil amplification factor

Peak Rock Acceleration(*PRA*) = 1.589 * *Y*

- *Y* :bedrock motion calculated in step 2
- According to PRA, find corresponding soil amplification factor from following Table A-1 and A-2. Call the SAF as S(1.0), and S(0.3)

Step 12. Calculate of On-site Spectral Capacity

- damage state 3,4,5,& 2 governed by longer period
  $C''(1.0)_{i,m} = \exp\left(Q(1.0)_{i,m}\right)$

- for damage state 2 governed by short period)
  $C''(0.3)_{i,m} = \exp\left(Q(0.3)_{i,m}\right)$

- $Q_{i,m}$: Capacity with uncertainty calculated in step 10.
- S :Modified soil amplification faction calculated in step 11

Step 13. Determine Damage States

- Compare the demand surface calculated in Step 4 with on-site spectral capacity calculated in Step 12, for each of damage states
- For deterministic analysis, if the demand surface motion is higher than the on site spectral capacity for damage state "i", the bridge is assumed to have damage state "i" or higher.
- For probabilistic analysis, if demand surface motion is the same as on-site spectral capacity, the probability of being damaged is 50%.

Table A-1 Lookup Table for Short Period (0.3 second)

NEHRP Site Condition	Modified Peak Rock Acceleration, $(PRA)_B$				
	≤ 0.1 g	0.2 g	0.3 g	0.4 g	≥ 0.5 g
A	0.8	0.8	0.8	0.8	0.8
B	1.0	1.0	1.0	1.0	1.0
C	1.2	1.2	1.1	1.0	1.0
D	1.6	1.4	1.2	1.1	1.0
E	2.5	1.7	1.2	0.9	0.6

Table A-2 Lookup Table for Long Period (1.0 second)

NEHRP Site Condition	Modified Peak Rock Acceleration, $(PRA)_B$				
	≤ 0.1 g	0.2 g	0.3 g	0.4 g	≥ 0.5 g
A	0.8	0.8	0.8	0.8	0.8
B	1.0	1.0	1.0	1.0	1.0
C	1.7	1.6	1.5	1.4	1.3
D	2.4	2.0	1.8	1.6	1.5
E	3.5	3.2	2.8	2.4	2.0

APPENDIX B
REDARS RESPONSE TO VARIOUS GROUND MOTION INPUT

It is important to recognize that a sensitivity analysis of ground motion is outside the scope of this project, as REDARS 1 does not import ground motions, and does not have attenuation functions available for the west coast. However, there is considerable variation in the number of damaged bridges with ground motions based on the Northridge earthquake alone. The ground motions themselves from the earthquake vary considerably, even when published by the same source. This section compares REDARS estimations, from the various ground motion input with regard to the number and distribution of damaged bridges. Although it is not our intent to validate any particular ground motion source, a few issues are identified for future versions of REDARS that will incorporate recorded ground motions.

As reviewed in Appendix A, REDARS relies on spectral acceleration measures. Three sets of spectral acceleration ground motion data are examined – TriNet March 1999, TriNet Dec 2002, Somerville, 1995. USGS data (Borchardt, 94) only gives PGA. However, these data, in conjunction with Somerville, 1995 were used by the developers of the bridge model for validation. According to the AASHTO spectral shape, for site class B, it is possible to estimate spectral acceleration from PGA: SA 0.3 second = 2.5 * PGA, and SA 1.0 second = PGA. Using this conversion, PGA from TriNet (both of Mar 99, and Dec 02) and Somerville, 1996 provide an additional set of spectral acceleration ground motions. This assumption was used by the developers while validating the Mander model (Basöz, personal communication). The purpose here is to test the applicability of this assumption for validation. The REDARS results of the following seven ground motion data sets are examined in this section:

1) Spectral acceleration from TriNet data published in March of 1999. This data set is used throughout much of the report.
2) Spectral acceleration from TriNet data published in December of 2002.
3) Spectral acceleration from Somerville, published in 1995
4) Spectral accelerations estimated from peak ground accelerations from USGS OFR-94-197
5) Spectral acceleration (estimated from peak ground accelerations) from TriNet data published in March of 1999.
6) Spectral acceleration (estimated from peak ground accelerations) from TriNet data published in December of 2002.
7) Spectral acceleration (estimated from peak ground accelerations) from Somerville, published in 1995.

The number of damaged bridges varies significantly based on the source of ground motion (see Table B-1). The highest number of damaged bridges is about twice the minimum number. Somerville, 1995 (PGA) results in 214 damaged bridges out of 940 sample bridges, while TriNet-Mar 99-PGA results in 417 damaged bridges. The number of collapsed bridges ranges from 11 to 102 bridges. Overall, ground motion data sets based on PGA (i.e., calculated as SA 0.3 second=2.5 * PGA, and SA 1.0 second = PGA) predict fewer collapsed bridges than estimates based directly on spectral acceleration.

PGA based Somerville's ground motion is closest to matching the actual number of damaged bridges, both in terms of the number of bridges damaged and collapsed. Direct use of Spectral Acceleration at 1.0 second rather than conversion from PGA has the greatest influence on the results. As reviewed in Section 2.3, the published spectral accelerations are 70-80% higher than PGA. Assuming that spectral acceleration at 1.0 second is equal to PGA results in a number of damaged (and collapsed) bridges that is very close to the actual number, which may have led to incorrect conclusions during the validation of the Mander's model.

Table B-1 Estimated Numbers of Damaged Bridges vs Ground Motion Data

Ground Motion Data	DS5 Collapsed	DS4 Major	DS3 Moderate	DS2 Minor	Sum
TriNet-March 1999-SA	102	98	72	91	363
TriNet-Dec 2002-SA	80	72	70	120	342
Somerville-95-SA	52	53	37	113	255
USGS-94-PGA to SA	11	47	49	123	230
TriNet-March 1999-PGA to SA	25	88	88	216	417
TriNet-Dec 2002-PGA to SA	11	61	27	148	247
Somerville-95-PGA to SA	12	47	50	105	214
Actual	7	35	78	70	190

The Mander bridge model was validated based on the assumption that peak ground acceleration is equal to spectral acceleration, which does not hold given soil types in the region. Therefore, the Mander model should be revisited or another model should be used. Additionally, TriNet ShakeMap reports peak horizontal ground motions, rather than geometric means. Although documentation of the Mander's model is not explicit, geometric means are probably more appropriate. If TriNet ground motions are to be used in the future, an adjustment should be made.

Multidisciplinary Center for Earthquake Engineering Research
List of Technical Reports

The Multidisciplinary Center for Earthquake Engineering Research (MCEER) publishes technical reports on a variety of subjects related to earthquake engineering written by authors funded through MCEER. These reports are available from both MCEER Publications and the National Technical Information Service (NTIS). Requests for reports should be directed to MCEER Publications, Multidisciplinary Center for Earthquake Engineering Research, State University of New York at Buffalo, Red Jacket Quadrangle, Buffalo, New York 14261. Reports can also be requested through NTIS, 5285 Port Royal Road, Springfield, Virginia 22161. NTIS accession numbers are shown in parenthesis, if available.

NCEER-87-0001 "First-Year Program in Research, Education and Technology Transfer," 3/5/87, (PB88-134275, A04, MF-A01).

NCEER-87-0002 "Experimental Evaluation of Instantaneous Optimal Algorithms for Structural Control," by R.C. Lin, T.T. Soong and A.M. Reinhorn, 4/20/87, (PB88-134341, A04, MF-A01).

NCEER-87-0003 "Experimentation Using the Earthquake Simulation Facilities at University at Buffalo," by A.M. Reinhorn and R.L. Ketter, to be published.

NCEER-87-0004 "The System Characteristics and Performance of a Shaking Table," by J.S. Hwang, K.C. Chang and G.C. Lee, 6/1/87, (PB88-134259, A03, MF-A01). This report is available only through NTIS (see address given above).

NCEER-87-0005 "A Finite Element Formulation for Nonlinear Viscoplastic Material Using a Q Model," by O. Gyebi and G. Dasgupta, 11/2/87, (PB88-213764, A08, MF-A01).

NCEER-87-0006 "Symbolic Manipulation Program (SMP) - Algebraic Codes for Two and Three Dimensional Finite Element Formulations," by X. Lee and G. Dasgupta, 11/9/87, (PB88-218522, A05, MF-A01).

NCEER-87-0007 "Instantaneous Optimal Control Laws for Tall Buildings Under Seismic Excitations," by J.N. Yang, A. Akbarpour and P. Ghaemmaghami, 6/10/87, (PB88-134333, A06, MF-A01). This report is only available through NTIS (see address given above).

NCEER-87-0008 "IDARC: Inelastic Damage Analysis of Reinforced Concrete Frame - Shear-Wall Structures," by Y.J. Park, A.M. Reinhorn and S.K. Kunnath, 7/20/87, (PB88-134325, A09, MF-A01). This report is only available through NTIS (see address given above).

NCEER-87-0009 "Liquefaction Potential for New York State: A Preliminary Report on Sites in Manhattan and Buffalo," by M. Budhu, V. Vijayakumar, R.F. Giese and L. Baumgras, 8/31/87, (PB88-163704, A03, MF-A01). This report is available only through NTIS (see address given above).

NCEER-87-0010 "Vertical and Torsional Vibration of Foundations in Inhomogeneous Media," by A.S. Veletsos and K.W. Dotson, 6/1/87, (PB88-134291, A03, MF-A01). This report is only available through NTIS (see address given above).

NCEER-87-0011 "Seismic Probabilistic Risk Assessment and Seismic Margins Studies for Nuclear Power Plants," by Howard H.M. Hwang, 6/15/87, (PB88-134267, A03, MF-A01). This report is only available through NTIS (see address given above).

NCEER-87-0012 "Parametric Studies of Frequency Response of Secondary Systems Under Ground-Acceleration Excitations," by Y. Yong and Y.K. Lin, 6/10/87, (PB88-134309, A03, MF-A01). This report is only available through NTIS (see address given above).

NCEER-87-0013 "Frequency Response of Secondary Systems Under Seismic Excitation," by J.A. HoLung, J. Cai and Y.K. Lin, 7/31/87, (PB88-134317, A05, MF-A01). This report is only available through NTIS (see address given above).

NCEER-87-0014 "Modelling Earthquake Ground Motions in Seismically Active Regions Using Parametric Time Series Methods," by G.W. Ellis and A.S. Cakmak, 8/25/87, (PB88-134283, A08, MF-A01). This report is only available through NTIS (see address given above).

NCEER-87-0015 "Detection and Assessment of Seismic Structural Damage," by E. DiPasquale and A.S. Cakmak, 8/25/87, (PB88-163712, A05, MF-A01). This report is only available through NTIS (see address given above).

NCEER-87-0016 "Pipeline Experiment at Parkfield, California," by J. Isenberg and E. Richardson, 9/15/87, (PB88-163720, A03, MF-A01). This report is available only through NTIS (see address given above).

NCEER-87-0017 "Digital Simulation of Seismic Ground Motion," by M. Shinozuka, G. Deodatis and T. Harada, 8/31/87, (PB88-155197, A04, MF-A01). This report is available only through NTIS (see address given above).

NCEER-87-0018 "Practical Considerations for Structural Control: System Uncertainty, System Time Delay and Truncation of Small Control Forces," J.N. Yang and A. Akbarpour, 8/10/87, (PB88-163738, A08, MF-A01). This report is only available through NTIS (see address given above).

NCEER-87-0019 "Modal Analysis of Nonclassically Damped Structural Systems Using Canonical Transformation," by J.N. Yang, S. Sarkani and F.X. Long, 9/27/87, (PB88-187851, A04, MF-A01).

NCEER-87-0020 "A Nonstationary Solution in Random Vibration Theory," by J.R. Red-Horse and P.D. Spanos, 11/3/87, (PB88-163746, A03, MF-A01).

NCEER-87-0021 "Horizontal Impedances for Radially Inhomogeneous Viscoelastic Soil Layers," by A.S. Veletsos and K.W. Dotson, 10/15/87, (PB88-150859, A04, MF-A01).

NCEER-87-0022 "Seismic Damage Assessment of Reinforced Concrete Members," by Y.S. Chung, C. Meyer and M. Shinozuka, 10/9/87, (PB88-150867, A05, MF-A01). This report is available only through NTIS (see address given above).

NCEER-87-0023 "Active Structural Control in Civil Engineering," by T.T. Soong, 11/11/87, (PB88-187778, A03, MF-A01).

NCEER-87-0024 "Vertical and Torsional Impedances for Radially Inhomogeneous Viscoelastic Soil Layers," by K.W. Dotson and A.S. Veletsos, 12/87, (PB88-187786, A03, MF-A01).

NCEER-87-0025 "Proceedings from the Symposium on Seismic Hazards, Ground Motions, Soil-Liquefaction and Engineering Practice in Eastern North America," October 20-22, 1987, edited by K.H. Jacob, 12/87, (PB88-188115, A23, MF-A01). This report is available only through NTIS (see address given above).

NCEER-87-0026 "Report on the Whittier-Narrows, California, Earthquake of October 1, 1987," by J. Pantelic and A. Reinhorn, 11/87, (PB88-187752, A03, MF-A01). This report is available only through NTIS (see address given above).

NCEER-87-0027 "Design of a Modular Program for Transient Nonlinear Analysis of Large 3-D Building Structures," by S. Srivastav and J.F. Abel, 12/30/87, (PB88-187950, A05, MF-A01). This report is only available through NTIS (see address given above).

NCEER-87-0028 "Second-Year Program in Research, Education and Technology Transfer," 3/8/88, (PB88-219480, A04, MF-A01).

NCEER-88-0001 "Workshop on Seismic Computer Analysis and Design of Buildings With Interactive Graphics," by W. McGuire, J.F. Abel and C.H. Conley, 1/18/88, (PB88-187760, A03, MF-A01). This report is only available through NTIS (see address given above).

NCEER-88-0002 "Optimal Control of Nonlinear Flexible Structures," by J.N. Yang, F.X. Long and D. Wong, 1/22/88, (PB88-213772, A06, MF-A01).

NCEER-88-0003 "Substructuring Techniques in the Time Domain for Primary-Secondary Structural Systems," by G.D. Manolis and G. Juhn, 2/10/88, (PB88-213780, A04, MF-A01).

NCEER-88-0004 "Iterative Seismic Analysis of Primary-Secondary Systems," by A. Singhal, L.D. Lutes and P.D. Spanos, 2/23/88, (PB88-213798, A04, MF-A01).

NCEER-88-0005 "Stochastic Finite Element Expansion for Random Media," by P.D. Spanos and R. Ghanem, 3/14/88, (PB88-213806, A03, MF-A01).

NCEER-88-0006 "Combining Structural Optimization and Structural Control," by F.Y. Cheng and C.P. Pantelides, 1/10/88, (PB88-213814, A05, MF-A01).

NCEER-88-0007 "Seismic Performance Assessment of Code-Designed Structures," by H.H-M. Hwang, J-W. Jaw and H-J. Shau, 3/20/88, (PB88-219423, A04, MF-A01). This report is only available through NTIS (see address given above).

NCEER-88-0008 "Reliability Analysis of Code-Designed Structures Under Natural Hazards," by H.H-M. Hwang, H. Ushiba and M. Shinozuka, 2/29/88, (PB88-229471, A07, MF-A01). This report is only available through NTIS (see address given above).

NCEER-88-0009 "Seismic Fragility Analysis of Shear Wall Structures," by J-W Jaw and H.H-M. Hwang, 4/30/88, (PB89-102867, A04, MF-A01).

NCEER-88-0010 "Base Isolation of a Multi-Story Building Under a Harmonic Ground Motion - A Comparison of Performances of Various Systems," by F-G Fan, G. Ahmadi and I.G. Tadjbakhsh, 5/18/88, (PB89-122238, A06, MF-A01). This report is only available through NTIS (see address given above).

NCEER-88-0011 "Seismic Floor Response Spectra for a Combined System by Green's Functions," by F.M. Lavelle, L.A. Bergman and P.D. Spanos, 5/1/88, (PB89-102875, A03, MF-A01).

NCEER-88-0012 "A New Solution Technique for Randomly Excited Hysteretic Structures," by G.Q. Cai and Y.K. Lin, 5/16/88, (PB89-102883, A03, MF-A01).

NCEER-88-0013 "A Study of Radiation Damping and Soil-Structure Interaction Effects in the Centrifuge," by K. Weissman, supervised by J.H. Prevost, 5/24/88, (PB89-144703, A06, MF-A01).

NCEER-88-0014 "Parameter Identification and Implementation of a Kinematic Plasticity Model for Frictional Soils," by J.H. Prevost and D.V. Griffiths, to be published.

NCEER-88-0015 "Two- and Three- Dimensional Dynamic Finite Element Analyses of the Long Valley Dam," by D.V. Griffiths and J.H. Prevost, 6/17/88, (PB89-144711, A04, MF-A01).

NCEER-88-0016 "Damage Assessment of Reinforced Concrete Structures in Eastern United States," by A.M. Reinhorn, M.J. Seidel, S.K. Kunnath and Y.J. Park, 6/15/88, (PB89-122220, A04, MF-A01). This report is only available through NTIS (see address given above).

NCEER-88-0017 "Dynamic Compliance of Vertically Loaded Strip Foundations in Multilayered Viscoelastic Soils," by S. Ahmad and A.S.M. Israil, 6/17/88, (PB89-102891, A04, MF-A01).

NCEER-88-0018 "An Experimental Study of Seismic Structural Response With Added Viscoelastic Dampers," by R.C. Lin, Z. Liang, T.T. Soong and R.H. Zhang, 6/30/88, (PB89-122212, A05, MF-A01). This report is available only through NTIS (see address given above).

NCEER-88-0019 "Experimental Investigation of Primary - Secondary System Interaction," by G.D. Manolis, G. Juhn and A.M. Reinhorn, 5/27/88, (PB89-122204, A04, MF-A01).

NCEER-88-0020 "A Response Spectrum Approach For Analysis of Nonclassically Damped Structures," by J.N. Yang, S. Sarkani and F.X. Long, 4/22/88, (PB89-102909, A04, MF-A01).

NCEER-88-0021 "Seismic Interaction of Structures and Soils: Stochastic Approach," by A.S. Veletsos and A.M. Prasad, 7/21/88, (PB89-122196, A04, MF-A01). This report is only available through NTIS (see address given above).

NCEER-88-0022 "Identification of the Serviceability Limit State and Detection of Seismic Structural Damage," by E. DiPasquale and A.S. Cakmak, 6/15/88, (PB89-122188, A05, MF-A01). This report is available only through NTIS (see address given above).

NCEER-88-0023 "Multi-Hazard Risk Analysis: Case of a Simple Offshore Structure," by B.K. Bhartia and E.H. Vanmarcke, 7/21/88, (PB89-145213, A05, MF-A01).

NCEER-88-0024 "Automated Seismic Design of Reinforced Concrete Buildings," by Y.S. Chung, C. Meyer and M. Shinozuka, 7/5/88, (PB89-122170, A06, MF-A01). This report is available only through NTIS (see address given above).

NCEER-88-0025 "Experimental Study of Active Control of MDOF Structures Under Seismic Excitations," by L.L. Chung, R.C. Lin, T.T. Soong and A.M. Reinhorn, 7/10/88, (PB89-122600, A04, MF-A01).

NCEER-88-0026 "Earthquake Simulation Tests of a Low-Rise Metal Structure," by J.S. Hwang, K.C. Chang, G.C. Lee and R.L. Ketter, 8/1/88, (PB89-102917, A04, MF-A01).

NCEER-88-0027 "Systems Study of Urban Response and Reconstruction Due to Catastrophic Earthquakes," by F. Kozin and H.K. Zhou, 9/22/88, (PB90-162348, A04, MF-A01).

NCEER-88-0028 "Seismic Fragility Analysis of Plane Frame Structures," by H.H-M. Hwang and Y.K. Low, 7/31/88, (PB89-131445, A06, MF-A01).

NCEER-88-0029 "Response Analysis of Stochastic Structures," by A. Kardara, C. Bucher and M. Shinozuka, 9/22/88, (PB89-174429, A04, MF-A01).

NCEER-88-0030 "Nonnormal Accelerations Due to Yielding in a Primary Structure," by D.C.K. Chen and L.D. Lutes, 9/19/88, (PB89-131437, A04, MF-A01).

NCEER-88-0031 "Design Approaches for Soil-Structure Interaction," by A.S. Veletsos, A.M. Prasad and Y. Tang, 12/30/88, (PB89-174437, A03, MF-A01). This report is available only through NTIS (see address given above).

NCEER-88-0032 "A Re-evaluation of Design Spectra for Seismic Damage Control," by C.J. Turkstra and A.G. Tallin, 11/7/88, (PB89-145221, A05, MF-A01).

NCEER-88-0033 "The Behavior and Design of Noncontact Lap Splices Subjected to Repeated Inelastic Tensile Loading," by V.E. Sagan, P. Gergely and R.N. White, 12/8/88, (PB89-163737, A08, MF-A01).

NCEER-88-0034 "Seismic Response of Pile Foundations," by S.M. Mamoon, P.K. Banerjee and S. Ahmad, 11/1/88, (PB89-145239, A04, MF-A01).

NCEER-88-0035 "Modeling of R/C Building Structures With Flexible Floor Diaphragms (IDARC2)," by A.M. Reinhorn, S.K. Kunnath and N. Panahshahi, 9/7/88, (PB89-207153, A07, MF-A01).

NCEER-88-0036 "Solution of the Dam-Reservoir Interaction Problem Using a Combination of FEM, BEM with Particular Integrals, Modal Analysis, and Substructuring," by C-S. Tsai, G.C. Lee and R.L. Ketter, 12/31/88, (PB89-207146, A04, MF-A01).

NCEER-88-0037 "Optimal Placement of Actuators for Structural Control," by F.Y. Cheng and C.P. Pantelides, 8/15/88, (PB89-162846, A05, MF-A01).

NCEER-88-0038 "Teflon Bearings in Aseismic Base Isolation: Experimental Studies and Mathematical Modeling," by A. Mokha, M.C. Constantinou and A.M. Reinhorn, 12/5/88, (PB89-218457, A10, MF-A01). This report is available only through NTIS (see address given above).

NCEER-88-0039 "Seismic Behavior of Flat Slab High-Rise Buildings in the New York City Area," by P. Weidlinger and M. Ettouney, 10/15/88, (PB90-145681, A04, MF-A01).

NCEER-88-0040 "Evaluation of the Earthquake Resistance of Existing Buildings in New York City," by P. Weidlinger and M. Ettouney, 10/15/88, to be published.

NCEER-88-0041 "Small-Scale Modeling Techniques for Reinforced Concrete Structures Subjected to Seismic Loads," by W. Kim, A. El-Attar and R.N. White, 11/22/88, (PB89-189625, A05, MF-A01).

NCEER-88-0042 "Modeling Strong Ground Motion from Multiple Event Earthquakes," by G.W. Ellis and A.S. Cakmak, 10/15/88, (PB89-174445, A03, MF-A01).

NCEER-88-0043 "Nonstationary Models of Seismic Ground Acceleration," by M. Grigoriu, S.E. Ruiz and E. Rosenblueth, 7/15/88, (PB89-189617, A04, MF-A01).

NCEER-88-0044 "SARCF User's Guide: Seismic Analysis of Reinforced Concrete Frames," by Y.S. Chung, C. Meyer and M. Shinozuka, 11/9/88, (PB89-174452, A08, MF-A01).

NCEER-88-0045 "First Expert Panel Meeting on Disaster Research and Planning," edited by J. Pantelic and J. Stoyle, 9/15/88, (PB89-174460, A05, MF-A01).

NCEER-88-0046 "Preliminary Studies of the Effect of Degrading Infill Walls on the Nonlinear Seismic Response of Steel Frames," by C.Z. Chrysostomou, P. Gergely and J.F. Abel, 12/19/88, (PB89-208383, A05, MF-A01).

NCEER-88-0047 "Reinforced Concrete Frame Component Testing Facility - Design, Construction, Instrumentation and Operation," by S.P. Pessiki, C. Conley, T. Bond, P. Gergely and R.N. White, 12/16/88, (PB89-174478, A04, MF-A01).

NCEER-89-0001 "Effects of Protective Cushion and Soil Compliancy on the Response of Equipment Within a Seismically Excited Building," by J.A. HoLung, 2/16/89, (PB89-207179, A04, MF-A01).

NCEER-89-0002 "Statistical Evaluation of Response Modification Factors for Reinforced Concrete Structures," by H.H-M. Hwang and J-W. Jaw, 2/17/89, (PB89-207187, A05, MF-A01).

NCEER-89-0003 "Hysteretic Columns Under Random Excitation," by G-Q. Cai and Y.K. Lin, 1/9/89, (PB89-196513, A03, MF-A01).

NCEER-89-0004 "Experimental Study of `Elephant Foot Bulge' Instability of Thin-Walled Metal Tanks," by Z-H. Jia and R.L. Ketter, 2/22/89, (PB89-207195, A03, MF-A01).

NCEER-89-0005 "Experiment on Performance of Buried Pipelines Across San Andreas Fault," by J. Isenberg, E. Richardson and T.D. O'Rourke, 3/10/89, (PB89-218440, A04, MF-A01). This report is available only through NTIS (see address given above).

NCEER-89-0006 "A Knowledge-Based Approach to Structural Design of Earthquake-Resistant Buildings," by M. Subramani, P. Gergely, C.H. Conley, J.F. Abel and A.H. Zaghw, 1/15/89, (PB89-218465, A06, MF-A01).

NCEER-89-0007 "Liquefaction Hazards and Their Effects on Buried Pipelines," by T.D. O'Rourke and P.A. Lane, 2/1/89, (PB89-218481, A09, MF-A01).

NCEER-89-0008 "Fundamentals of System Identification in Structural Dynamics," by H. Imai, C-B. Yun, O. Maruyama and M. Shinozuka, 1/26/89, (PB89-207211, A04, MF-A01).

NCEER-89-0009 "Effects of the 1985 Michoacan Earthquake on Water Systems and Other Buried Lifelines in Mexico," by A.G. Ayala and M.J. O'Rourke, 3/8/89, (PB89-207229, A06, MF-A01).

NCEER-89-R010 "NCEER Bibliography of Earthquake Education Materials," by K.E.K. Ross, Second Revision, 9/1/89, (PB90-125352, A05, MF-A01). This report is replaced by NCEER-92-0018.

NCEER-89-0011 "Inelastic Three-Dimensional Response Analysis of Reinforced Concrete Building Structures (IDARC-3D), Part I - Modeling," by S.K. Kunnath and A.M. Reinhorn, 4/17/89, (PB90-114612, A07, MF-A01). This report is available only through NTIS (see address given above).

NCEER-89-0012 "Recommended Modifications to ATC-14," by C.D. Poland and J.O. Malley, 4/12/89, (PB90-108648, A15, MF-A01).

NCEER-89-0013 "Repair and Strengthening of Beam-to-Column Connections Subjected to Earthquake Loading," by M. Corazao and A.J. Durrani, 2/28/89, (PB90-109885, A06, MF-A01).

NCEER-89-0014 "Program EXKAL2 for Identification of Structural Dynamic Systems," by O. Maruyama, C-B. Yun, M. Hoshiya and M. Shinozuka, 5/19/89, (PB90-109877, A09, MF-A01).

NCEER-89-0015 "Response of Frames With Bolted Semi-Rigid Connections, Part I - Experimental Study and Analytical Predictions," by P.J. DiCorso, A.M. Reinhorn, J.R. Dickerson, J.B. Radziminski and W.L. Harper, 6/1/89, to be published.

NCEER-89-0016 "ARMA Monte Carlo Simulation in Probabilistic Structural Analysis," by P.D. Spanos and M.P. Mignolet, 7/10/89, (PB90-109893, A03, MF-A01).

NCEER-89-P017 "Preliminary Proceedings from the Conference on Disaster Preparedness - The Place of Earthquake Education in Our Schools," Edited by K.E.K. Ross, 6/23/89, (PB90-108606, A03, MF-A01).

NCEER-89-0017 "Proceedings from the Conference on Disaster Preparedness - The Place of Earthquake Education in Our Schools," Edited by K.E.K. Ross, 12/31/89, (PB90-207895, A012, MF-A02). This report is available only through NTIS (see address given above).

NCEER-89-0018 "Multidimensional Models of Hysteretic Material Behavior for Vibration Analysis of Shape Memory Energy Absorbing Devices, by E.J. Graesser and F.A. Cozzarelli, 6/7/89, (PB90-164146, A04, MF-A01).

NCEER-89-0019 "Nonlinear Dynamic Analysis of Three-Dimensional Base Isolated Structures (3D-BASIS)," by S. Nagarajaiah, A.M. Reinhorn and M.C. Constantinou, 8/3/89, (PB90-161936, A06, MF-A01). This report has been replaced by NCEER-93-0011.

NCEER-89-0020 "Structural Control Considering Time-Rate of Control Forces and Control Rate Constraints," by F.Y. Cheng and C.P. Pantelides, 8/3/89, (PB90-120445, A04, MF-A01).

NCEER-89-0021 "Subsurface Conditions of Memphis and Shelby County," by K.W. Ng, T-S. Chang and H-H.M. Hwang, 7/26/89, (PB90-120437, A03, MF-A01).

NCEER-89-0022 "Seismic Wave Propagation Effects on Straight Jointed Buried Pipelines," by K. Elhmadi and M.J. O'Rourke, 8/24/89, (PB90-162322, A10, MF-A02).

NCEER-89-0023 "Workshop on Serviceability Analysis of Water Delivery Systems," edited by M. Grigoriu, 3/6/89, (PB90-127424, A03, MF-A01).

NCEER-89-0024 "Shaking Table Study of a 1/5 Scale Steel Frame Composed of Tapered Members," by K.C. Chang, J.S. Hwang and G.C. Lee, 9/18/89, (PB90-160169, A04, MF-A01).

NCEER-89-0025 "DYNA1D: A Computer Program for Nonlinear Seismic Site Response Analysis - Technical Documentation," by Jean H. Prevost, 9/14/89, (PB90-161944, A07, MF-A01). This report is available only through NTIS (see address given above).

NCEER-89-0026 "1:4 Scale Model Studies of Active Tendon Systems and Active Mass Dampers for Aseismic Protection," by A.M. Reinhorn, T.T. Soong, R.C. Lin, Y.P. Yang, Y. Fukao, H. Abe and M. Nakai, 9/15/89, (PB90-173246, A10, MF-A02). This report is available only through NTIS (see address given above).

NCEER-89-0027 "Scattering of Waves by Inclusions in a Nonhomogeneous Elastic Half Space Solved by Boundary Element Methods," by P.K. Hadley, A. Askar and A.S. Cakmak, 6/15/89, (PB90-145699, A07, MF-A01).

NCEER-89-0028 "Statistical Evaluation of Deflection Amplification Factors for Reinforced Concrete Structures," by H.H.M. Hwang, J-W. Jaw and A.L. Ch'ng, 8/31/89, (PB90-164633, A05, MF-A01).

NCEER-89-0029 "Bedrock Accelerations in Memphis Area Due to Large New Madrid Earthquakes," by H.H.M. Hwang, C.H.S. Chen and G. Yu, 11/7/89, (PB90-162330, A04, MF-A01).

NCEER-89-0030 "Seismic Behavior and Response Sensitivity of Secondary Structural Systems," by Y.Q. Chen and T.T. Soong, 10/23/89, (PB90-164658, A08, MF-A01).

NCEER-89-0031 "Random Vibration and Reliability Analysis of Primary-Secondary Structural Systems," by Y. Ibrahim, M. Grigoriu and T.T. Soong, 11/10/89, (PB90-161951, A04, MF-A01).

NCEER-89-0032 "Proceedings from the Second U.S. - Japan Workshop on Liquefaction, Large Ground Deformation and Their Effects on Lifelines, September 26-29, 1989," Edited by T.D. O'Rourke and M. Hamada, 12/1/89, (PB90-209388, A22, MF-A03).

NCEER-89-0033 "Deterministic Model for Seismic Damage Evaluation of Reinforced Concrete Structures," by J.M. Bracci, A.M. Reinhorn, J.B. Mander and S.K. Kunnath, 9/27/89, (PB91-108803, A06, MF-A01).

NCEER-89-0034 "On the Relation Between Local and Global Damage Indices," by E. DiPasquale and A.S. Cakmak, 8/15/89, (PB90-173865, A05, MF-A01).

NCEER-89-0035 "Cyclic Undrained Behavior of Nonplastic and Low Plasticity Silts," by A.J. Walker and H.E. Stewart, 7/26/89, (PB90-183518, A10, MF-A01).

NCEER-89-0036 "Liquefaction Potential of Surficial Deposits in the City of Buffalo, New York," by M. Budhu, R. Giese and L. Baumgrass, 1/17/89, (PB90-208455, A04, MF-A01).

NCEER-89-0037 "A Deterministic Assessment of Effects of Ground Motion Incoherence," by A.S. Veletsos and Y. Tang, 7/15/89, (PB90-164294, A03, MF-A01).

NCEER-89-0038 "Workshop on Ground Motion Parameters for Seismic Hazard Mapping," July 17-18, 1989, edited by R.V. Whitman, 12/1/89, (PB90-173923, A04, MF-A01).

NCEER-89-0039 "Seismic Effects on Elevated Transit Lines of the New York City Transit Authority," by C.J. Costantino, C.A. Miller and E. Heymsfield, 12/26/89, (PB90-207887, A06, MF-A01).

NCEER-89-0040 "Centrifugal Modeling of Dynamic Soil-Structure Interaction," by K. Weissman, Supervised by J.H. Prevost, 5/10/89, (PB90-207879, A07, MF-A01).

NCEER-89-0041 "Linearized Identification of Buildings With Cores for Seismic Vulnerability Assessment," by I-K. Ho and A.E. Aktan, 11/1/89, (PB90-251943, A07, MF-A01).

NCEER-90-0001 "Geotechnical and Lifeline Aspects of the October 17, 1989 Loma Prieta Earthquake in San Francisco," by T.D. O'Rourke, H.E. Stewart, F.T. Blackburn and T.S. Dickerman, 1/90, (PB90-208596, A05, MF-A01).

NCEER-90-0002 "Nonnormal Secondary Response Due to Yielding in a Primary Structure," by D.C.K. Chen and L.D. Lutes, 2/28/90, (PB90-251976, A07, MF-A01).

NCEER-90-0003 "Earthquake Education Materials for Grades K-12," by K.E.K. Ross, 4/16/90, (PB91-251984, A05, MF-A05). This report has been replaced by NCEER-92-0018.

NCEER-90-0004 "Catalog of Strong Motion Stations in Eastern North America," by R.W. Busby, 4/3/90, (PB90-251984, A05, MF-A01).

NCEER-90-0005 "NCEER Strong-Motion Data Base: A User Manual for the GeoBase Release (Version 1.0 for the Sun3)," by P. Friberg and K. Jacob, 3/31/90 (PB90-258062, A04, MF-A01).

NCEER-90-0006 "Seismic Hazard Along a Crude Oil Pipeline in the Event of an 1811-1812 Type New Madrid Earthquake," by H.H.M. Hwang and C-H.S. Chen, 4/16/90, (PB90-258054, A04, MF-A01).

NCEER-90-0007 "Site-Specific Response Spectra for Memphis Sheahan Pumping Station," by H.H.M. Hwang and C.S. Lee, 5/15/90, (PB91-108811, A05, MF-A01).

NCEER-90-0008 "Pilot Study on Seismic Vulnerability of Crude Oil Transmission Systems," by T. Ariman, R. Dobry, M. Grigoriu, F. Kozin, M. O'Rourke, T. O'Rourke and M. Shinozuka, 5/25/90, (PB91-108837, A06, MF-A01).

NCEER-90-0009 "A Program to Generate Site Dependent Time Histories: EQGEN," by G.W. Ellis, M. Srinivasan and A.S. Cakmak, 1/30/90, (PB91-108829, A04, MF-A01).

NCEER-90-0010 "Active Isolation for Seismic Protection of Operating Rooms," by M.E. Talbott, Supervised by M. Shinozuka, 6/8/9, (PB91-110205, A05, MF-A01).

NCEER-90-0011 "Program LINEARID for Identification of Linear Structural Dynamic Systems," by C-B. Yun and M. Shinozuka, 6/25/90, (PB91-110312, A08, MF-A01).

NCEER-90-0012 "Two-Dimensional Two-Phase Elasto-Plastic Seismic Response of Earth Dams," by A.N. Yiagos, Supervised by J.H. Prevost, 6/20/90, (PB91-110197, A13, MF-A02).

NCEER-90-0013 "Secondary Systems in Base-Isolated Structures: Experimental Investigation, Stochastic Response and Stochastic Sensitivity," by G.D. Manolis, G. Juhn, M.C. Constantinou and A.M. Reinhorn, 7/1/90, (PB91-110320, A08, MF-A01).

NCEER-90-0014 "Seismic Behavior of Lightly-Reinforced Concrete Column and Beam-Column Joint Details," by S.P. Pessiki, C.H. Conley, P. Gergely and R.N. White, 8/22/90, (PB91-108795, A11, MF-A02).

NCEER-90-0015 "Two Hybrid Control Systems for Building Structures Under Strong Earthquakes," by J.N. Yang and A. Danielians, 6/29/90, (PB91-125393, A04, MF-A01).

NCEER-90-0016 "Instantaneous Optimal Control with Acceleration and Velocity Feedback," by J.N. Yang and Z. Li, 6/29/90, (PB91-125401, A03, MF-A01).

NCEER-90-0017 "Reconnaissance Report on the Northern Iran Earthquake of June 21, 1990," by M. Mehrain, 10/4/90, (PB91-125377, A03, MF-A01).

NCEER-90-0018 "Evaluation of Liquefaction Potential in Memphis and Shelby County," by T.S. Chang, P.S. Tang, C.S. Lee and H. Hwang, 8/10/90, (PB91-125427, A09, MF-A01).

NCEER-90-0019 "Experimental and Analytical Study of a Combined Sliding Disc Bearing and Helical Steel Spring Isolation System," by M.C. Constantinou, A.S. Mokha and A.M. Reinhorn, 10/4/90, (PB91-125385, A06, MF-A01). This report is available only through NTIS (see address given above).

NCEER-90-0020 "Experimental Study and Analytical Prediction of Earthquake Response of a Sliding Isolation System with a Spherical Surface," by A.S. Mokha, M.C. Constantinou and A.M. Reinhorn, 10/11/90, (PB91-125419, A05, MF-A01).

NCEER-90-0021 "Dynamic Interaction Factors for Floating Pile Groups," by G. Gazetas, K. Fan, A. Kaynia and E. Kausel, 9/10/90, (PB91-170381, A05, MF-A01).

NCEER-90-0022 "Evaluation of Seismic Damage Indices for Reinforced Concrete Structures," by S. Rodriguez-Gomez and A.S. Cakmak, 9/30/90, PB91-171322, A06, MF-A01).

NCEER-90-0023 "Study of Site Response at a Selected Memphis Site," by H. Desai, S. Ahmad, E.S. Gazetas and M.R. Oh, 10/11/90, (PB91-196857, A03, MF-A01).

NCEER-90-0024 "A User's Guide to Strongmo: Version 1.0 of NCEER's Strong-Motion Data Access Tool for PCs and Terminals," by P.A. Friberg and C.A.T. Susch, 11/15/90, (PB91-171272, A03, MF-A01).

NCEER-90-0025 "A Three-Dimensional Analytical Study of Spatial Variability of Seismic Ground Motions," by L-L. Hong and A.H.-S. Ang, 10/30/90, (PB91-170399, A09, MF-A01).

NCEER-90-0026 "MUMOID User's Guide - A Program for the Identification of Modal Parameters," by S. Rodriguez-Gomez and E. DiPasquale, 9/30/90, (PB91-171298, A04, MF-A01).

NCEER-90-0027 "SARCF-II User's Guide - Seismic Analysis of Reinforced Concrete Frames," by S. Rodriguez-Gomez, Y.S. Chung and C. Meyer, 9/30/90, (PB91-171280, A05, MF-A01).

NCEER-90-0028 "Viscous Dampers: Testing, Modeling and Application in Vibration and Seismic Isolation," by N. Makris and M.C. Constantinou, 12/20/90 (PB91-190561, A06, MF-A01).

NCEER-90-0029 "Soil Effects on Earthquake Ground Motions in the Memphis Area," by H. Hwang, C.S. Lee, K.W. Ng and T.S. Chang, 8/2/90, (PB91-190751, A05, MF-A01).

NCEER-91-0001 "Proceedings from the Third Japan-U.S. Workshop on Earthquake Resistant Design of Lifeline Facilities and Countermeasures for Soil Liquefaction, December 17-19, 1990," edited by T.D. O'Rourke and M. Hamada, 2/1/91, (PB91-179259, A99, MF-A04).

NCEER-91-0002 "Physical Space Solutions of Non-Proportionally Damped Systems," by M. Tong, Z. Liang and G.C. Lee, 1/15/91, (PB91-179242, A04, MF-A01).

NCEER-91-0003 "Seismic Response of Single Piles and Pile Groups," by K. Fan and G. Gazetas, 1/10/91, (PB92-174994, A04, MF-A01).

NCEER-91-0004 "Damping of Structures: Part 1 - Theory of Complex Damping," by Z. Liang and G. Lee, 10/10/91, (PB92-197235, A12, MF-A03).

NCEER-91-0005 "3D-BASIS - Nonlinear Dynamic Analysis of Three Dimensional Base Isolated Structures: Part II," by S. Nagarajaiah, A.M. Reinhorn and M.C. Constantinou, 2/28/91, (PB91-190553, A07, MF-A01). This report has been replaced by NCEER-93-0011.

NCEER-91-0006 "A Multidimensional Hysteretic Model for Plasticity Deforming Metals in Energy Absorbing Devices," by E.J. Graesser and F.A. Cozzarelli, 4/9/91, (PB92-108364, A04, MF-A01).

NCEER-91-0007 "A Framework for Customizable Knowledge-Based Expert Systems with an Application to a KBES for Evaluating the Seismic Resistance of Existing Buildings," by E.G. Ibarra-Anaya and S.J. Fenves, 4/9/91, (PB91-210930, A08, MF-A01).

NCEER-91-0008 "Nonlinear Analysis of Steel Frames with Semi-Rigid Connections Using the Capacity Spectrum Method," by G.G. Deierlein, S-H. Hsieh, Y-J. Shen and J.F. Abel, 7/2/91, (PB92-113828, A05, MF-A01).

NCEER-91-0009 "Earthquake Education Materials for Grades K-12," by K.E.K. Ross, 4/30/91, (PB91-212142, A06, MF-A01). This report has been replaced by NCEER-92-0018.

NCEER-91-0010 "Phase Wave Velocities and Displacement Phase Differences in a Harmonically Oscillating Pile," by N. Makris and G. Gazetas, 7/8/91, (PB92-108356, A04, MF-A01).

NCEER-91-0011 "Dynamic Characteristics of a Full-Size Five-Story Steel Structure and a 2/5 Scale Model," by K.C. Chang, G.C. Yao, G.C. Lee, D.S. Hao and Y.C. Yeh," 7/2/91, (PB93-116648, A06, MF-A02).

NCEER-91-0012 "Seismic Response of a 2/5 Scale Steel Structure with Added Viscoelastic Dampers," by K.C. Chang, T.T. Soong, S-T. Oh and M.L. Lai, 5/17/91, (PB92-110816, A05, MF-A01).

NCEER-91-0013 "Earthquake Response of Retaining Walls; Full-Scale Testing and Computational Modeling," by S. Alampalli and A-W.M. Elgamal, 6/20/91, to be published.

NCEER-91-0014 "3D-BASIS-M: Nonlinear Dynamic Analysis of Multiple Building Base Isolated Structures," by P.C. Tsopelas, S. Nagarajaiah, M.C. Constantinou and A.M. Reinhorn, 5/28/91, (PB92-113885, A09, MF-A02).

NCEER-91-0015 "Evaluation of SEAOC Design Requirements for Sliding Isolated Structures," by D. Theodossiou and M.C. Constantinou, 6/10/91, (PB92-114602, A11, MF-A03).

NCEER-91-0016 "Closed-Loop Modal Testing of a 27-Story Reinforced Concrete Flat Plate-Core Building," by H.R. Somaprasad, T. Toksoy, H. Yoshiyuki and A.E. Aktan, 7/15/91, (PB92-129980, A07, MF-A02).

NCEER-91-0017 "Shake Table Test of a 1/6 Scale Two-Story Lightly Reinforced Concrete Building," by A.G. El-Attar, R.N. White and P. Gergely, 2/28/91, (PB92-222447, A06, MF-A02).

NCEER-91-0018 "Shake Table Test of a 1/8 Scale Three-Story Lightly Reinforced Concrete Building," by A.G. El-Attar, R.N. White and P. Gergely, 2/28/91, (PB93-116630, A08, MF-A02).

NCEER-91-0019 "Transfer Functions for Rigid Rectangular Foundations," by A.S. Veletsos, A.M. Prasad and W.H. Wu, 7/31/91, to be published.

NCEER-91-0020 "Hybrid Control of Seismic-Excited Nonlinear and Inelastic Structural Systems," by J.N. Yang, Z. Li and A. Danielians, 8/1/91, (PB92-143171, A06, MF-A02).

NCEER-91-0021 "The NCEER-91 Earthquake Catalog: Improved Intensity-Based Magnitudes and Recurrence Relations for U.S. Earthquakes East of New Madrid," by L. Seeber and J.G. Armbruster, 8/28/91, (PB92-176742, A06, MF-A02).

NCEER-91-0022 "Proceedings from the Implementation of Earthquake Planning and Education in Schools: The Need for Change - The Roles of the Changemakers," by K.E.K. Ross and F. Winslow, 7/23/91, (PB92-129998, A12, MF-A03).

NCEER-91-0023 "A Study of Reliability-Based Criteria for Seismic Design of Reinforced Concrete Frame Buildings," by H.H.M. Hwang and H-M. Hsu, 8/10/91, (PB92-140235, A09, MF-A02).

NCEER-91-0024 "Experimental Verification of a Number of Structural System Identification Algorithms," by R.G. Ghanem, H. Gavin and M. Shinozuka, 9/18/91, (PB92-176577, A18, MF-A04).

NCEER-91-0025 "Probabilistic Evaluation of Liquefaction Potential," by H.H.M. Hwang and C.S. Lee," 11/25/91, (PB92-143429, A05, MF-A01).

NCEER-91-0026 "Instantaneous Optimal Control for Linear, Nonlinear and Hysteretic Structures - Stable Controllers," by J.N. Yang and Z. Li, 11/15/91, (PB92-163807, A04, MF-A01).

NCEER-91-0027 "Experimental and Theoretical Study of a Sliding Isolation System for Bridges," by M.C. Constantinou, A. Kartoum, A.M. Reinhorn and P. Bradford, 11/15/91, (PB92-176973, A10, MF-A03).

NCEER-92-0001 "Case Studies of Liquefaction and Lifeline Performance During Past Earthquakes, Volume 1: Japanese Case Studies," Edited by M. Hamada and T. O'Rourke, 2/17/92, (PB92-197243, A18, MF-A04).

NCEER-92-0002 "Case Studies of Liquefaction and Lifeline Performance During Past Earthquakes, Volume 2: United States Case Studies," Edited by T. O'Rourke and M. Hamada, 2/17/92, (PB92-197250, A20, MF-A04).

NCEER-92-0003 "Issues in Earthquake Education," Edited by K. Ross, 2/3/92, (PB92-222389, A07, MF-A02).

NCEER-92-0004 "Proceedings from the First U.S. - Japan Workshop on Earthquake Protective Systems for Bridges," Edited by I.G. Buckle, 2/4/92, (PB94-142239, A99, MF-A06).

NCEER-92-0005 "Seismic Ground Motion from a Haskell-Type Source in a Multiple-Layered Half-Space," A.P. Theoharis, G. Deodatis and M. Shinozuka, 1/2/92, to be published.

NCEER-92-0006 "Proceedings from the Site Effects Workshop," Edited by R. Whitman, 2/29/92, (PB92-197201, A04, MF-A01).

NCEER-92-0007 "Engineering Evaluation of Permanent Ground Deformations Due to Seismically-Induced Liquefaction," by M.H. Baziar, R. Dobry and A-W.M. Elgamal, 3/24/92, (PB92-222421, A13, MF-A03).

NCEER-92-0008 "A Procedure for the Seismic Evaluation of Buildings in the Central and Eastern United States," by C.D. Poland and J.O. Malley, 4/2/92, (PB92-222439, A20, MF-A04).

NCEER-92-0009 "Experimental and Analytical Study of a Hybrid Isolation System Using Friction Controllable Sliding Bearings," by M.Q. Feng, S. Fujii and M. Shinozuka, 5/15/92, (PB93-150282, A06, MF-A02).

NCEER-92-0010 "Seismic Resistance of Slab-Column Connections in Existing Non-Ductile Flat-Plate Buildings," by A.J. Durrani and Y. Du, 5/18/92, (PB93-116812, A06, MF-A02).

NCEER-92-0011 "The Hysteretic and Dynamic Behavior of Brick Masonry Walls Upgraded by Ferrocement Coatings Under Cyclic Loading and Strong Simulated Ground Motion," by H. Lee and S.P. Prawel, 5/11/92, to be published.

NCEER-92-0012 "Study of Wire Rope Systems for Seismic Protection of Equipment in Buildings," by G.F. Demetriades, M.C. Constantinou and A.M. Reinhorn, 5/20/92, (PB93-116655, A08, MF-A02).

NCEER-92-0013 "Shape Memory Structural Dampers: Material Properties, Design and Seismic Testing," by P.R. Witting and F.A. Cozzarelli, 5/26/92, (PB93-116663, A05, MF-A01).

NCEER-92-0014 "Longitudinal Permanent Ground Deformation Effects on Buried Continuous Pipelines," by M.J. O'Rourke, and C. Nordberg, 6/15/92, (PB93-116671, A08, MF-A02).

NCEER-92-0015 "A Simulation Method for Stationary Gaussian Random Functions Based on the Sampling Theorem," by M. Grigoriu and S. Balopoulou, 6/11/92, (PB93-127496, A05, MF-A01).

NCEER-92-0016 "Gravity-Load-Designed Reinforced Concrete Buildings: Seismic Evaluation of Existing Construction and Detailing Strategies for Improved Seismic Resistance," by G.W. Hoffmann, S.K. Kunnath, A.M. Reinhorn and J.B. Mander, 7/15/92, (PB94-142007, A08, MF-A02).

NCEER-92-0017 "Observations on Water System and Pipeline Performance in the Limón Area of Costa Rica Due to the April 22, 1991 Earthquake," by M. O'Rourke and D. Ballantyne, 6/30/92, (PB93-126811, A06, MF-A02).

NCEER-92-0018 "Fourth Edition of Earthquake Education Materials for Grades K-12," Edited by K.E.K. Ross, 8/10/92, (PB93-114023, A07, MF-A02).

NCEER-92-0019 "Proceedings from the Fourth Japan-U.S. Workshop on Earthquake Resistant Design of Lifeline Facilities and Countermeasures for Soil Liquefaction," Edited by M. Hamada and T.D. O'Rourke, 8/12/92, (PB93-163939, A99, MF-E11).

NCEER-92-0020 "Active Bracing System: A Full Scale Implementation of Active Control," by A.M. Reinhorn, T.T. Soong, R.C. Lin, M.A. Riley, Y.P. Wang, S. Aizawa and M. Higashino, 8/14/92, (PB93-127512, A06, MF-A02).

NCEER-92-0021 "Empirical Analysis of Horizontal Ground Displacement Generated by Liquefaction-Induced Lateral Spreads," by S.F. Bartlett and T.L. Youd, 8/17/92, (PB93-188241, A06, MF-A02).

NCEER-92-0022 "IDARC Version 3.0: Inelastic Damage Analysis of Reinforced Concrete Structures," by S.K. Kunnath, A.M. Reinhorn and R.F. Lobo, 8/31/92, (PB93-227502, A07, MF-A02).

NCEER-92-0023 "A Semi-Empirical Analysis of Strong-Motion Peaks in Terms of Seismic Source, Propagation Path and Local Site Conditions, by M. Kamiyama, M.J. O'Rourke and R. Flores-Berrones, 9/9/92, (PB93-150266, A08, MF-A02).

NCEER-92-0024 "Seismic Behavior of Reinforced Concrete Frame Structures with Nonductile Details, Part I: Summary of Experimental Findings of Full Scale Beam-Column Joint Tests," by A. Beres, R.N. White and P. Gergely, 9/30/92, (PB93-227783, A05, MF-A01).

NCEER-92-0025 "Experimental Results of Repaired and Retrofitted Beam-Column Joint Tests in Lightly Reinforced Concrete Frame Buildings," by A. Beres, S. El-Borgi, R.N. White and P. Gergely, 10/29/92, (PB93-227791, A05, MF-A01).

NCEER-92-0026 "A Generalization of Optimal Control Theory: Linear and Nonlinear Structures," by J.N. Yang, Z. Li and S. Vongchavalitkul, 11/2/92, (PB93-188621, A05, MF-A01).

NCEER-92-0027 "Seismic Resistance of Reinforced Concrete Frame Structures Designed Only for Gravity Loads: Part I - Design and Properties of a One-Third Scale Model Structure," by J.M. Bracci, A.M. Reinhorn and J.B. Mander, 12/1/92, (PB94-104502, A08, MF-A02).

NCEER-92-0028 "Seismic Resistance of Reinforced Concrete Frame Structures Designed Only for Gravity Loads: Part II - Experimental Performance of Subassemblages," by L.E. Aycardi, J.B. Mander and A.M. Reinhorn, 12/1/92, (PB94-104510, A08, MF-A02).

NCEER-92-0029 "Seismic Resistance of Reinforced Concrete Frame Structures Designed Only for Gravity Loads: Part III - Experimental Performance and Analytical Study of a Structural Model," by J.M. Bracci, A.M. Reinhorn and J.B. Mander, 12/1/92, (PB93-227528, A09, MF-A01).

NCEER-92-0030 "Evaluation of Seismic Retrofit of Reinforced Concrete Frame Structures: Part I - Experimental Performance of Retrofitted Subassemblages," by D. Choudhuri, J.B. Mander and A.M. Reinhorn, 12/8/92, (PB93-198307, A07, MF-A02).

NCEER-92-0031 "Evaluation of Seismic Retrofit of Reinforced Concrete Frame Structures: Part II - Experimental Performance and Analytical Study of a Retrofitted Structural Model," by J.M. Bracci, A.M. Reinhorn and J.B. Mander, 12/8/92, (PB93-198315, A09, MF-A03).

NCEER-92-0032 "Experimental and Analytical Investigation of Seismic Response of Structures with Supplemental Fluid Viscous Dampers," by M.C. Constantinou and M.D. Symans, 12/21/92, (PB93-191435, A10, MF-A03). This report is available only through NTIS (see address given above).

NCEER-92-0033 "Reconnaissance Report on the Cairo, Egypt Earthquake of October 12, 1992," by M. Khater, 12/23/92, (PB93-188621, A03, MF-A01).

NCEER-92-0034 "Low-Level Dynamic Characteristics of Four Tall Flat-Plate Buildings in New York City," by H. Gavin, S. Yuan, J. Grossman, E. Pekelis and K. Jacob, 12/28/92, (PB93-188217, A07, MF-A02).

NCEER-93-0001 "An Experimental Study on the Seismic Performance of Brick-Infilled Steel Frames With and Without Retrofit," by J.B. Mander, B. Nair, K. Wojtkowski and J. Ma, 1/29/93, (PB93-227510, A07, MF-A02).

NCEER-93-0002 "Social Accounting for Disaster Preparedness and Recovery Planning," by S. Cole, E. Pantoja and V. Razak, 2/22/93, (PB94-142114, A12, MF-A03).

NCEER-93-0003 "Assessment of 1991 NEHRP Provisions for Nonstructural Components and Recommended Revisions," by T.T. Soong, G. Chen, Z. Wu, R-H. Zhang and M. Grigoriu, 3/1/93, (PB93-188639, A06, MF-A02).

NCEER-93-0004 "Evaluation of Static and Response Spectrum Analysis Procedures of SEAOC/UBC for Seismic Isolated Structures," by C.W. Winters and M.C. Constantinou, 3/23/93, (PB93-198299, A10, MF-A03).

NCEER-93-0005 "Earthquakes in the Northeast - Are We Ignoring the Hazard? A Workshop on Earthquake Science and Safety for Educators," edited by K.E.K. Ross, 4/2/93, (PB94-103066, A09, MF-A02).

NCEER-93-0006 "Inelastic Response of Reinforced Concrete Structures with Viscoelastic Braces," by R.F. Lobo, J.M. Bracci, K.L. Shen, A.M. Reinhorn and T.T. Soong, 4/5/93, (PB93-227486, A05, MF-A02).

NCEER-93-0007 "Seismic Testing of Installation Methods for Computers and Data Processing Equipment," by K. Kosar, T.T. Soong, K.L. Shen, J.A. HoLung and Y.K. Lin, 4/12/93, (PB93-198299, A07, MF-A02).

NCEER-93-0008 "Retrofit of Reinforced Concrete Frames Using Added Dampers," by A. Reinhorn, M. Constantinou and C. Li, to be published.

NCEER-93-0009 "Seismic Behavior and Design Guidelines for Steel Frame Structures with Added Viscoelastic Dampers," by K.C. Chang, M.L. Lai, T.T. Soong, D.S. Hao and Y.C. Yeh, 5/1/93, (PB94-141959, A07, MF-A02).

NCEER-93-0010 "Seismic Performance of Shear-Critical Reinforced Concrete Bridge Piers," by J.B. Mander, S.M. Waheed, M.T.A. Chaudhary and S.S. Chen, 5/12/93, (PB93-227494, A08, MF-A02).

NCEER-93-0011 "3D-BASIS-TABS: Computer Program for Nonlinear Dynamic Analysis of Three Dimensional Base Isolated Structures," by S. Nagarajaiah, C. Li, A.M. Reinhorn and M.C. Constantinou, 8/2/93, (PB94-141819, A09, MF-A02).

NCEER-93-0012 "Effects of Hydrocarbon Spills from an Oil Pipeline Break on Ground Water," by O.J. Helweg and H.H.M. Hwang, 8/3/93, (PB94-141942, A06, MF-A02).

NCEER-93-0013 "Simplified Procedures for Seismic Design of Nonstructural Components and Assessment of Current Code Provisions," by M.P. Singh, L.E. Suarez, E.E. Matheu and G.O. Maldonado, 8/4/93, (PB94-141827, A09, MF-A02).

NCEER-93-0014 "An Energy Approach to Seismic Analysis and Design of Secondary Systems," by G. Chen and T.T. Soong, 8/6/93, (PB94-142767, A11, MF-A03).

NCEER-93-0015 "Proceedings from School Sites: Becoming Prepared for Earthquakes - Commemorating the Third Anniversary of the Loma Prieta Earthquake," Edited by F.E. Winslow and K.E.K. Ross, 8/16/93, (PB94-154275, A16, MF-A02).

NCEER-93-0016 "Reconnaissance Report of Damage to Historic Monuments in Cairo, Egypt Following the October 12, 1992 Dahshur Earthquake," by D. Sykora, D. Look, G. Croci, E. Karaesmen and E. Karaesmen, 8/19/93, (PB94-142221, A08, MF-A02).

NCEER-93-0017 "The Island of Guam Earthquake of August 8, 1993," by S.W. Swan and S.K. Harris, 9/30/93, (PB94-141843, A04, MF-A01).

NCEER-93-0018 "Engineering Aspects of the October 12, 1992 Egyptian Earthquake," by A.W. Elgamal, M. Amer, K. Adalier and A. Abul-Fadl, 10/7/93, (PB94-141983, A05, MF-A01).

NCEER-93-0019 "Development of an Earthquake Motion Simulator and its Application in Dynamic Centrifuge Testing," by I. Krstelj, Supervised by J.H. Prevost, 10/23/93, (PB94-181773, A-10, MF-A03).

NCEER-93-0020 "NCEER-Taisei Corporation Research Program on Sliding Seismic Isolation Systems for Bridges: Experimental and Analytical Study of a Friction Pendulum System (FPS)," by M.C. Constantinou, P. Tsopelas, Y-S. Kim and S. Okamoto, 11/1/93, (PB94-142775, A08, MF-A02).

NCEER-93-0021 "Finite Element Modeling of Elastomeric Seismic Isolation Bearings," by L.J. Billings, Supervised by R. Shepherd, 11/8/93, to be published.

NCEER-93-0022 "Seismic Vulnerability of Equipment in Critical Facilities: Life-Safety and Operational Consequences," by K. Porter, G.S. Johnson, M.M. Zadeh, C. Scawthorn and S. Eder, 11/24/93, (PB94-181765, A16, MF-A03).

NCEER-93-0023 "Hokkaido Nansei-oki, Japan Earthquake of July 12, 1993, by P.I. Yanev and C.R. Scawthorn, 12/23/93, (PB94-181500, A07, MF-A01).

NCEER-94-0001 "An Evaluation of Seismic Serviceability of Water Supply Networks with Application to the San Francisco Auxiliary Water Supply System," by I. Markov, Supervised by M. Grigoriu and T. O'Rourke, 1/21/94, (PB94-204013, A07, MF-A02).

NCEER-94-0002 "NCEER-Taisei Corporation Research Program on Sliding Seismic Isolation Systems for Bridges: Experimental and Analytical Study of Systems Consisting of Sliding Bearings, Rubber Restoring Force Devices and Fluid Dampers," Volumes I and II, by P. Tsopelas, S. Okamoto, M.C. Constantinou, D. Ozaki and S. Fujii, 2/4/94, (PB94-181740, A09, MF-A02 and PB94-181757, A12, MF-A03).

NCEER-94-0003 "A Markov Model for Local and Global Damage Indices in Seismic Analysis," by S. Rahman and M. Grigoriu, 2/18/94, (PB94-206000, A12, MF-A03).

NCEER-94-0004 "Proceedings from the NCEER Workshop on Seismic Response of Masonry Infills," edited by D.P. Abrams, 3/1/94, (PB94-180783, A07, MF-A02).

NCEER-94-0005 "The Northridge, California Earthquake of January 17, 1994: General Reconnaissance Report," edited by J.D. Goltz, 3/11/94, (PB94-193943, A10, MF-A03).

NCEER-94-0006 "Seismic Energy Based Fatigue Damage Analysis of Bridge Columns: Part I - Evaluation of Seismic Capacity," by G.A. Chang and J.B. Mander, 3/14/94, (PB94-219185, A11, MF-A03).

NCEER-94-0007 "Seismic Isolation of Multi-Story Frame Structures Using Spherical Sliding Isolation Systems," by T.M. Al-Hussaini, V.A. Zayas and M.C. Constantinou, 3/17/94, (PB94-193745, A09, MF-A02).

NCEER-94-0008 "The Northridge, California Earthquake of January 17, 1994: Performance of Highway Bridges," edited by I.G. Buckle, 3/24/94, (PB94-193851, A06, MF-A02).

NCEER-94-0009 "Proceedings of the Third U.S.-Japan Workshop on Earthquake Protective Systems for Bridges," edited by I.G. Buckle and I. Friedland, 3/31/94, (PB94-195815, A99, MF-A06).

NCEER-94-0010 "3D-BASIS-ME: Computer Program for Nonlinear Dynamic Analysis of Seismically Isolated Single and Multiple Structures and Liquid Storage Tanks," by P.C. Tsopelas, M.C. Constantinou and A.M. Reinhorn, 4/12/94, (PB94-204922, A09, MF-A02).

NCEER-94-0011 "The Northridge, California Earthquake of January 17, 1994: Performance of Gas Transmission Pipelines," by T.D. O'Rourke and M.C. Palmer, 5/16/94, (PB94-204989, A05, MF-A01).

NCEER-94-0012 "Feasibility Study of Replacement Procedures and Earthquake Performance Related to Gas Transmission Pipelines," by T.D. O'Rourke and M.C. Palmer, 5/25/94, (PB94-206638, A09, MF-A02).

NCEER-94-0013 "Seismic Energy Based Fatigue Damage Analysis of Bridge Columns: Part II - Evaluation of Seismic Demand," by G.A. Chang and J.B. Mander, 6/1/94, (PB95-18106, A08, MF-A02).

NCEER-94-0014 "NCEER-Taisei Corporation Research Program on Sliding Seismic Isolation Systems for Bridges: Experimental and Analytical Study of a System Consisting of Sliding Bearings and Fluid Restoring Force/Damping Devices," by P. Tsopelas and M.C. Constantinou, 6/13/94, (PB94-219144, A10, MF-A03).

NCEER-94-0015 "Generation of Hazard-Consistent Fragility Curves for Seismic Loss Estimation Studies," by H. Hwang and J-R. Huo, 6/14/94, (PB95-181996, A09, MF-A02).

NCEER-94-0016 "Seismic Study of Building Frames with Added Energy-Absorbing Devices," by W.S. Pong, C.S. Tsai and G.C. Lee, 6/20/94, (PB94-219136, A10, A03).

NCEER-94-0017 "Sliding Mode Control for Seismic-Excited Linear and Nonlinear Civil Engineering Structures," by J. Yang, J. Wu, A. Agrawal and Z. Li, 6/21/94, (PB95-138483, A06, MF-A02).

NCEER-94-0018 "3D-BASIS-TABS Version 2.0: Computer Program for Nonlinear Dynamic Analysis of Three Dimensional Base Isolated Structures," by A.M. Reinhorn, S. Nagarajaiah, M.C. Constantinou, P. Tsopelas and R. Li, 6/22/94, (PB95-182176, A08, MF-A02).

NCEER-94-0019 "Proceedings of the International Workshop on Civil Infrastructure Systems: Application of Intelligent Systems and Advanced Materials on Bridge Systems," Edited by G.C. Lee and K.C. Chang, 7/18/94, (PB95-252474, A20, MF-A04).

NCEER-94-0020 "Study of Seismic Isolation Systems for Computer Floors," by V. Lambrou and M.C. Constantinou, 7/19/94, (PB95-138533, A10, MF-A03).

NCEER-94-0021 "Proceedings of the U.S.-Italian Workshop on Guidelines for Seismic Evaluation and Rehabilitation of Unreinforced Masonry Buildings," Edited by D.P. Abrams and G.M. Calvi, 7/20/94, (PB95-138749, A13, MF-A03).

NCEER-94-0022 "NCEER-Taisei Corporation Research Program on Sliding Seismic Isolation Systems for Bridges: Experimental and Analytical Study of a System Consisting of Lubricated PTFE Sliding Bearings and Mild Steel Dampers," by P. Tsopelas and M.C. Constantinou, 7/22/94, (PB95-182184, A08, MF-A02).

NCEER-94-0023 “Development of Reliability-Based Design Criteria for Buildings Under Seismic Load,” by Y.K. Wen, H. Hwang and M. Shinozuka, 8/1/94, (PB95-211934, A08, MF-A02).

NCEER-94-0024 “Experimental Verification of Acceleration Feedback Control Strategies for an Active Tendon System,” by S.J. Dyke, B.F. Spencer, Jr., P. Quast, M.K. Sain, D.C. Kaspari, Jr. and T.T. Soong, 8/29/94, (PB95-212320, A05, MF-A01).

NCEER-94-0025 “Seismic Retrofitting Manual for Highway Bridges,” Edited by I.G. Buckle and I.F. Friedland, published by the Federal Highway Administration (PB95-212676, A15, MF-A03).

NCEER-94-0026 “Proceedings from the Fifth U.S.-Japan Workshop on Earthquake Resistant Design of Lifeline Facilities and Countermeasures Against Soil Liquefaction,” Edited by T.D. O’Rourke and M. Hamada, 11/7/94, (PB95-220802, A99, MF-E08).

NCEER-95-0001 "Experimental and Analytical Investigation of Seismic Retrofit of Structures with Supplemental Damping: Part 1 - Fluid Viscous Damping Devices," by A.M. Reinhorn, C. Li and M.C. Constantinou, 1/3/95, (PB95-266599, A09, MF-A02).

NCEER-95-0002 "Experimental and Analytical Study of Low-Cycle Fatigue Behavior of Semi-Rigid Top-And-Seat Angle Connections," by G. Pekcan, J.B. Mander and S.S. Chen, 1/5/95, (PB95-220042, A07, MF-A02).

NCEER-95-0003 "NCEER-ATC Joint Study on Fragility of Buildings," by T. Anagnos, C. Rojahn and A.S. Kiremidjian, 1/20/95, (PB95-220026, A06, MF-A02).

NCEER-95-0004 "Nonlinear Control Algorithms for Peak Response Reduction," by Z. Wu, T.T. Soong, V. Gattulli and R.C. Lin, 2/16/95, (PB95-220349, A05, MF-A01).

NCEER-95-0005 "Pipeline Replacement Feasibility Study: A Methodology for Minimizing Seismic and Corrosion Risks to Underground Natural Gas Pipelines," by R.T. Eguchi, H.A. Seligson and D.G. Honegger, 3/2/95, (PB95-252326, A06, MF-A02).

NCEER-95-0006 "Evaluation of Seismic Performance of an 11-Story Frame Building During the 1994 Northridge Earthquake," by F. Naeim, R. DiSulio, K. Benuska, A. Reinhorn and C. Li, to be published.

NCEER-95-0007 "Prioritization of Bridges for Seismic Retrofitting," by N. Basöz and A.S. Kiremidjian, 4/24/95, (PB95-252300, A08, MF-A02).

NCEER-95-0008 "Method for Developing Motion Damage Relationships for Reinforced Concrete Frames," by A. Singhal and A.S. Kiremidjian, 5/11/95, (PB95-266607, A06, MF-A02).

NCEER-95-0009 "Experimental and Analytical Investigation of Seismic Retrofit of Structures with Supplemental Damping: Part II - Friction Devices," by C. Li and A.M. Reinhorn, 7/6/95, (PB96-128087, A11, MF-A03).

NCEER-95-0010 "Experimental Performance and Analytical Study of a Non-Ductile Reinforced Concrete Frame Structure Retrofitted with Elastomeric Spring Dampers," by G. Pekcan, J.B. Mander and S.S. Chen, 7/14/95, (PB96-137161, A08, MF-A02).

NCEER-95-0011 "Development and Experimental Study of Semi-Active Fluid Damping Devices for Seismic Protection of Structures," by M.D. Symans and M.C. Constantinou, 8/3/95, (PB96-136940, A23, MF-A04).

NCEER-95-0012 "Real-Time Structural Parameter Modification (RSPM): Development of Innervated Structures," by Z. Liang, M. Tong and G.C. Lee, 4/11/95, (PB96-137153, A06, MF-A01).

NCEER-95-0013 "Experimental and Analytical Investigation of Seismic Retrofit of Structures with Supplemental Damping: Part III - Viscous Damping Walls," by A.M. Reinhorn and C. Li, 10/1/95, (PB96-176409, A11, MF-A03).

NCEER-95-0014 "Seismic Fragility Analysis of Equipment and Structures in a Memphis Electric Substation," by J-R. Huo and H.H.M. Hwang, 8/10/95, (PB96-128087, A09, MF-A02).

NCEER-95-0015 "The Hanshin-Awaji Earthquake of January 17, 1995: Performance of Lifelines," Edited by M. Shinozuka, 11/3/95, (PB96-176383, A15, MF-A03).

NCEER-95-0016 "Highway Culvert Performance During Earthquakes," by T.L. Youd and C.J. Beckman, available as NCEER-96-0015.

NCEER-95-0017 "The Hanshin-Awaji Earthquake of January 17, 1995: Performance of Highway Bridges," Edited by I.G. Buckle, 12/1/95, to be published.

NCEER-95-0018 "Modeling of Masonry Infill Panels for Structural Analysis," by A.M. Reinhorn, A. Madan, R.E. Valles, Y. Reichmann and J.B. Mander, 12/8/95, (PB97-110886, MF-A01, A06).

NCEER-95-0019 "Optimal Polynomial Control for Linear and Nonlinear Structures," by A.K. Agrawal and J.N. Yang, 12/11/95, (PB96-168737, A07, MF-A02).

NCEER-95-0020 "Retrofit of Non-Ductile Reinforced Concrete Frames Using Friction Dampers," by R.S. Rao, P. Gergely and R.N. White, 12/22/95, (PB97-133508, A10, MF-A02).

NCEER-95-0021 "Parametric Results for Seismic Response of Pile-Supported Bridge Bents," by G. Mylonakis, A. Nikolaou and G. Gazetas, 12/22/95, (PB97-100242, A12, MF-A03).

NCEER-95-0022 "Kinematic Bending Moments in Seismically Stressed Piles," by A. Nikolaou, G. Mylonakis and G. Gazetas, 12/23/95, (PB97-113914, MF-A03, A13).

NCEER-96-0001 "Dynamic Response of Unreinforced Masonry Buildings with Flexible Diaphragms," by A.C. Costley and D.P. Abrams," 10/10/96, (PB97-133573, MF-A03, A15).

NCEER-96-0002 "State of the Art Review: Foundations and Retaining Structures," by I. Po Lam, to be published.

NCEER-96-0003 "Ductility of Rectangular Reinforced Concrete Bridge Columns with Moderate Confinement," by N. Wehbe, M. Saiidi, D. Sanders and B. Douglas, 11/7/96, (PB97-133557, A06, MF-A02).

NCEER-96-0004 "Proceedings of the Long-Span Bridge Seismic Research Workshop," edited by I.G. Buckle and I.M. Friedland, to be published.

NCEER-96-0005 "Establish Representative Pier Types for Comprehensive Study: Eastern United States," by J. Kulicki and Z. Prucz, 5/28/96, (PB98-119217, A07, MF-A02).

NCEER-96-0006 "Establish Representative Pier Types for Comprehensive Study: Western United States," by R. Imbsen, R.A. Schamber and T.A. Osterkamp, 5/28/96, (PB98-118607, A07, MF-A02).

NCEER-96-0007 "Nonlinear Control Techniques for Dynamical Systems with Uncertain Parameters," by R.G. Ghanem and M.I. Bujakov, 5/27/96, (PB97-100259, A17, MF-A03).

NCEER-96-0008 "Seismic Evaluation of a 30-Year Old Non-Ductile Highway Bridge Pier and Its Retrofit," by J.B. Mander, B. Mahmoodzadegan, S. Bhadra and S.S. Chen, 5/31/96, (PB97-110902, MF-A03, A10).

NCEER-96-0009 "Seismic Performance of a Model Reinforced Concrete Bridge Pier Before and After Retrofit," by J.B. Mander, J.H. Kim and C.A. Ligozio, 5/31/96, (PB97-110910, MF-A02, A10).

NCEER-96-0010 "IDARC2D Version 4.0: A Computer Program for the Inelastic Damage Analysis of Buildings," by R.E. Valles, A.M. Reinhorn, S.K. Kunnath, C. Li and A. Madan, 6/3/96, (PB97-100234, A17, MF-A03).

NCEER-96-0011 "Estimation of the Economic Impact of Multiple Lifeline Disruption: Memphis Light, Gas and Water Division Case Study," by S.E. Chang, H.A. Seligson and R.T. Eguchi, 8/16/96, (PB97-133490, A11, MF-A03).

NCEER-96-0012 "Proceedings from the Sixth Japan-U.S. Workshop on Earthquake Resistant Design of Lifeline Facilities and Countermeasures Against Soil Liquefaction, Edited by M. Hamada and T. O'Rourke, 9/11/96, (PB97-133581, A99, MF-A06).

NCEER-96-0013 "Chemical Hazards, Mitigation and Preparedness in Areas of High Seismic Risk: A Methodology for Estimating the Risk of Post-Earthquake Hazardous Materials Release," by H.A. Seligson, R.T. Eguchi, K.J. Tierney and K. Richmond, 11/7/96, (PB97-133565, MF-A02, A08).

NCEER-96-0014 "Response of Steel Bridge Bearings to Reversed Cyclic Loading," by J.B. Mander, D-K. Kim, S.S. Chen and G.J. Premus, 11/13/96, (PB97-140735, A12, MF-A03).

NCEER-96-0015 "Highway Culvert Performance During Past Earthquakes," by T.L. Youd and C.J. Beckman, 11/25/96, (PB97-133532, A06, MF-A01).

NCEER-97-0001 "Evaluation, Prevention and Mitigation of Pounding Effects in Building Structures," by R.E. Valles and A.M. Reinhorn, 2/20/97, (PB97-159552, A14, MF-A03).

NCEER-97-0002 "Seismic Design Criteria for Bridges and Other Highway Structures," by C. Rojahn, R. Mayes, D.G. Anderson, J. Clark, J.H. Hom, R.V. Nutt and M.J. O'Rourke, 4/30/97, (PB97-194658, A06, MF-A03).

NCEER-97-0003 “Proceedings of the U.S.-Italian Workshop on Seismic Evaluation and Retrofit,” Edited by D.P. Abrams and G.M. Calvi, 3/19/97, (PB97-194666, A13, MF-A03).

NCEER-97-0004 "Investigation of Seismic Response of Buildings with Linear and Nonlinear Fluid Viscous Dampers," by A.A. Seleemah and M.C. Constantinou, 5/21/97, (PB98-109002, A15, MF-A03).

NCEER-97-0005 "Proceedings of the Workshop on Earthquake Engineering Frontiers in Transportation Facilities," edited by G.C. Lee and I.M. Friedland, 8/29/97, (PB98-128911, A25, MR-A04).

NCEER-97-0006 "Cumulative Seismic Damage of Reinforced Concrete Bridge Piers," by S.K. Kunnath, A. El-Bahy, A. Taylor and W. Stone, 9/2/97, (PB98-108814, A11, MF-A03).

NCEER-97-0007 "Structural Details to Accommodate Seismic Movements of Highway Bridges and Retaining Walls," by R.A. Imbsen, R.A. Schamber, E. Thorkildsen, A. Kartoum, B.T. Martin, T.N. Rosser and J.M. Kulicki, 9/3/97, (PB98-108996, A09, MF-A02).

NCEER-97-0008 "A Method for Earthquake Motion-Damage Relationships with Application to Reinforced Concrete Frames," by A. Singhal and A.S. Kiremidjian, 9/10/97, (PB98-108988, A13, MF-A03).

NCEER-97-0009 "Seismic Analysis and Design of Bridge Abutments Considering Sliding and Rotation," by K. Fishman and R. Richards, Jr., 9/15/97, (PB98-108897, A06, MF-A02).

NCEER-97-0010 "Proceedings of the FHWA/NCEER Workshop on the National Representation of Seismic Ground Motion for New and Existing Highway Facilities," edited by I.M. Friedland, M.S. Power and R.L. Mayes, 9/22/97, (PB98-128903, A21, MF-A04).

NCEER-97-0011 "Seismic Analysis for Design or Retrofit of Gravity Bridge Abutments," by K.L. Fishman, R. Richards, Jr. and R.C. Divito, 10/2/97, (PB98-128937, A08, MF-A02).

NCEER-97-0012 "Evaluation of Simplified Methods of Analysis for Yielding Structures," by P. Tsopelas, M.C. Constantinou, C.A. Kircher and A.S. Whittaker, 10/31/97, (PB98-128929, A10, MF-A03).

NCEER-97-0013 "Seismic Design of Bridge Columns Based on Control and Repairability of Damage," by C-T. Cheng and J.B. Mander, 12/8/97, (PB98-144249, A11, MF-A03).

NCEER-97-0014 "Seismic Resistance of Bridge Piers Based on Damage Avoidance Design," by J.B. Mander and C-T. Cheng, 12/10/97, (PB98-144223, A09, MF-A02).

NCEER-97-0015 “Seismic Response of Nominally Symmetric Systems with Strength Uncertainty,” by S. Balopoulou and M. Grigoriu, 12/23/97, (PB98-153422, A11, MF-A03).

NCEER-97-0016 “Evaluation of Seismic Retrofit Methods for Reinforced Concrete Bridge Columns,” by T.J. Wipf, F.W. Klaiber and F.M. Russo, 12/28/97, (PB98-144215, A12, MF-A03).

NCEER-97-0017 “Seismic Fragility of Existing Conventional Reinforced Concrete Highway Bridges,” by C.L. Mullen and A.S. Cakmak, 12/30/97, (PB98-153406, A08, MF-A02).

NCEER-97-0018 “Loss Asssessment of Memphis Buildings,” edited by D.P. Abrams and M. Shinozuka, 12/31/97, (PB98-144231, A13, MF-A03).

NCEER-97-0019 “Seismic Evaluation of Frames with Infill Walls Using Quasi-static Experiments,” by K.M. Mosalam, R.N. White and P. Gergely, 12/31/97, (PB98-153455, A07, MF-A02).

NCEER-97-0020 “Seismic Evaluation of Frames with Infill Walls Using Pseudo-dynamic Experiments,” by K.M. Mosalam, R.N. White and P. Gergely, 12/31/97, (PB98-153430, A07, MF-A02).

NCEER-97-0021 “Computational Strategies for Frames with Infill Walls: Discrete and Smeared Crack Analyses and Seismic Fragility,” by K.M. Mosalam, R.N. White and P. Gergely, 12/31/97, (PB98-153414, A10, MF-A02).

NCEER-97-0022 "Proceedings of the NCEER Workshop on Evaluation of Liquefaction Resistance of Soils," edited by T.L. Youd and I.M. Idriss, 12/31/97, (PB98-155617, A15, MF-A03).

MCEER-98-0001 "Extraction of Nonlinear Hysteretic Properties of Seismically Isolated Bridges from Quick-Release Field Tests," by Q. Chen, B.M. Douglas, E.M. Maragakis and I.G. Buckle, 5/26/98, (PB99-118838, A06, MF-A01).

MCEER-98-0002 "Methodologies for Evaluating the Importance of Highway Bridges," by A. Thomas, S. Eshenaur and J. Kulicki, 5/29/98, (PB99-118846, A10, MF-A02).

MCEER-98-0003 "Capacity Design of Bridge Piers and the Analysis of Overstrength," by J.B. Mander, A. Dutta and P. Goel, 6/1/98, (PB99-118853, A09, MF-A02).

MCEER-98-0004 "Evaluation of Bridge Damage Data from the Loma Prieta and Northridge, California Earthquakes," by N. Basoz and A. Kiremidjian, 6/2/98, (PB99-118861, A15, MF-A03).

MCEER-98-0005 "Screening Guide for Rapid Assessment of Liquefaction Hazard at Highway Bridge Sites," by T. L. Youd, 6/16/98, (PB99-118879, A06, not available on microfiche).

MCEER-98-0006 "Structural Steel and Steel/Concrete Interface Details for Bridges," by P. Ritchie, N. Kauhl and J. Kulicki, 7/13/98, (PB99-118945, A06, MF-A01).

MCEER-98-0007 "Capacity Design and Fatigue Analysis of Confined Concrete Columns," by A. Dutta and J.B. Mander, 7/14/98, (PB99-118960, A14, MF-A03).

MCEER-98-0008 "Proceedings of the Workshop on Performance Criteria for Telecommunication Services Under Earthquake Conditions," edited by A.J. Schiff, 7/15/98, (PB99-118952, A08, MF-A02).

MCEER-98-0009 "Fatigue Analysis of Unconfined Concrete Columns," by J.B. Mander, A. Dutta and J.H. Kim, 9/12/98, (PB99-123655, A10, MF-A02).

MCEER-98-0010 "Centrifuge Modeling of Cyclic Lateral Response of Pile-Cap Systems and Seat-Type Abutments in Dry Sands," by A.D. Gadre and R. Dobry, 10/2/98, (PB99-123606, A13, MF-A03).

MCEER-98-0011 "IDARC-BRIDGE: A Computational Platform for Seismic Damage Assessment of Bridge Structures," by A.M. Reinhorn, V. Simeonov, G. Mylonakis and Y. Reichman, 10/2/98, (PB99-162919, A15, MF-A03).

MCEER-98-0012 "Experimental Investigation of the Dynamic Response of Two Bridges Before and After Retrofitting with Elastomeric Bearings," by D.A. Wendichansky, S.S. Chen and J.B. Mander, 10/2/98, (PB99-162927, A15, MF-A03).

MCEER-98-0013 "Design Procedures for Hinge Restrainers and Hinge Sear Width for Multiple-Frame Bridges," by R. Des Roches and G.L. Fenves, 11/3/98, (PB99-140477, A13, MF-A03).

MCEER-98-0014 "Response Modification Factors for Seismically Isolated Bridges," by M.C. Constantinou and J.K. Quarshie, 11/3/98, (PB99-140485, A14, MF-A03).

MCEER-98-0015 "Proceedings of the U.S.-Italy Workshop on Seismic Protective Systems for Bridges," edited by I.M. Friedland and M.C. Constantinou, 11/3/98, (PB2000-101711, A22, MF-A04).

MCEER-98-0016 "Appropriate Seismic Reliability for Critical Equipment Systems: Recommendations Based on Regional Analysis of Financial and Life Loss," by K. Porter, C. Scawthorn, C. Taylor and N. Blais, 11/10/98, (PB99-157265, A08, MF-A02).

MCEER-98-0017 "Proceedings of the U.S. Japan Joint Seminar on Civil Infrastructure Systems Research," edited by M. Shinozuka and A. Rose, 11/12/98, (PB99-156713, A16, MF-A03).

MCEER-98-0018 "Modeling of Pile Footings and Drilled Shafts for Seismic Design," by I. PoLam, M. Kapuskar and D. Chaudhuri, 12/21/98, (PB99-157257, A09, MF-A02).

MCEER-99-0001 "Seismic Evaluation of a Masonry Infilled Reinforced Concrete Frame by Pseudodynamic Testing," by S.G. Buonopane and R.N. White, 2/16/99, (PB99-162851, A09, MF-A02).

MCEER-99-0002 "Response History Analysis of Structures with Seismic Isolation and Energy Dissipation Systems: Verification Examples for Program SAP2000," by J. Scheller and M.C. Constantinou, 2/22/99, (PB99-162869, A08, MF-A02).

MCEER-99-0003 "Experimental Study on the Seismic Design and Retrofit of Bridge Columns Including Axial Load Effects," by A. Dutta, T. Kokorina and J.B. Mander, 2/22/99, (PB99-162877, A09, MF-A02).

MCEER-99-0004 "Experimental Study of Bridge Elastomeric and Other Isolation and Energy Dissipation Systems with Emphasis on Uplift Prevention and High Velocity Near-source Seismic Excitation," by A. Kasalanati and M. C. Constantinou, 2/26/99, (PB99-162885, A12, MF-A03).

MCEER-99-0005 "Truss Modeling of Reinforced Concrete Shear-flexure Behavior," by J.H. Kim and J.B. Mander, 3/8/99, (PB99-163693, A12, MF-A03).

MCEER-99-0006 "Experimental Investigation and Computational Modeling of Seismic Response of a 1:4 Scale Model Steel Structure with a Load Balancing Supplemental Damping System," by G. Pekcan, J.B. Mander and S.S. Chen, 4/2/99, (PB99-162893, A11, MF-A03).

MCEER-99-0007 "Effect of Vertical Ground Motions on the Structural Response of Highway Bridges," by M.R. Button, C.J. Cronin and R.L. Mayes, 4/10/99, (PB2000-101411, A10, MF-A03).

MCEER-99-0008 "Seismic Reliability Assessment of Critical Facilities: A Handbook, Supporting Documentation, and Model Code Provisions," by G.S. Johnson, R.E. Sheppard, M.D. Quilici, S.J. Eder and C.R. Scawthorn, 4/12/99, (PB2000-101701, A18, MF-A04).

MCEER-99-0009 "Impact Assessment of Selected MCEER Highway Project Research on the Seismic Design of Highway Structures," by C. Rojahn, R. Mayes, D.G. Anderson, J.H. Clark, D'Appolonia Engineering, S. Gloyd and R.V. Nutt, 4/14/99, (PB99-162901, A10, MF-A02).

MCEER-99-0010 "Site Factors and Site Categories in Seismic Codes," by R. Dobry, R. Ramos and M.S. Power, 7/19/99, (PB2000-101705, A08, MF-A02).

MCEER-99-0011 "Restrainer Design Procedures for Multi-Span Simply-Supported Bridges," by M.J. Randall, M. Saiidi, E. Maragakis and T. Isakovic, 7/20/99, (PB2000-101702, A10, MF-A02).

MCEER-99-0012 "Property Modification Factors for Seismic Isolation Bearings," by M.C. Constantinou, P. Tsopelas, A. Kasalanati and E. Wolff, 7/20/99, (PB2000-103387, A11, MF-A03).

MCEER-99-0013 "Critical Seismic Issues for Existing Steel Bridges," by P. Ritchie, N. Kauhl and J. Kulicki, 7/20/99, (PB2000-101697, A09, MF-A02).

MCEER-99-0014 "Nonstructural Damage Database," by A. Kao, T.T. Soong and A. Vender, 7/24/99, (PB2000-101407, A06, MF-A01).

MCEER-99-0015 "Guide to Remedial Measures for Liquefaction Mitigation at Existing Highway Bridge Sites," by H.G. Cooke and J. K. Mitchell, 7/26/99, (PB2000-101703, A11, MF-A03).

MCEER-99-0016 "Proceedings of the MCEER Workshop on Ground Motion Methodologies for the Eastern United States," edited by N. Abrahamson and A. Becker, 8/11/99, (PB2000-103385, A07, MF-A02).

MCEER-99-0017 "Quindío, Colombia Earthquake of January 25, 1999: Reconnaissance Report," by A.P. Asfura and P.J. Flores, 10/4/99, (PB2000-106893, A06, MF-A01).

MCEER-99-0018 "Hysteretic Models for Cyclic Behavior of Deteriorating Inelastic Structures," by M.V. Sivaselvan and A.M. Reinhorn, 11/5/99, (PB2000-103386, A08, MF-A02).

MCEER-99-0019 "Proceedings of the 7th U.S.- Japan Workshop on Earthquake Resistant Design of Lifeline Facilities and Countermeasures Against Soil Liquefaction," edited by T.D. O'Rourke, J.P. Bardet and M. Hamada, 11/19/99, (PB2000-103354, A99, MF-A06).

MCEER-99-0020 "Development of Measurement Capability for Micro-Vibration Evaluations with Application to Chip Fabrication Facilities," by G.C. Lee, Z. Liang, J.W. Song, J.D. Shen and W.C. Liu, 12/1/99, (PB2000-105993, A08, MF-A02).

MCEER-99-0021 "Design and Retrofit Methodology for Building Structures with Supplemental Energy Dissipating Systems," by G. Pekcan, J.B. Mander and S.S. Chen, 12/31/99, (PB2000-105994, A11, MF-A03).

MCEER-00-0001 "The Marmara, Turkey Earthquake of August 17, 1999: Reconnaissance Report," edited by C. Scawthorn; with major contributions by M. Bruneau, R. Eguchi, T. Holzer, G. Johnson, J. Mander, J. Mitchell, W. Mitchell, A. Papageorgiou, C. Scaethorn, and G. Webb, 3/23/00, (PB2000-106200, A11, MF-A03).

MCEER-00-0002 "Proceedings of the MCEER Workshop for Seismic Hazard Mitigation of Health Care Facilities," edited by G.C. Lee, M. Ettouney, M. Grigoriu, J. Hauer and J. Nigg, 3/29/00, (PB2000-106892, A08, MF-A02).

MCEER-00-0003 "The Chi-Chi, Taiwan Earthquake of September 21, 1999: Reconnaissance Report," edited by G.C. Lee and C.H. Loh, with major contributions by G.C. Lee, M. Bruneau, I.G. Buckle, S.E. Chang, P.J. Flores, T.D. O'Rourke, M. Shinozuka, T.T. Soong, C-H. Loh, K-C. Chang, Z-J. Chen, J-S. Hwang, M-L. Lin, G-Y. Liu, K-C. Tsai, G.C. Yao and C-L. Yen, 4/30/00, (PB2001-100980, A10, MF-A02).

MCEER-00-0004 "Seismic Retrofit of End-Sway Frames of Steel Deck-Truss Bridges with a Supplemental Tendon System: Experimental and Analytical Investigation," by G. Pekcan, J.B. Mander and S.S. Chen, 7/1/00, (PB2001-100982, A10, MF-A02).

MCEER-00-0005 "Sliding Fragility of Unrestrained Equipment in Critical Facilities," by W.H. Chong and T.T. Soong, 7/5/00, (PB2001-100983, A08, MF-A02).

MCEER-00-0006 "Seismic Response of Reinforced Concrete Bridge Pier Walls in the Weak Direction," by N. Abo-Shadi, M. Saiidi and D. Sanders, 7/17/00, (PB2001-100981, A17, MF-A03).

MCEER-00-0007 "Low-Cycle Fatigue Behavior of Longitudinal Reinforcement in Reinforced Concrete Bridge Columns," by J. Brown and S.K. Kunnath, 7/23/00, (PB2001-104392, A08, MF-A02).

MCEER-00-0008 "Soil Structure Interaction of Bridges for Seismic Analysis," I. PoLam and H. Law, 9/25/00, (PB2001-105397, A08, MF-A02).

MCEER-00-0009 "Proceedings of the First MCEER Workshop on Mitigation of Earthquake Disaster by Advanced Technologies (MEDAT-1), edited by M. Shinozuka, D.J. Inman and T.D. O'Rourke, 11/10/00, (PB2001-105399, A14, MF-A03).

MCEER-00-0010 "Development and Evaluation of Simplified Procedures for Analysis and Design of Buildings with Passive Energy Dissipation Systems," by O.M. Ramirez, M.C. Constantinou, C.A. Kircher, A.S. Whittaker, M.W. Johnson, J.D. Gomez and C. Chrysostomou, 11/16/01, (PB2001-105523, A23, MF-A04).

MCEER-00-0011 "Dynamic Soil-Foundation-Structure Interaction Analyses of Large Caissons," by C-Y. Chang, C-M. Mok, Z-L. Wang, R. Settgast, F. Waggoner, M.A. Ketchum, H.M. Gonnermann and C-C. Chin, 12/30/00, (PB2001-104373, A07, MF-A02).

MCEER-00-0012 "Experimental Evaluation of Seismic Performance of Bridge Restrainers," by A.G. Vlassis, E.M. Maragakis and M. Saiid Saiidi, 12/30/00, (PB2001-104354, A09, MF-A02).

MCEER-00-0013 "Effect of Spatial Variation of Ground Motion on Highway Structures," by M. Shinozuka, V. Saxena and G. Deodatis, 12/31/00, (PB2001-108755, A13, MF-A03).

MCEER-00-0014 "A Risk-Based Methodology for Assessing the Seismic Performance of Highway Systems," by S.D. Werner, C.E. Taylor, J.E. Moore, II, J.S. Walton and S. Cho, 12/31/00, (PB2001-108756, A14, MF-A03).

MCEER-01-0001 "Experimental Investigation of P-Delta Effects to Collapse During Earthquakes," by D. Vian and M. Bruneau, 6/25/01, (PB2002-100534, A17, MF-A03).

MCEER-01-0002 "Proceedings of the Second MCEER Workshop on Mitigation of Earthquake Disaster by Advanced Technologies (MEDAT-2)," edited by M. Bruneau and D.J. Inman, 7/23/01, (PB2002-100434, A16, MF-A03).

MCEER-01-0003 "Sensitivity Analysis of Dynamic Systems Subjected to Seismic Loads," by C. Roth and M. Grigoriu, 9/18/01, (PB2003-100884, A12, MF-A03).

MCEER-01-0004 "Overcoming Obstacles to Implementing Earthquake Hazard Mitigation Policies: Stage 1 Report," by D.J. Alesch and W.J. Petak, 12/17/01, (PB2002-107949, A07, MF-A02).

MCEER-01-0005 "Updating Real-Time Earthquake Loss Estimates: Methods, Problems and Insights," by C.E. Taylor, S.E. Chang and R.T. Eguchi, 12/17/01, (PB2002-107948, A05, MF-A01).

MCEER-01-0006 "Experimental Investigation and Retrofit of Steel Pile Foundations and Pile Bents Under Cyclic Lateral Loadings," by A. Shama, J. Mander, B. Blabac and S. Chen, 12/31/01, (PB2002-107950, A13, MF-A03).

MCEER-02-0001 "Assessment of Performance of Bolu Viaduct in the 1999 Duzce Earthquake in Turkey" by P.C. Roussis, M.C. Constantinou, M. Erdik, E. Durukal and M. Dicleli, 5/8/02, (PB2003-100883, A08, MF-A02).

MCEER-02-0002 "Seismic Behavior of Rail Counterweight Systems of Elevators in Buildings," by M.P. Singh, Rildova and L.E. Suarez, 5/27/02. (PB2003-100882, A11, MF-A03).

MCEER-02-0003 "Development of Analysis and Design Procedures for Spread Footings," by G. Mylonakis, G. Gazetas, S. Nikolaou and A. Chauncey, 10/02/02, (PB2004-101636, A13, MF-A03, CD-A13).

MCEER-02-0004 "Bare-Earth Algorithms for Use with SAR and LIDAR Digital Elevation Models," by C.K. Huyck, R.T. Eguchi and B. Houshmand, 10/16/02, (PB2004-101637, A07, CD-A07).

MCEER-02-0005 "Review of Energy Dissipation of Compression Members in Concentrically Braced Frames," by K.Lee and M. Bruneau, 10/18/02, (PB2004-101638, A10, CD-A10).

MCEER-03-0001 "Experimental Investigation of Light-Gauge Steel Plate Shear Walls for the Seismic Retrofit of Buildings" by J. Berman and M. Bruneau, 5/2/03, (PB2004-101622, A10, MF-A03, CD-A10).

MCEER-03-0002 "Statistical Analysis of Fragility Curves," by M. Shinozuka, M.Q. Feng, H. Kim, T. Uzawa and T. Ueda, 6/16/03, (PB2004-101849, A09, CD-A09).

MCEER-03-0003 "Proceedings of the Eighth U.S.-Japan Workshop on Earthquake Resistant Design f Lifeline Facilities and Countermeasures Against Liquefaction," edited by M. Hamada, J.P. Bardet and T.D. O'Rourke, 6/30/03, (PB2004-104386, A99, CD-A99).

MCEER-03-0004 "Proceedings of the PRC-US Workshop on Seismic Analysis and Design of Special Bridges," edited by L.C. Fan and G.C. Lee, 7/15/03, (PB2004-104387, A14, CD-A14).

MCEER-03-0005 "Urban Disaster Recovery: A Framework and Simulation Model," by S.B. Miles and S.E. Chang, 7/25/03, (PB2004-104388, A07, CD-A07).

MCEER-03-0006 "Behavior of Underground Piping Joints Due to Static and Dynamic Loading," by R.D. Meis, M. Maragakis and R. Siddharthan, 11/17/03, (PB2005-102194, A13, MF-A03, CD-A00).

MCEER-03-0007 "Seismic Vulnerability of Timber Bridges and Timber Substructures," by A.A. Shama, J.B. Mander, I.M. Friedland and D.R. Allicock, 12/15/03.

MCEER-04-0001 "Experimental Study of Seismic Isolation Systems with Emphasis on Secondary System Response and Verification of Accuracy of Dynamic Response History Analysis Methods," by E. Wolff and M. Constantinou, 1/16/04 (PB2005-102195, A99, MF-E08, CD-A00).

MCEER-04-0002 "Tension, Compression and Cyclic Testing of Engineered Cementitious Composite Materials," by K. Kesner and S.L. Billington, 3/1/04, (PB2005-102196, A08, CD-A08).

MCEER-04-0003 "Cyclic Testing of Braces Laterally Restrained by Steel Studs to Enhance Performance During Earthquakes," by O.C. Celik, J.W. Berman and M. Bruneau, 3/16/04, (PB2005-102197, A13, MF-A03, CD-A00).

MCEER-04-0004 "Methodologies for Post Earthquake Building Damage Detection Using SAR and Optical Remote Sensing: Application to the August 17, 1999 Marmara, Turkey Earthquake," by C.K. Huyck, B.J. Adams, S. Cho, R.T. Eguchi, B. Mansouri and B. Houshmand, 6/15/04, (PB2005-104888, A10, CD-A00).

MCEER-04-0005 "Nonlinear Structural Analysis Towards Collapse Simulation: A Dynamical Systems Approach," by M.V. Sivaselvan and A.M. Reinhorn, 6/16/04, (PB2005-104889, A11, MF-A03, CD-A00).

MCEER-04-0006 "Proceedings of the Second PRC-US Workshop on Seismic Analysis and Design of Special Bridges," edited by G.C. Lee and L.C. Fan, 6/25/04, (PB2005-104890, A16, CD-A00).

MCEER-04-0007 "Seismic Vulnerability Evaluation of Axially Loaded Steel Built-up Laced Members," by K. Lee and M. Bruneau, 6/30/04, (PB2005-104891, A16, CD-A00).

MCEER-04-0008 "Evaluation of Accuracy of Simplified Methods of Analysis and Design of Buildings with Damping Systems for Near-Fault and for Soft-Soil Seismic Motions," by E.A. Pavlou and M.C. Constantinou, 8/16/04, (PB2005-104892, A08, MF-A02, CD-A00).

MCEER-04-0009 "Assessment of Geotechnical Issues in Acute Care Facilities in California," by M. Lew, T.D. O'Rourke, R. Dobry and M. Koch, 9/15/04, (PB2005-104893, A08, CD-A00).

MCEER-04-0010 "Scissor-Jack-Damper Energy Dissipation System," by A.N. Sigaher-Boyle and M.C. Constantinou, 12/1/04 (PB2005-108221).

MCEER-04-0011 "Seismic Retrofit of Bridge Steel Truss Piers Using a Controlled Rocking Approach," by M. Pollino and M. Bruneau, 12/20/04 (PB2006-105795).

MCEER-05-0001 "Experimental and Analytical Studies of Structures Seismically Isolated with an Uplift-Restraint Isolation System," by P.C. Roussis and M.C. Constantinou, 1/10/05 (PB2005-108222).

MCEER-05-0002 "A Versatile Experimentation Model for Study of Structures Near Collapse Applied to Seismic Evaluation of Irregular Structures," by D. Kusumastuti, A.M. Reinhorn and A. Rutenberg, 3/31/05 (PB2006-101523).

MCEER-05-0003 "Proceedings of the Third PRC-US Workshop on Seismic Analysis and Design of Special Bridges," edited by L.C. Fan and G.C. Lee, 4/20/05, (PB2006-105796).

MCEER-05-0004 "Approaches for the Seismic Retrofit of Braced Steel Bridge Piers and Proof-of-Concept Testing of an Eccentrically Braced Frame with Tubular Link," by J.W. Berman and M. Bruneau, 4/21/05 (PB2006-101524).

MCEER-05-0005 "Simulation of Strong Ground Motions for Seismic Fragility Evaluation of Nonstructural Components in Hospitals," by A. Wanitkorkul and A. Filiatrault, 5/26/05 (PB2006-500027).

MCEER-05-0006 "Seismic Safety in California Hospitals: Assessing an Attempt to Accelerate the Replacement or Seismic Retrofit of Older Hospital Facilities," by D.J. Alesch, L.A. Arendt and W.J. Petak, 6/6/05 (PB2006-105794).

MCEER-05-0007 "Development of Seismic Strengthening and Retrofit Strategies for Critical Facilities Using Engineered Cementitious Composite Materials," by K. Kesner and S.L. Billington, 8/29/05.

MCEER-05-0008 "Experimental and Analytical Studies of Base Isolation Systems for Seismic Protection of Power Transformers," by N. Murota, M.Q. Feng and G-Y. Liu, 9/30/05.

MCEER-05-0009 "3D-BASIS-ME-MB: Computer Program for Nonlinear Dynamic Analysis of Seismically Isolated Structures," by P.C. Tsopelas, P.C. Roussis, M.C. Constantinou, R. Buchanan and A.M. Reinhorn, 10/3/05.

MCEER-05-0010 "Steel Plate Shear Walls for Seismic Design and Retrofit of Building Structures," by D. Vian and M. Bruneau, 12/15/05.

MCEER-05-0011 "The Performance-Based Design Paradigm," by M.J. Astrella and A. Whittaker, 12/15/05.

MCEER-06-0001 "Seismic Fragility of Suspended Ceiling Systems," H. Badillo-Almaraz, A.S. Whittaker, A.M. Reinhorn and G.P. Cimellaro, 2/4/06.

MCEER-06-00002 "Multi-Dimensional Fragility of Structures," by G.P. Cimellaro, A.M. Reinhorn and M. Bruneau, 3/1/06.

MCEER-06-0003 "Built-Up Shear Links as Energy Dissipators for Seismic Protection of Bridges," by P. Dusicka, A.M. Itani and I.G. Buckle, 3/15/06.

MCEER-06-0004 "Analytical Investigation of the Structural Fuse Concept," by R.E. Vargas and M. Bruneau, 3/16/06.

MCEER-06-0005 "Experimental Investigation of the Structural Fuse Concept," by R.E. Vargas and M. Bruneau, 3/17/06.

MCEER-06-0006 "Further Development of Tubular Eccentrically Braced Frame Links for the Seismic Retrofit of Braced Steel Truss Bridge Piers," by J.W. Berman and M. Bruneau, 3/27/06.

MCEER-06-0007 "REDARS Validation Report," by S. Cho, C.K. Huyck, S. Ghosh and R.T. Eguchi, 8/8/06.

MCEER
EARTHQUAKE ENGINEERING TO EXTREME EVENTS
University at Buffalo, The State University of New York
Red Jacket Quadrangle ▪ Buffalo, New York 14261
Phone: (716) 645-3391 ▪ Fax: (716) 645-3399
E-mail: *mceer@buffalo.edu* ▪ WWW Site *http://mceer.buffalo.edu*
University at Buffalo *The State University of New York*

ISSN 1520-295X